1-1-2012

ATM Deficiency -- A Multifaceted Defect in Lymphocyte Development

Beth Helmink
Washington University in St. Louis

WASHINGTON UNIVERSITY IN ST. LOUIS

Division of Biology and Biomedical Sciences

Immunology

Dissertation Examination Committee:
Barry P. Sleckman, Chair
Jason Mills
Eugene Oltz
Sheila Stewart
Wojciech Swat
Herbert W. “Skip” Virgin
Zhongsheng You

ATM-deficiency – A Multifaceted Defect in Lymphocyte Development

by

Beth Ann Helmink

A dissertation presented to the
Graduate School of Arts and Sciences
of Washington University in
partial fulfillment of the
requirements for the degree of
Doctor of Philosophy

May 2012

Saint Louis, Missouri

ABSTRACT OF THE DISSERTATION

ATM Deficiency -- A Multifaceted Defect in Lymphocyte Development

by

Beth Ann Helmink

Doctor of Philosophy in Biology and Biomedical Sciences

(Immunology)

Washington University in St. Louis, 2012

Professor Barry P. Sleckman, Chairperson

The generation of a functional antigen receptor gene in developing lymphocytes requires that the second exon be assembled through a process known as V(D)J recombination, a process that necessarily involves the generation and repair of DNA double-strand breaks made by the Rag endonuclease. Double strand breaks incurred during G1 of the cell cycle activate ATM, a PI3-kinase-like kinase that, in response to genotoxic DNA damage, is known to phosphorylate hundreds of proteins with unique and diverse functions. Notably, deficiencies in ATM lead to ataxia-telangiectasia, a syndrome characterized by lymphopenia, genomic instability and a predisposition to tumors involving antigen receptor loci suggesting that ATM likely plays a similar critical role downstream of Rag-mediated DNA DSBs during V(D)J recombination. In this body of work, I describe three distinct pathways activated by ATM in response to Rag DNA DSBs and how defects in these pathways would impair lymphocyte development and contribute to the phenotype of ATM-deficient mice and humans. First, ATM-deficient lymphocytes have a defect in the repair of Rag DNA DSBs characterized by an accumulation of unrepaired coding ends and an increase in aberrant hybrid joint formation during rearrangement by inversion. Furthermore, these coding ends drift apart and are frequently aberrantly resolved as translocations. We determine that ATM contributes to the repair of Rag DNA DSBs by maintaining the unrepaired ends in a stable post-cleavage complex possibly through the phosphorylation of components of the MRN complex. Secondly, in G1-phase lymphocytes, the ATM-dependent phosphorylation of

histone H2AX inhibits the robust CtIP-dependent opening and resection of hairpin-sealed coding ends thereby preventing their aberrant resolution by alternative repair pathways. Finally, in response to Rag DSBs, through the activation of NFκB and other transcription factors, ATM activates a broad genetic program that transcends the canonical DNA damage response and includes genes whose known functions are integral to lymphocyte development. While this work has significantly increased our understanding of the cellular response to Rag DNA DSBs, given the diversity of the other known substrates of ATM, it seems likely that we have only begun to unravel the complexities of the ATM-deficient phenotype.

Acknowledgements

This work was supported through funding provided by various NIH grants awarded to Dr. Barry P. Sleckman as well as through the MSTP training grant awarded to Washington University in St. Louis.

Special thanks to Dr. Barry P. Sleckman and all members of the Sleckman lab past and present for an enlightening and enjoyable four-years and to the faculty and staff of the Medical Scientist Training Program at Washington University in St. Louis.

Table of Contents

List of Tables and Figures

Chapter 1

Background

The immune system has two component arms, the innate and the adaptive immune systems. The innate immune system is able to rapidly and broadly defend against large numbers of potential pathogens based on commonalities amongst them. Conversely, the adaptive immune system, while slow to activate, can recognize and defend against any given pathogen in a specific manner based on that pathogen's unique molecular characteristics. Importantly, the adaptive immune system has memory that enables a more rapid and forceful response on subsequent encounters. The adaptive immune system relies on B and T lymphocytes each of which contains a unique receptor (B- and T-cell receptors or BCRs and TCRs, respectively) that enable the cell to recognize individual foreign antigens either alone (BCR) or in complex with MHC molecules on antigen presenting cells (TCR)(1).

The BCR is composed of two identical paired immunoglobulin heavy chain (IgH) molecules and two identical paired immunoglobulin light chain (IgL) molecules of either the lambda or kappa variety (IgLλ or IgLκ, respectively). The component chains each contain a unique variable region that confers the specificity of binding and a constant region that provides structure and enables for a cellular signaling cascade in response to antigen binding. These four molecules are covalently linked by multiple disulfide bonds and are arranged such that the variable regions of the light and heavy chains are terminally located and together comprise the variable region that binds antigen. Similarly, the TCR consists of molecules with both variable and constant regions. A TCR consists of a single TCR alpha chain (TCRα) and TCR beta chain (TCRβ) for $\alpha\beta$ T cells or a single TCR gamma chain (TCRγ) and TCR delta chain (TCRδ) for TCR$\gamma\delta$ cells. The terminus of the assembled TCR also consists of a variable region that binds antigen in complex with the MHC molecules(1).

The genes encoding the individual components of the BCR and TCR are unique in that they do not exist in a functional state in the germline configuration. Rather, the genetic loci encoding these receptor components consist of hundreds of different gene segments (grouped as V, D and J gene segments) that are joined together somatically to form the functional antigen receptor gene during a process known as V(D)J recombination(1-3). The formation of a

functional gene requires a single gene segment from each of these component groups to be joined together (V and J gene segments for IgL and TCRα and TCRγ, and V, D, and J gene segments for IgH, TCRδ and TCRβ) and attached to a constant region gene segment(1).

The combination of different component chains and different gene segments for each component chain results in the diversity of the resultant BCRs or TCRs that is known as combinatorial diversity. This combined with unique aspects of the V(D)J recombination reaction discussed below (generating junctional diversity) generates heterogeneity within the cohort of antigen receptors that would be unattainable by any other means. It is this diversity that enables the adaptive immune system to recognize a near unlimited number of possible antigens(1). The development of this powerful arm of the immune system via V(D)J recombination, though, is not without risk, as this recombination event requires the generation and repair of DNA double-strand breaks (DSBs) generated by the lymphocyte-specific recombination activating gene (RAG) endonuclease. Any form of DNA damage including chemical modifications of nucleotide bases, base-pair mismatches, single-stranded DNA nicks or DSBs is inherently dangerous as it poses a threat to genomic integrity. The DNA DSB, however, is the most hazardous(4, 5). As such, DNA DSBs trigger within the cell a collection of pathways known as the DNA damage response that serves to limit the repercussions of these DNA lesions(6).

The focus of this body of work lies in further characterizing the response to and repair of the RAG-induced DNA DSB generated in developing lymphocytes undergoing V(D)J recombination in an attempt to generate a functional antigen receptor gene. We begin with a brief discussion of the RAG endonuclease and the generation of RAG-mediated DNA DSBs (RAG DNA DSBs).

The RAG Endonuclease

The RAG endonuclease consists of two protein components, RAG-1 and RAG-2, that are expressed exclusively in developing lymphocytes; these components can exist singly or as a heterodimeric pair that can form in the absence of DNA(2, 7, 8). RAG endonuclease activity requires both RAG-1 and RAG-2(2, 7, 8). As RAG-2 is rapidly degraded upon entry into S-phase

secondary to its phosphorylation at T490 by a cell cycle dependent kinase, RAG endonuclease activity is limited to the G1-phase of the cell cycle(9-11). The RAG complex, *in vitro*, also consists of the HMG (high mobility group) proteins that bind DNA non-specifically and, in doing so, alter the three-dimensional structure of the double-stranded helix bending the DNA strands (12, 13). The contribution of the HMG proteins to V(D)J recombination *in vivo* is not known(14).

The RAG-1 and RAG-2 proteins consist of core regions that are necessary and sufficient for V(D)J recombination and non-core regions(15, 16). The C-terminal core region of RAG-1 contains DNA binding domains (nonamer-binding domain and heptamer-binding domain), Rag-2 binding sites, a zinc finger domain that may facilitate RAG-2 binding, as well as the DDE motif that is shared amongst the transposases from which it is evolutionarily derived and affords RAG-1 its enzymatic activity(17-19). The N-terminal non-core region of RAG-1 contains a RING domain that may have ubiquitylation activity (of histone H3) as well as the second of two zinc finger domains(17, 19). In contrast to RAG-1, the N-terminus of RAG-2 constitutes its core region and consists of multiple repeats of a domain that promotes protein-protein binding. Additionally, RAG-2 contains a C-terminal acidic region that enhances interaction with histone proteins and a PHD domain that binds methylated histone H3 (specifically H3K4me3)(20-22). RAG-2 has no enzymatic activity. However, various mutations in RAG-2 affect the catalytic activity of RAG-1 *in vitro* suggesting that it may somehow facilitate RAG-1 enzymatic activity, perhaps by contributing to the active site of the RAG holocomplex(17, 19, 23). Interestingly, the non-core regions of both RAG-1 and RAG-2 are highly conserved. Specific functions for these regions are not known this time; however, many speculate that these non-core regions may have critical activities in the regulation or enhancement of RAG endonuclease activity or the joining of the resultant DNA DSBs(17, 19).

RAG DNA DSB Generation

The enzymatic activity of RAG-1 activates hydroxyl groups (-OH) to target the phosphodiester bond of the sugar-phosphate back of a DNA strand. The active site of RAG-1 consists of three negatively charged acidic residues (the DDE motif) that can bind divalent cations

(Mg^{2+} *in vivo* and Mn^{2+} *in vitro*) that are critical for the activation of the hydroxyl groups as nucleophiles(24-26). When the activated –OH group is from a water molecule, the result is a single-stranded DNA nick. When the activated –OH group, however, is the free 3' OH at the site of a single-stranded DNA nick, the result is intra-molecular trans-esterification reaction that results in the formation of a DNA double-strand break with one hairpin-sealed end and a second blunt phosphorylated end(27-30).

Each of the gene segments comprising the antigen receptor loci is flanked by specific sequences of DNA recognized by the RAG endonuclease. These are termed recombination signal sequences or RSSs and consist of a highly conserved heptamer (5'-CACAGTG-3') and nonamer (5'-ACAAAAACC-3') separated by a more variable 12- or 23-base-pair spacer sequence. The RSS is oriented such that the heptamer abuts the coding region of the gene segment(1).

Rag-1 and Rag-2 may both have DNA binding abilities(31, 32). However, Rag-2 binds DNA with very low affinity and in a non-specific manner(31, 32). In contrast, RAG-1 specifically recognizes the RSS, initially binding the nonamer via its nonamer-binding domain and later making contact with the heptamer(33-35). RAG-2 may facilitate interaction of RAG-1 with the heptamer sequence(31, 32). It is thought that the bending action of the HMG proteins on DNA may also be required to allow for the joining of the more distantly separated heptamer and nonamer of a 23-bp RSS. In agreement with this notion, the HMG proteins do not enhance RAG cleavage at the 12-bp RSS as significantly as they do at the 23-bp RSS *in vitro*(12). Again, however, no role for the HMG proteins *in vivo* during V(D)J recombination has been demonstrated.

Overall, RAG binds 12- or 23-bp RSSs with near equal affinity(36-38). When RAG binds a single RSS (forming what is known as a signal complex or SC), single-stranded DNA nicks can occur. The nick is made precisely at the junction of the heptamer and the coding region(39). RAG, however, does not make DNA DSBs in the setting of a SC *in vivo*(36-38). DNA DSB generation occurs only when two gene segments with RSSs of different spacer lengths

individually bound to RAG are brought together in a pre-cleavage complex known as a paired complex or PC(36-38). This requirement is known as the 12/23 rule and is important to allow for efficient joining of the resultant broken DNA ends and to ensure that the antigen receptor gene contains the right type and number of V, D, and J gene segments. For example, a D gene segment flanked by 23-bp RSSs will recombine only with upstream V gene segments with 12-bp RSSs and downstream J gene segments with 12-bp RSSs. Two V, two D, or two J gene segments will not recombine nor will a V gene segment recombine with a J gene segment when a D gene segment is required. It is important to note that not all gene segment pairs consisting of 12- and 23-base pair spacers can recombine. An additional level of regulation must exist to govern the joining of different gene segments. This is known as the Beyond 12/23 rule; however the mechanism by which this additional level of regulation occurs is not known(40, 41).

Although RAG can bind and nick 12- or 23-bp RSSs with near equal efficiency, only rarely are 23-BP RSS-containing gene segments found with single-stranded nicks(36-38). Additionally, 12-bp RSS-containing SCs have a preference for binding 23-bp RSS-containing SCs over other 12-bp RSS-containing SCCs(42). 23-bp RSS-containing SCs do not exhibit such specificity. Based on these observations, researchers have proposed a stepwise model for RAG cleavage that may explain the existence of the 12/23 rule(42, 43). In this model, a 12-bp RSS-containing SC with a single-stranded nick subsequently captures a 23-bp RSS forming a paired complex (PC)(7, 28, 38, 42). Then and only then does it introduce a single-stranded nick at the analogous location on the 23-bp RSS(38). The -OH groups of the resulting nicks are activated by RAG-1 active site to undergo intra-molecular trans-esterification reactions resulting in two hairpin-sealed DNA ends bordering the two coding regions of the gene segments to be recombined (coding ends or CEs) and two blunt phosphorylated ends at the ends containing the RSS (signal ends or SEs)(28, 43, 44).

The two hairpin-sealed coding ends must be joined together to form a coding joint (CJ) in subsequent steps to complete V(D)J recombination. The signal ends are likewise joined to from

signal joints (SJs). The processing of these DNA ends and the joining step are described in detail in subsequent sections.

Regulation of RAG DNA DSB Generation

Importantly, DNA exists in the context of chromatin that that does not generally allow for RAG binding or DSB generation. Indeed, in experiments carried out in fibroblasts, the RAG endonuclease will cleave plasmid substrates existing as naked DNA but will not cleave at the endogenous antigen receptor locus or elsewhere in the genome(19, 45). Thus, V(D)J recombination must be preceded by alterations in the chromatin environment that enable RAG binding and subsequent DNA DSB generation(19, 46). These alterations are thought to be direct or indirect consequences of the germline transcription of the antigen receptor loci that occurs coincident with the initiation of V(D)J recombination(19, 45, 46). For one, it is thought that transcription factor binding and the activity of transcriptional promoters and enhancers that drive germ-line transcription may directly influence RAG binding(19, 46, 47). For example, Pax5 binding to consensus sites in the distal V gene segments of the IgH locus has been proposed to facilitate binding of RAG to D gene segments(48-50). Additionally, the types and extent of histone modifications in the surrounding chromatin distinguish transcriptionally active loci differ from transcriptionally inactive loci. Histone acetylation and H3K4 methylation, for example, are increased in areas of the genome actively undergoing V(D)J recombination. These post-translational modifications of histone proteins might result in the alteration of chromatin structure that would reveal the RSS allowing for RAG binding. The aforementioned PHD domain of Rag-2 specifically recognizes H3K4me3 and may target RAG to transcriptionally active loci and may boost the catalytic activity of RAG(20-22). Furthermore, chromatin remodeling complexes like the Swi-Snf remodeling complex may shift nucleosomes so as to reveal the RSS; an RSS situated on a nucleosome is resistant to RAG-mediated cleavage(51, 52). The recruitment of RNA Pol II by these chromatin remodeling complexes and transcriptional elongation are likewise important(46, 53). All of these activities that promote transcription would also affect the accessibility of a given antigen receptor locus to the activity of the RAG endonuclease.

Additionally, the antigen receptor loci condense and de-condense in a manner that correlates with their recombination. A condensed locus allows for joining between gene segments separated by great distances(49, 54-57). Finally, just as gene silencing can occur near the nuclear membrane, actively recombining antigen receptor loci may need to move away from these circumferential "silencing" environments(19, 41, 46, 57, 58). All these changes occur in a highly regulated manner that enables tight regulation of the generation of RAG DNA DSBs(47). The regulation of RAG activity and V(D)J recombination at each of these levels ensures that as few as possible DNA DSBs are present in the cell at any given time.

These levels of regulation, in addition to preventing unnecessary and potentially dangerous RAG DNA DSBs, may allow for the multidimensional regulation of antigen receptor genetic recombination(19, 59). Specifically, V(D)J recombination occurs in a cell-type- and developmental-stage-specific fashion(1). The genetic loci encoding the BCR rearrange only in B cells. Similarly, the TCR loci rearrange only in T cells. Additionally, pro-B cells rearrange the IgH heavy chain. It is not until the developing B cell produces a functional IgH heavy chain, progresses to the pre-B cell stage and undergoes proliferation that it begins to rearrange the light chain (IgLκ or IgLλ) components of the BCR. Again, the same is true for the TCR. The rearrangement of each locus is ordered with DJ rearrangement occurring before V to DJ rearrangement. This is termed intra-allelic exclusion(1). Finally, V(D)J recombination occurs at a single allele prior to rearrangement of the second allele of a given antigen receptor locus. This additional level of regulation is thought to ensure that each lymphocyte expresses a single antigen receptor with a single antigen specificity and is termed inter-allelic exclusion(1).

Aberrant RAG DNA DSB Generation

Despite these numerous critical safeguards, aberrant RAG break generation can and does occur within developing lymphocytes. For instance, the RAG proteins can recognize DNA sequences elsewhere in the genome that resemble RSSs and cleave at these sites(60). Additionally, RAG can cleave at certain three-dimensional DNA structures, specifically at the junction of B and non-B DNA structures(60, 61). Furthermore, the core RAG proteins retain some

of the activity of the transposases from which they have evolved *in vitro* under specific conditions; however, RAG-mediated transposition is not observed to any great extent *in vivo*(62).

Defects in RAG DNA DSB Generation

As the expression of an assembled antigen receptor gene is absolutely required for lymphocyte development to proceed, defects in V(D)J recombination would be expected to lead to decreased numbers of lymphocytes. Proliferation of this smaller cohort of lymphocytes would also lead to a decreased diversity of the adaptive immune system. Thus, one would expect these defects to result in both lymphopenia and immunodeficiency. Such is the case. In fact, the inability to initiate V(D)J recombination as occurs in the absence of a functional RAG endonuclease leads to a complete absence of B and T cells known as severe combined immunodeficiency or SCID(63-65). Deficiencies in RAG activity can lead to a less severe phenotype known as Omenn Syndrome(65-68).

The DNA DSB Response

The generation of DNA DSBs in such a programmed fashion within a cell is unique and is limited to V(D)J recombination and immunoglobulin class switch recombination (CSR) in the developing lymphocyte and to crossover in meiosis in all dividing cells. Most often, we think of the DNA DSBs that occur in response to ionizing radiation, chemotherapeutic agents, and reactive oxygen species. In contrast to physiologic DNA DSBs, these genotoxic DNA double-strand breaks can only prove deleterious to the cells. Indeed, their aberrant resolution can lead to chromosomal deletions, inversions, or translocations. Such aberrant joints can, in some cases, lead to malignant transformation through, for example, the deletion of a tumor suppressor gene, the dysregulation of the expression of an oncogene via the proximity to a strong promoter sequence, or the creation of a fusion protein that has unique and harmful activities. Indeed, defects in the various forms of DNA repair including DNA DSB repair are implicated in some human cancer syndromes(69).

Cells are primed to rapidly activate a multifunctional signaling pathway in response to DNA DSBs that is commonly referred to as the DNA damage response(69). The initiation of this

response requires sensors, transducers, and effectors(6). The major sensor of DNA damage is G1-phase cells is the MRN complex consisting of Mre11, Rad50, and Nbs1(70). The primary transducer is the ATM (ataxia-telangiectasia mutated) kinase that may phosphorylate over 700 substrates in response to genotoxic DNA damage(71, 72). Given their implication in cancer etiology and cancer treatment, the pathways activated in the cellular response to genotoxic DSBs have been extensively characterized(69). This response encompasses pathways that promote DNA DSB repair, initiate cell cycle checkpoints and cell death pathways. However, given the sheer number and variety of ATM substrates, the depth and breadth of the DNA damage response is likely far greater than we appreciate at this point(6, 69, 73, 74).

Only recently has attention turned to the characterization of the cellular response to physiologic DNA DSBs such as the RAG DNA DSB. The DNA damage response activated in developing lymphocytes in response to RAG-mediated DNA DSBs and that activated in all cells in response to genotoxic breaks exhibit significant similarities and differences that are addressed below and have important implications for both lymphocyte development and function.

MRN as DNA Damage Sensor

The sensor component of the DNA damage response must have two critical capabilities. First, it must be able to immediately recognize the presence of DNA damage and to localize to that site. Secondly, it must be able to efficiently recruit and assist in the activation of the transducer components of the damage response. These roles are fulfilled by a single complex consisting of three proteins, Mre11, Rad50 and Nbs1. Importantly, the independent factors that constitute the MRN complex function only in the context of this holocomplex(75, 76). The properties of these individual components as well as the unique three-dimensional structure of the resulting protein complex afford MRN the ability to translocate to a DNA break site rapidly during all phases of the cell cycle and to recruit ATM(77).

The DNA binding ability of the MRN complex is mediated by Mre11 and Rad50 which form a heterotetramer (M2R2)(78-80). The C-terminal domain of Mre11 contains a DNA binding domain and also enables association with Rad50(81). The N-terminus of Mre11 contains a

phosphoesterase domain(81). Rad50 consists of N- and C-terminal ATP-binding cassette (ABC)–ATPase domains (Walker A and B motifs), while the mid-section consists of two coiled-coil motifs oriented in an anti-parallel fashion and separated by a conserved CxxC motif. The Walker A and B motifs come together and the coiled-coil motifs intertwine forming a three-dimensional structure that has a globular end with an extended arm containing a CxxC motif at the tip of that extension. The CxxC motifs of individual Rad50 molecules can interact through the coordination of a zinc ion(79, 82-86). When bound to ATP, the globular ends of Rad50 containing the Walker A and B motifs can dimerize and bind DNA(82, 87).

The N-terminus of Nbs contains an FHA-BRCT-BRCT domain. The C-terminus enables binding to both Mre11 and ATM(88, 89). Thus, Nbs1 is the link between DNA damage recognition and localization and transducer recruitment(77). The activation of ATM can be enhanced by the MRN complex(70, 75, 90-92).

ATM as Transducer of DNA Damage Response

ATM, DNA-PKcs (DNA-dependent protein kinase catalytic subunit), and ATR (ATM- and Rad3-related) comprise a family of serine/threonine protein kinases that structurally resemble kinases that phosphorylate inositol phospholipids and are therefore termed phosphoinositide3-kinase like kinases (PIKKs). These PIKKs preferentially phosphorylate serine or threonine residues followed by glutamate (SQ or TQ motifs) (93, 94). ATR is primarily activated by ssDNA during the S-G2-M phases of the cell cycle. In contrast, DNA-PKcs and ATM are activated by DNA DSBs during all phases of the cell cycle but predominantly during the G1 phase(69, 71, 73). As RAG DNA DSBs are initiated in the G1 phase of the cell cycle, here we focus on ATM and DNA-PKcs activity and not ATR activity. While these kinases have unique substrates, they also have overlapping cohorts of substrates and some overlapping functions(95-98).

ATM and other PIKK family members are large proteins; ATM is comprised of over 3000 amino acid residues. The catalytic region shared by PIKK family members is located in the far C-terminal portion of the protein. The functions of the various non-catalytic portions of the protein remain ill-defined but are required to promote the stability of this protein(99). The non-catalytic

portions of ATM include multiple nuclear localization signals, a leucine zipper, a HEAT repeat (domain shared by Huntington (H), elongation factor 3 (E), ATM (A), and TRRAP (T) proteins), and FAT and FATC (domain shared by FRAP (F), ATM (A), and TRRAP (T) proteins) domains(73, 99).

ATM is recruited to DNA DSBs through the binding of protein components like MRN located at the break site(70, 75, 90-92). ATM, however, does possess some intrinsic DNA binding capabilities(100). At the site of a DNA DSB, ATM undergoes auto-phosphorylation which promotes a conversion from its inactive multimeric state to its active monomeric state(101). ATM can be activated even when this auto-phosphorylation site (serine 1981) has been mutated however; thus auto-phosphorylation is not absolutely required for its activation(102).

Interaction with the MRN complex bound to broken DNA ends enhances ATM activity(70, 75, 90-92). Moreover, simply targeting ATM to DNA even in the absence of a DNA DSB can lead to its activation and the phosphorylation of downstream substrates(101, 103). These two findings underscore the importance of localization and concentration of ATM at a break site in the activation of downstream pathways. However, this requirement for localization of ATM at the site of a DNA DSB for activation is debated as ATM activation can be achieved in the absence of a functional MRN complex where localization of ATM is impaired(76, 104).

ATM activates hundreds of different proteins in response to DNA damage; these proteins function in numerous diverse cellular pathways. Functional categorization of these 700 different potential substrates results in the identification of pathways that vary from DNA DSB repair to the initiation of cell cycle checkpoints and apoptotic pathways to cellular migration and metabolism(71, 72).

Sensor and Transducer in the Response to RAG DNA DSBs

NBS localizes to sites of RAG DNA DSBs (105). Moreover, RAG DNA DSBs, similar to genotoxic DNA DSBs, activate ATM (106-110). Thus, during V(D)J recombination in developing lymphocytes, ATM is likely the predominant regulator of the DNA damage response.

Phenotype of an Impaired DNA Damage Response

ATM is the kinase mutated in ataxia telangiectasia, a human disease characterized by cerebellar degeneration leading to ataxia and the development of both ocular and cutaneous telangiectasias. In addition to these more visible characteristics, ATM patients exhibit retarded growth patterns and gonadal atrophy and undergo premature aging. Furthermore, they have high rates of malignancies, especially lymphoid malignancies and breast cancer. Cells isolated from these patients exhibit sensitivity to ionizing radiation and have large numbers of chromosomal aberrations indicating genomic instability(111-116). Similarly, patients with deficiencies in components of the MRN complex have also been described. Hypomorphic mutations in Mre11 cause ATLD (ataxia telangiectasia like disease), deficiencies in Nbs cause Nijmegen break syndrome and mutations in Rad50 cause Nijmejen-break-syndrome-like-disorder (NBSLD). Like A-T patients, these patients exhibit sensitivity to ionizing radiation and a propensity towards tumor development (6, 117-122). Phenotypes shared by these patients underscore the importance of the DNA damage response and the roles of MRN and ATM as primary sensors and transducers of this response.

Component Pathways of the ATM-dependent DNA Damage Response

Discussed in more detail below are three important pathways activated by ATM as components of the DNA damage response during the G1 phase of the cell cycle. First and foremost, these pathways support the repair of the DNA DSB. Secondly, they allow for the formation of a DNA repair focus. Finally, ATM activates cell cycle checkpoint and initiates transcriptional pathways that ultimately determine cell survival versus death.

DNA Repair Pathways

As the persistence or aberrant repair of DNA DSBs can lead to potentially oncogenic chromosomal lesions, it is critical that DNA lesions be repaired with both accuracy and efficiency. As such, numerous conserved cellular DNA repair pathways exist with each specifically tailored for a particular type of DNA damage. DNA DSB repair pathways have historically been dichotomized into pathways that rely on homologous sequences to template repair (homologous

mediated repair or HR) and pathways that simply join two broken DNA ends (non-homologous end joining or NHEJ)(123). However, recent work has revealed a number of pathways that bridge that divide, requiring short tracts of homology to join the two ends. Below we discuss these distinct DNA repair pathways.

Homology-Mediated Repair

Homologous recombination (HR) occurs primarily during post-replicative (S-G2-M) phases of the cell cycle when the replicated sister chromatid or paired homologous chromosome is readily available to serve as a template for repair and/or recombination respectively (124-126). HR begins with the 5' to 3' resection of the DNA end generating a long 3' ssDNA overhang on the opposing strand that is bound by ssDNA binding proteins, replication protein A (RPA), and subsequently Rad51(125, 127, 128). This end resection is initiated by Mre11, which possesses both endonucleolytic and exonucleolytic activities (3' to 5') and CtIP, a homologue of yeast endonuclease Sae2(76, 129-136). Further resection is carried out by other nucleases and/or helicases including Exo1, Dna2, and the RecQ family members(137). The resulting ssDNA overhang base-pairs with the homologous sequence on the sister chromatid or homologous chromosome known as the template strand, and, in doing so, disrupts that native DNA strand (138). This results in the formation of a branched DNA structure known as a Holliday junction that is subsequently resolved into the two original, distinct DNA fragments(139).

Variants of HR exist including break-induced repair (BIR) which is primarily used to repair DNA lesions that can occur at a stalled replication fork during the process of DNA replication and similarly requires long tracts of homology. A second variant of HR is single-stranded annealing (SSA). For SSA to occur, both broken DNA ends of a single break are resected to form ssDNA overhangs. These overhangs do not invade homologous sequences *in trans*, that is on the sister chromatid or homologous chromosome. Rather, the resection reveals long tracts of homology *in cis* that allow for intra-chromosomal joining. Notably, this results in the deletion of the intervening sequence potentially leading to large chromosomal deletions depending on the amount of resection that took place(139).

Non-homologous End Joining

During repair by NHEJ, the two broken DNA ends from a single DNA DSB are simply re-joined. Thus, unlike HR, NHEJ does not rely on long tracts of homology to mediate joining. The ligation of the two ends must occur efficiently so as to limit processing of those DNA ends prior to their joining as such processing would result in the alteration or loss of genetic information(140). If multiple DNA DSBs occur simultaneously within the cell, these broken ends could theoretically be ligated together by NHEJ, forming chromosomal translocations. The efficiency of NHEJ, effectively limiting the time and space that these broken ends occupy, is inversely related to the rate of formation of translocations(140).

NHEJ requires a cohort of factors: the DNA-PK (DNA-dependent protein kinase) holoenzyme complex consisting of Ku70, Ku80, and DNA-PKcs and the DNA ligase complex including XRCC4, XLF, and DNA Ligase IV(140). Artemis is another factor that is occasionally required for NHEJ(140). Ku70 and Ku80 have no known enzymatic activity(140). Rather, they possess sequence-independent affinity for broken DNA ends, preferentially binding those that are blunt or those with minimal overhangs but also binding single-stranded nicks and hairpin-sealed DNA ends(140-142). The three-dimensional structure of the Ku heterodimer reveals a ring-like structure with a central cavitary pore well-suited for the binding of a DNA double-stranded helix(141). Ku binding to the broken DNA end results in the recruitment of the final subunit of the DNA-PK holocomplex, the catalytic subunit of DNA-PK (DNA-PKcs)(140, 143). Binding of DNA-PKcs to the C-terminus of Ku80 causes the inward translocation of the Ku heterodimer onto the broken DNA strand and allows DNA-PKcs to also bind the broken DNA end and undergo the unique DNA-dependent activation of its kinase activity(42). Interestingly, the region of Ku80 that binds DNA-PKcs is homologous to the region of Nbs that mediates binding of fellow PIKK family member ATM(4). Among the key targets of DNA-PKcs kinase activity are DNA-PKcs itself and Artemis(42, 144). The phenotype resulting from DNA-PKcs deficiency and kinase inactivity are different, suggesting that DNA-PKcs may also have structural roles in NHEJ(145). DNA-PKcs can bridge broken DNA ends together through kinase-independent DNA binding; this may be

done in combination with the Ku proteins which also have DNA binding activity and bind DNA ends in such a way as to facilitate their alignment(146-149). While this binding by the DNA-PK complex may initially facilitate the joining of two DNA ends, it may be subsequently inhibitory to joining. Evidence suggests that the active removal of DNA-PKcs from the broken DNA end perhaps mediated by an auto-phosphorylation event is required for joining to take place(144, 145). This finding has interesting implications for DNA repair. Specifically, as auto-phosphorylation is thought to occur *in trans*, this requirement may function to ensure that a broken DNA end has another broken DNA end similarly bound to DNA-PKcs that is readily available to ligate to. Furthermore, the DNA-PK holoenzyme complex may protect DNA ends from any processing or chemical modification up until the ligation event occurs.

That ligation event is catalyzed by DNA Ligase IV, one of three known mammalian DNA ligases(140, 150, 151). The DNA-PK holoenzyme complex recruits the ligase complex containing DNA Ligase IV, XRCC4 and XLF (XRCC4 like factor)(150-152). XRCC4, like the DNA-PK holoenzyme complex components, may play some ill-defined role in aligning broken DNA ends. XRCC4, however, is also required to maintain Ligase IV levels within the cell; deficiency in XRCC4 is effectively a deficiency in Ligase IV(150, 151). On the other hand, while XLF is structurally similar to XRCC4, XLF is not shown to have DNA binding abilities and its levels do not affect Ligase IV levels(153, 154). Both XRCC4 and XLF can promote the activity of Ligase IV(152). XRCC4 promotes the enzymatic activity of Ligase IV by facilitating the adenylation of its key catalytic residues(150, 151). XLF, on the other hand, facilitates the joining of DNA ends with small ssDNA overhangs that are not otherwise immediately amenable to ligation by Ligase IV(155-157). A final NHEJ factor, Artemis, has exonuclease activity but acquires endonuclease activity upon its phosphorylation by DNA-PKcs(158, 159). Artemis activity is not required for the repair of all DNA DSBs; in fact, in the setting of ionizing radiation, all but ~10% of breaks are repaired efficiently in the absence of Artemis. The remaining 10% of breaks are thought to have undergone chemical modifications that require Artemis-mediated processing prior to their joining(160-162).

Alternative End Joining

The black and white view of DNA repair by either HR or NHEJ is being replaced by the notion that multiple additional pathways exist which have characteristics in common with both HR and NHEJ(163). This is evidenced by the fact that most IR-induced breaks in NHEJ-deficient cells do eventually join in a manner that is not dependent on HR factors (140, 164-166). AEJ is currently defined as joining that takes place in the absence of core NHEJ factors. DNA ends undergo significant amounts of resection prior to joining. Thus, the joints that form exhibit large deletions(163). Secondly, AEJ is likely mediated by small regions of homology revealed by the end resection as the joints form at sequences shared by the two DNA ends(163). In this regard, AEJ is similar to SSA. The protein components required for and the mechanism of these potentially multiple AEJ pathways are unknown at this time. As this joining occurs, by definition, in the absence of Ligase IV, one of the other two mammalian DNA ligases, Ligase I or Ligase III must function in AEJ(163, 167, 168). Other proteins implicated in this pathway include Mre11 and CtIP which are suggested to initiate the end resection that would reveal potential microhomologies as they do in homology mediated repair(80, 163, 169-171).

AEJ has been implicated in the formation of translocations. AEJ pathways are normally suppressed by classical NHEJ. In the absence of classical NHEJ factors, both the frequencies of AEJ and translocations increase(163, 171, 172). The sequences of translocations found in NHEJ deficient cells do not differ significantly from those that form in NHEJ-proficient (wild-type or WT) cells suggesting that even in WT cells, AEJ may be the primary mode of DNA repair that allows for translocations(172).

DNA Repair Pathway Choice

DNA repair pathway choice is largely determined by the stage of the cell cycle the cell occupies when that break occurs(139, 173). HR is the predominant repair pathways during the S-G2- and M phases of the cell cycle where a sister chromatid or paired homologous chromosome is readily available. NHEJ, on the other hand, occurs primarily during the G1-phase of the cell cycle but can function at all stages of the cell cycle. All required DNA repair factors for

both HR and NHEJ are present throughout the cell cycle. Thus, DNA repair pathway choice relies on both cell cycle-dependent and cell cycle-independent factors(139, 173). Accessing the inappropriate repair pathway would have negative consequences. For example, attempting HR during G1 in the absence of a sister chromatid or paired homologous chromosome could lead to loss of heterozygosity if a mutant homologous chromosome is used as a substrate or chromosomal deletions, inversions, or translocations if an unrelated but similar sequence is utilized for repair(139, 173).

DNA repair pathway choice likely occurs early on during the repair process, perhaps depending on the proteins that initially recognize and bind the broken DNA end and the initial processing of that end (139, 143). Ku deficiency rescues the embryonic lethality of Ligase IV deficiency, providing evidence for Ku binding as a key determinant of repair pathway choice(174). The absence of Ku in cells where NHEJ is crippled (Ligase IV-deficient cells) might allow broken DNA ends to access alternative repair pathways and enable the cell to escape the activation of apoptotic pathways(174). Indeed, levels of homology-mediated repair are substantially increased in Ku70-deficient cells(175). Secondly, end resection is thought to promote homology-mediated repair and simultaneously prevent NHEJ, as DNA ends with significant overhangs do not bind Ku efficiently(140-142, 176). End resection can be regulated in a cell cycle-dependent fashion, as Sae2 (CtIP homologue) activity is enhanced upon phosphorylation of Ser267 (corresponding to T847 in CtIP) by the cyclin dependent kinase Cdc28 (CDK1)(130, 176-178). The Sae2 mutant S267E exhibits end resection inappropriately during all stages of the cell cycle including G1 disrupting NHEJ. Conversely, the Sae2 mutant S267A is defective in end resection and is more apt to repair breaks by NHEJ even in the presence of sister chromatid or a paired homologous chromosome during the S-G2-M phases of the cell cycle(176).

Repair of RAG DNA DSBs

Defects in the initiation of V(D)J recombination can lead to SCID as discussed above, but what occurs to developing lymphocytes when RAG-mediated DNA DSBs breaks are mishandled? Interestingly, subsets of patients with SCID have been identified that, in addition to profound

lymphopenia and immunodeficiency, also have a sensitivity to ionizing radiation and exhibit genomic instability and a propensity towards tumor development, specifically lymphoid tumors. This phenotype is known as radiosensitive SCID or RS SCID(65, 179). These additional features indicate a defect in DNA repair pathways and suggest that defects in the repair of RAG DNA DSBs might contribute not only to lymphopenia and a resulting immunodeficiency but also to lymphoid tumor formation.

Analysis of V(D)J recombination in lymphocytes derived from RS SCID patients and in mouse models of these diseases have led to many important discoveries regarding the pathways by which RAG DNA DSBs are repaired. In this regard, humans with RS SCID have been identified with mutations in Ligase IV, Artemis, DNA-PKcs, and Cernunnos(65, 150). All are components of the NHEJ pathway of DNA DSB repair. Moreover, mouse models with deficiencies in any of the core components of the NHEJ DNA repair pathway (collectively referred to here as NHEJ-deficient mice) exhibit a similar phenotype. Notably, deletion of some NHEJ factors in mice leads to exhibit embryonic lethality; in these cases, conditional knockout mice have been shown to have defects in V(D)J recombination(150). While RAG proteins are expressed exclusively in lymphocytes and RAG-mediated DNA DSBs occur only in developing lymphocytes, the repair of these breaks occurs via general DNA repair mechanisms, specifically non-homologous end joining.

Furthermore, just as the mishandling of genotoxic DNA DSBs can result in chromosomal deletions, inversions, and translocations, the mishandling of RAG DNA DSB can lead to chromosomal lesions with oncogenic potential. Follicular lymphoma is caused by a translocation (t14:18) that results in the IgH promoter driving bcl-2 expression(179). *IgH* to *c-myc* translocations (t8:14) in Burkitt's lymphoma similarly dysregulates the expression of an oncogene leading to cellular transformation(179). Furthermore, deletion of the tumor suppressor *Mts1* in developing lymphocytes is a frequent cause of T-ALL(180).

As discussed above, RAG-mediated DNA DSBs result in the formation of two hairpin-sealed coding ends and two blunt phospohylated signal ends that must be joined together to form coding joints (CJs) and signal joints (SJs) respectively.

During V(D)J recombination, the unrepaired signal ends remain bound to RAG in a post-cleavage complex(181, 182). RAG must be actively removed from the signal ends to allow for joining(181, 182). Just as occurs during the NHEJ-mediated repair of genotoxic DNA DSBs, these broken signal ends recruit the DNA-PK complex consisting of Ku70, Ku80 and DNA-PKcs. The blunt phosphorylated signal ends can be joined directly by the XRCC4/DNA Ligase IV forming a signal joint (SJ)(150).

Coding ends, do not bind RAG with the same affinity that signal ends do; thus, other factors would be required to keep the four free DNA ends tethered to one another(181, 182). Whether and how coding ends are maintained in the post-cleavage complex is unknown. Furthermore, coding ends cannot be joined in their native state; these hairpin-sealed ends must undergo processing(150). As we discuss below, it is this processing that ultimately contributes to the incredible diversity of the resulting antigen receptors.

The processing of the hairpin-sealed coding ends is initiated by the non-core NHEJ factor Artemis. As discussed above, the association of Artemis with DNA-PKcs confers endonuclease activity to Artemis that enables it to “open up” hairpin-sealed DNA ends(158). Artemis creates a nick in the hairpin at a non-precise location causing it to open; although hairpin-opening does not occur at exactly the same nucleotide position each time, it more frequently occurs two nucleotides 3’ of the tip(158, 159, 183). In the absence of Artemis or DNA-PKcs, hairpin-sealed broken DNA ends accumulate and V(D)J recombination cannot be completed(150, 158, 161). These data suggest that, although proteins such as RAG possess endonuclease activity *in vitro*, Artemis is the primary endonuclease that opens hairpin-sealed coding ends during V(D)J recombination *in vivo*(184, 185). Importantly, Artemis is not required for SJ formation(186).

The asymmetric opening of the hairpin-sealed DNA end results in palindromic DNA sequences. The nucleotides comprising these palindromic sequences of varying length are

termed p nucleotides(150). Hairpin-opened coding ends are susceptible to the activity of nucleases presumably through those at the site of the RAG DNA DSB such as Artemis, terminal deoxynucleotidyl transferase (TdT), or RAG which has flap endonuclease activity(158, 187, 188). Finally, coding ends undergo a third form of processing. Additional nucleotides can be added to hairpin-opened coding ends in a non-templated fashion though the addition of (N) nucleotides by TdT or polymerase μ (158, 189, 190). The coding ends processed by these various modalities can subsequently be joined by the NHEJ ligase complex consisting of XRCC4 and DNA Ligase IV to form a coding joint (CJ)(150, 191). The processing of coding ends prior to ligation is unique to NHEJ during V(D)J recombination.

Some mutants of the RAG proteins are efficient in cleavage at the RSS-coding end junction *in vitro* but the resulting DNA ends do not join efficiently(192-194). Moreover, RAG-1 can bind the Ku heterodimer; thus, RAG may participate in recruiting NHEJ factors to the break site(195). These data suggest that the RAG endonuclease may also play some role in the joining step of V(D)J recombination**.** Any role for RAG in DNA end joining would be unique to V(D)J recombination and not a general component of NHEJ as RAG is expressed only in developing lymphocytes undergoing V(D)J recombination.

AEJ and RAG DNA DSB Repair

Though mice with deficiencies in core NHEJ factors are profoundly immunodeficient, they are not typically completely devoid of lymphocytes suggesting that alternative DNA repair pathways may allow for V(D)J recombination to take place at very low levels in these animals(140). Some RAG mutants (core RAG-1, core RAG-2 and RAG-2 FS361) allow for especially high rates of CJ formation in NHEJ-deficient cells(196). Interestingly, the CJs formed in these NHEJ-deficient cells exhibit significant deletions and microhomology at the site of the joint suggesting that they did indeed form via alternative end joining(196). Furthermore, cells expressing these mutant RAG proteins but with intact NHEJ pathways also utilize alternative end joining to join coding ends at low rates(164). These data suggest that alternative DNA repair pathways can function during V(D)J recombination(196-198). The RAG proteins themselves may

function to protect cells from accessing these aberrant repair pathways(196-198). Other cellular pathways may function to quell the use of alternative repair pathways. Utilization of these pathways during V(D)J recombination could lead to increased frequency of translocation events. Furthermore, the utilization of microhomologies to mediate end joining would lead to a decreased diversity in the antigen receptor repertoire(197, 198).

Deletional versus Inversional Rearrangement

The primary goal of NHEJ is to rapidly ligate the two broken DNA ends so as to preserve as much genomic information as possible. Deletions and inversions are both considered aberrant and potentially dangerous products of misguided DNA repair by NHEJ(140). While utilizing components of the NHEJ pathway, the repair of RAG-mediated DNA DSBs does not simply join two DNA DSBs together. In V(D)J recombination, rearrangement absolutely requires deletion (during rearrangement by deletion) or inversion (during rearrangement by inversion) of large regions of genomic DNA. Rearrangement by deletion or inversion occurs depending on the orientation of the RSS pair and the transcriptional orientation of the gene segments to be recombined. Gene segments that are in the same transcriptional orientation recombine by deletion wherein the intervening sequence is simply excised from the chromosome. The RSS pair remains on opposite ends of the segment that is excised from the chromosome; SJ formation leads to the formation of an episomal fragment of DNA that is subsequently lost during cellular division. Importantly, during rearrangement by deletion, joining of coding ends, but not signal ends, is required to maintain the linear integrity of the chromosome. Most rearrangements during V(D)J recombination occur by deletion. However, some antigen receptor loci, such as the IgL kappa locus, utilize inversional rearrangement with significant frequency. Gene segments that are in the opposite transcriptional orientation undergo rearrangement by inversion. Upon RAG-mediated cleavage, the segment of DNA located between the two RSSs must be inverted to allow for SJ and CJ formation. Notably, during inversional rearrangement, both coding and signal joint formation occur within the chromosomal context; as such, both are required to maintain the linear integrity of the chromosome. Two additional types of joints can occur that do not correctly pair

coding ends and signal ends and therefore do not result in functional antigen receptor genes. Importantly, these may exist as backup pathways that would function to preserve the linear integrity of the chromosome. Occasionally, the coding and signal ends simply rejoin in the original configuration forming open-and-shut joints. Additionally, hybrid joints can occur in which a signal end inappropriately joins to the other coding end. During rearrangement by deletion, hybrid joint formation would require the inversion of the intervening gene segment. During rearrangement by inversion, this would involve the inappropriate loss of the intervening gene segment(1, 150, 199).

V(D)J recombination, then, is only successful when NHEJ pathways allow for a controlled mis-repair, one that allows for deletion or inversion. The mechanism by which signal ends are joined to signal ends and coding ends to coding ends leading to these desirable deletions or inversions is not known. However, the answer to this conundrum likely lies in the components of and the structure of the post-cleavage complex. For example, RAG binding to signal ends may facilitate SJ formation and prevent open-and-shut and hybrid joint formation(181, 182).

Antigen Receptor Diversity

The unique aspects of the V(D)J recombination reaction described above generates CJs that vary in both size and sequence. This junctional diversity supplements combinatorial diversity and results in the diverse antigen receptor repertoire that is the cornerstone of adaptive immunity. As noted above, combinatorial diversity is a term used to denote the combination of different antigen receptor components for each functional antigen receptor and the different V, D, and J gene segments used to construct each receptor component. Neither combinatorial nor junctional diversity is without constraint. For example, it is clear that some gene segments are used more frequently than others. Additionally, in some cases, for example in the mouse, more than 95% of the B cells utilize the kappa light chain(200). With regards to junctional diversity, excessive deletion or addition of nucleotides to coding ends prior to joint formation would be deleterious. Some gene segments undergoing V(D)J recombination can be quite small, and large deletions could lead to the deletion of an entire gene segment and the formation of a non-functional antigen

receptor(201). Large nucleotide additions could similarly perturb the structure of the resultant antigen receptor such that it would no longer recognize antigen; this is especially true for the TCR which must recognize antigen in complex with an MHC molecule. Additionally, as discussed above, end resection may be a critical determinant of DNA repair pathway choice. Thus, excessive nuclease activity might allow RAG DNA DSBs to access homology-mediated alternative repair pathways that could potentially lead to the formation of a non-functional antigen receptor, limit the diversity or the resulting antigen receptor pool or lead to potentially oncogenic chromosomal lesions. Pathways must exist to govern the processes and protein factors that generate both combinatorial and junctional diversity(201).

A role for ATM in RAG DNA DSB Repair

Like RS-SCID patients, A-T patients exhibit characteristics suggesting deficiencies in the repair of RAG-mediated DNA DSBs in addition to the deficiencies in the repair of genotoxic DNA DSBs. First, they are lymphopenic and susceptible to infection. Secondly, they exhibit a high frequency of translocations involving the antigen receptor loci. For example, translocations involving the human TCRγ and the TCRδ locus and inversions involving the human TCRγ (Vγ) and TCRβ (Jβ) loci are found in circulating non-transformed peripheral T cells in the absence of ATM; translocations involving the TCRα locus can be found in up to 10% of circulating T cells in ATM-deficient mice(108, 113, 116, 202, 203). Additionally, A-T patients almost invariably develop lymphoid tumors, and these tumors harbor translocations involving the antigen receptor loci(111). This phenotype is recapitulated in ATM-deficient mice(204). These lymphoid tumors are likely a result of aberrant V(D)J recombination as they do not occur in mice unable to initiate recombination owing to an absence of RAG endonuclease components(114, 205). Thus, ATM-deficiency leads to decreased efficiency of RAG DNA DSB repair leading to lymphopenia and increased mis-repair leading to increased numbers of translocations and lymphoid tumor generation.

We have demonstrated a role for ATM in the repair of RAG DNA DSBs. Specifically, ATM functions to maintain coding ends within the post-cleavage complex. In its absence, we

note a decreased efficiency of RAG DNA DSB repair and an increase in the rates of aberrant repair including hybrid joint formation and translocations(107). Like DNA-PKcs, ATM may have both kinase dependent and independent functions, and this described role in RAG DNA DSB repair may directly rely on one or more of the non-catalytic regions of ATM(95-98). However, as this function requires ATM kinase activity, its role in maintaining DNA ends in the post-cleavage complex likely lies in the phosphorylation of one of its downstream substrates, possibly the MRN complex(107). We discuss this further in Chapter 3.

Formation and Function of DNA Repair Foci

In addition to ATM and MRN, many additional proteins are recruited to the site of a genotoxic DNA DSB forming what is often referred to as a DNA repair focus. The accumulation of factors at the break site occurs in a spatially and temporally regulated fashion(4). Creation of the DNA repair focus is a critical feature of the DNA damage response functioning to recruit various repair factors, to tether the broken DNA ends together allowing for efficient repair, and to potentiate signaling pathways by concentrating the component enzymes and their substrates at the break site(4).

The formation of the DNA repair focus begins with the phosphorylation of H2AX by ATM(206, 207). H2AX is a variant of the histone protein H2A and represents about 10% of the H2A in the genome(206-208). It is unknown whether H2AX is spread evenly throughout chromatin or whether it is concentrated in certain regions of the genome(208). Among the differences between H2AX and its H2A counterpart is the presence of approximately twenty additional amino acids at its C-terminus; this unique carboxy-terminal tail protrudes from the nucleosome core around which the DNA is wound(208). The serine residue four amino acids from the end of H2AX (-SQEY) comprises an SQ motif that is specifically phosphorylated by ATM (forming γ–H2AX) (206). While optimal phosphorylation relies on ATM, in its absence, DNA-PKcs can perform this function(209-211).

The phosphorylation of H2AX in the chromatin flanking the break is directly or indirectly required for the maintenance of a large percentage of the factors comprising the DNA repair

focus at the break site(208, 212). The initial re-localization of these factors to the break site can still occur in H2AX deficient cells, but in the absence of γ-H2AX, they drift from the break site more rapidly(213). A number of factors can bind phosphorylated tail of H2AX directly including Nbs1, 53BP1, and Mdc1(214-216). However, Mdc1, through its C-terminal tandem BRCT domains, does so with the highest efficiency and stability(214). How, then, are these other factors then retained in the DNA repair focus? Mdc1 recruits Rnf8 upon its phosphorylation by ATM at four TQXF sites (T699, T719, T752, and T765) (217, 218). Rnf8 is an E3 ubiquitin ligase that can catalyze the ubiquitylation of H2A and H2AX(219-221). This ubiquitylation event leads to further histone modification through the recruitment of additional ubiquitin ligases such as Rnf168 and also results in the direct recruitment of repair factors such as Rap80 and Brca1(222-224). However, these histone ubiquitylation events also alter the chromatin environment at the break site to reveal other histone marks making them available to bind factors such as 53BP1. These other histone modifications might be generated *de novo* in response to DSBs, similar to H2AX phosphorylation. Alternatively, they might exist constitutively in chromatin but be revealed only upon the chromatin rearrangement initiated by DNA damage responses(208, 225-227). Through these various pathways, then, H2AX is directly or indirectly responsible for the recruitment of a large number of factors at the break site.

Mdc1 binds γ-H2AX. However, it also binds ATM directly through its FHA-domain and indirectly by binding Nbs1 which can subsequently recruit ATM(228). Nbs1 contains an N-terminal FHA-BRCT-BRCT domain that binds the SDTD motifs of Mdc1 after the serine and threonine residues are phosphorylated by Ck2(229-231). Mdc1 physically links ATM to its substrate H2AX. This creates a feed-forward mechanism that would enable a cell to rapidly activate a large fraction of nuclear ATM and efficiently initiate ATM-dependent phosphorylation events and activate downstream pathways in the presence of a single DNA DSB(214, 217, 218, 228). As might be expected, γH2AX levels are lower in Mdc1 deficient cells(218, 228). Additionally, H2AX- and Mdc1-deficient cells are unable to efficiently activate cell cycle checkpoints in response to low dose irradiation, but both are able to do so effectively when the

number of DNA DSBs is increased using high dose irradiation(218, 228, 232). These data suggest that a critical function of the DNA repair focus is the potentiation of DNA damage response signaling pathways.

The DNA repair focus may also play a direct role in the repair of a DNA DSB. Indeed, the phenotype of H2AX-deficient mice is consistent with H2AX having a role in the actual repair of DNA DSBs. Specifically, this mouse is small in size, infertile, and exhibits genomic instability with sensitivity to ionizing radiation(208, 233-236). Mice with deficiencies in other known components of DNA repair foci likewise share these characteristics with H2AX-deficient mice. However, H2AX and these other components of DNA repair foci are not core components of any of the DNA repair pathways(140). A primary theory is that γ-H2AX and the resulting foci may function as a scaffold to hold broken DNA ends together, thereby facilitating efficient repair(237). .

DNA Repair Foci Formed at RAG DNA DSBs

Just as genotoxic DNA DSBs promote H2AX phosphorylation and repair focus formation, RAG DNA DSBs also induce H2AX phosphorylation within the chromatin at the site of a DNA DSB and at significant distances (> 200 kb) from the break site, and other components of DNA repair foci can be found at RAG DNA DSBs including 53BP1(105, 211, 238-240). Mice with deficiencies in some components of the DNA repair focus including H2AX and 53BP1 exhibit mild lymphopenia and an increased frequency of translocations involving antigen receptor genetic loci; when H2AX-deficient mice are bred onto a p53-deficient background, they exhibit lymphoid tumor formation(213, 233-235, 238, 241, 242). Additionally, RIDDLE (radiosensitivity (R), immunodeficiency (I), dysmorphic features (D), learning disabilities (L)) syndrome patients have a defect in the ubiquitin ligase Rnf168; components of this phenotype are shared with the RS-SCID phenotype(222, 223). All of these data suggest that whatever role that the DNA repair focus plays during the repair of genotoxic DNA DSBs, it likely also plays during V(D)J recombination.

Indeed, persistent unrepaired coding ends in H2AX-deficient cells do more frequently irreversibly separate and form translocations, perhaps as a result of the scaffolding function of H2AX and the DNA repair focus(233-236, 243). However, H2AX-deficient lymphocytes undergo

efficient V(D)J recombination (233, 235). Furthermore, H2AX-deficient lymphocytes do not show evidence of hybrid joint formation or the accumulation of unrepaired coding ends as we observe in the setting of ATM and MRN deficiency(243). The exact role of H2AX in the V(D)J recombination is not completely understood. In Chapter XX, we discuss an additional and novel role for H2AX in the repair of RAG DNA DSBs in preventing the resection of persistent unrepaired coding ends.

Transcriptional Pathways Activated by ATM

ATM activates a number of transcriptional pathways in response to genotoxic DNA damage. These primarily include pathways that mediate cell cycle arrest or influence cell survival including p53 and NFκB(244-247). The activation of p53 in response to DNA damage functions to halt cell cycle progression and to promote the death of cells with potentially dangerous chromosomal lesions. In support of this notion, p53-deficient mice exhibit genomic instability and develop tumors; furthermore, mutations in p53 and defects in p53-dependent pathways have been implicated in a number of human cancer syndromes(234, 248-250). On the other hand, NFκB is commonly described as a pro-survival transcription factor, as a large fraction of the genes regulated by NFκB have activities in promoting cell survival. Cells deficient in NFκB signaling pathways exhibit increased cell death in response to ionizing radiation(247). In response to many stimuli, however, NFkB promotes the expression of a large cohort of genes with diverse known activities(251-253).

The activity of p53 and its downstream pathways is tightly regulated both through the regulation of p53 protein levels within the cell and through various post-translational modifications. ATM activation of p53-dependent pathways relies on its ability to lead to the abnormal accumulation of p53 within the cell and as well as its ability to phosphorylate and activate p53(244). Mdm2 is an ubiquitin ligase that normally maintains p53 at negligible levels within the cell by mediating its degradation(254, 255). ATM phosphorylates Mdm2 in response to DNA damage and physically prevents its association with p53(244, 254, 255). ATM additionally activates p53 primarily via the direct phosphorylation of p53 at Ser15 but also indirectly through

the phosphorylation of Chk2(244, 256). Chk2 phosphorylation by ATM in response to DNA damage leads to the formation of catalytically active Chk2 dimers. Dimerized Chk2 subsequently phosphorylates p53 at a unique site, Ser20, further activating its transcriptional activity(244, 249, 256-260).

This ATM-dependent activation of p53 results in the initiation of the G1-S checkpoint. Progression from the G1-phase of the cell cycle to S-phase requires the activation of the Cdk2-cyclinE complex. This complex is activated by de-phosphorylation of Cdk2 by the phosphatase Cdc25a. Cdc25a, itself, is a target of the ATM-dependent kinase activity of Chk2, and phosphorylation of Cdc25a leads to its degradation(261). Cdc25a is therefore unable to dephosphorylate and activate Cdk2(261). The activation of p53 also affords transcriptional changes that contribute to the initiation of the G1-S checkpoint; specifically, the expression cyclin-dependent kinase inhibitor (p21) which prevents binding to Cdk-2 to cyclinE is driven by p53 transcription factor activity(94). In addition to promoting the G1-S cell cycle checkpoint, the p53 transcription factor also activates cell death pathways by promoting the transcription of pro-death factors including PUMA, Apaf1, NOXA, and Bax(262).

In response to genotoxic DNA damage, ATM simultaneously activates NFκB-dependent transcriptional activity. DNA damage induced activation of NFκB by ATM is unique as NFκB signaling is generally initiated through the binding of ligands to cell surface receptors(263, 264). The transcription factor NFκB, a dimer consisting of p50 and p65 subunits, resides in the cytoplasm as its nuclear localization signal is obscured by binding to IκBα (inhibitor of NFκB). It is only upon the phosphorylation of IκBα and its subsequent degradation that the p50/p65 heterodimer translocates to the nucleus, where it affects the transcription of a large cohort of genes(265-267). The binding of ligands such as LPS and TNF to their cell surface receptors is normally the stimulus that activates the IκBα kinase (IKK) complex (consisting of IKKα, IKKβ and the regulatory IKKγ (NEMO)) subunit through the phosphorylation of NEMO. All of these activating events occur within the cytoplasm. However, NEMO does shuttle in and out of the nucleus, and, interestingly, the balance of nuclear:cytoplasmic NEMO is shifted in response to

DNA damage by an unknown mechanism(268). In response to DNA damage, the nuclear fraction of NEMO is phosphorylated by ATM. The phosphorylated NEMO is subsequently monoubiquitinated and translocates back to the cytoplasm. There it binds IKKα/IKKβ, activates the IKK complex, and leads to the phosphorylation and degradation of IκBα and enables the translocation of the p50/p65 heterodimer to the nucleus(269). Gene products with pro-survival activities whose transcription is regulated by ATM and NFκB in response to genotoxic DNA damage include, among others, Pim2 and Bcl3(247, 270).

Activation of Transcriptional Pathways in Response to RAG DNA DSBs

Like genotoxic breaks, RAG DNA DSBs also activate transcriptional pathways in an ATM-dependent manner. ATM activates p53 in response to persistent RAG DNA DSBs(271). As a result, ATM-deficient cells are defective in activating the G1-S checkpoint, and unrepaired coding ends are detectable in ATM-deficient cells even at post-replicative stages of the cell cycle(202, 272). In fact, these unrepaired breaks remain even after the cell has undergone multiple cell divisions(202, 272). The activation of p53 by persistent RAG DNA DSBs also activates robust pro-apoptotic pathways that eliminate cells harboring these potentially dangerous DNA lesions(271). Although NHEJ-deficient mice cannot repair RAG-mediated DNA DSBs, they do not develop lymphoid tumors to any great extent(150). However, mice with deficiencies in p53 and NHEJ develop lymphoid malignancies at a young age(150, 271). These observations illustrate the oncogenic potential of RAG-mediated DNA DSBs and the necessity of ATM- and p53-dependent apoptotic pathways. In Chapter 5, we demonstrate that RAG DNA DSBs simultaneously activate NFκB transcriptional pathways. The activation of NFκB by RAG DNA DSBs and the implications of activating such a pleiotropic transcription factor in these developing cells is discussed.

Summary

Indeed, RAG DNA DSBs, similar to genotoxic DNA DSBs, activate an ATM-dependent DNA damage response. In the individual chapters that follow, we further define components of this response that occurs in developing lymphocytes undergoing V(D)J recombination.

Specifically, we discuss how ATM participates in the repair of the RAG DNA DSB (Chapter 3), how ATM regulates DNA end resection through modulation of H2AX phosphorylation and CtIP activity (Chapter 4) and, finally, how ATM significant alters gene expression patterns in developing lymphocytes undergoing V(D)J recombination (Chapter 5).

Chapter 2

Materials and Methods

Approach to Analyzing V(D)J Recombination

The difficulty of studying V(D)J recombination *in vivo* is two-fold. First, RAG DNA DSBs are made and repaired quickly in a non-synchronized fashion among the developing B cells in the bone marrow or T cells in the thymus; thus, to capture cells in bone marrow or thymus that are actively rearranging their antigen receptor loci is a daunting task. Additionally, antigen receptor loci are complex with hundreds of different V, D, and J gene segments spanning great distances within the genome. Though some segments are used preferentially, the sheer number of possible combinations that allows for the powerful adaptive immune system makes the analysis of rearrangement by methods such as Southern blotting impossible. Southern blotting of DNA isolated from lymphocytes undergoing V(D)J recombination demonstrates a distinct band representing the germline state of the un-rearranged alleles and a smear of rearrangement products of various sizes that is non-interpretable for the most part. An ideal system to analyze V(D)J recombination would allow for the synchronous induction of RAG DNA DSBs and would somehow limit the number of possible resultant recombination products. Attempts to develop these model systems are described here.

The rearrangement of plasmid substrates containing a single RSS pair (thus resulting in a single rearrangement product) can be analyzed in fibroblasts, CHO cell lines, or other non-lymphoid cells transfected with the RAG endonuclease or transformed B cells that naturally express the RAG endonuclease(273, 274). However, naked DNA (plasmid recombination substrates) does not recapitulate the natural chromatin environment that clearly plays a role in V(D)J recombination(46). Not unexpectedly, numerous proteins have effects in chromosomal repair but have no demonstrable defect in the repair of these plasmid substrates. In this regard, while multiple studies were unable to detect defects in CJ formation in *Atm*$^{-/-}$ cells by analysis of V(D)J recombination of extra-chromosomal substrates, we have clearly demonstrated a role for ATM in the repair of chromosomal RAG DNA DSBs(107, 275-277). Furthermore, assaying repair in lymphocytes rather than fibroblasts transfected with the RAG proteins is paramount as it is has

been demonstrated that the requirements for some NHEJ factors (notably XLF) for the repair of RAG DNA DSBs is different in these two cell types(278).

Significantly improved methods for studying V(D)J recombination have addressed these major weaknesses. These methods utilize B cells transformed with a temperature sensitive Abelson murine leukemia virus(279). This virus preferentially targets pre-B cells that are primed to undergo rearrangement of the endogenous IgL loci. However, once infected with the temperature sensitive Abelson virus (abl pre-B cells), these cells rapidly cycle and do not express the RAG proteins or undergo V(D)J recombination(279). Culturing them at non-permissive temperatures however, turns off abl kinase activity, arrests the cells in G1 where they begin to express the RAG proteins and undergo V(D)J recombination at the endogenous IgL kappa and lambda loci(279). The system utilized in the studies detailed in subsequent chapters is an adaptation of the above. Instead of infecting pre-B cells with the temperature sensitive Abelson leukemia virus, we introduce the abl kinase to bone marrow cultures via a retrovirus that similarly transforms the pre-B cell population. Instead of varying culture temperatures, we use a small molecule inhibitor of the abl kinase, STI571 or Gleevac, to stop cell division, arrest the cells in G1, and induce RAG endonucleolytic activity and V(D)J recombination(107, 280). Instead of analyzing rearrangement of the complex endogenous antigen receptor loci, we utilize retroviral recombination substrates that are integrated into the chromosome of these cells. These retroviral chromosomal recombination substrates, similar to the extrachromsomal plasmid substrates, contain a single pair of RSSs (Figure 1 and 2A). These retroviral recombination substrates can rearrange by deletion (pMX-DEL) or inversion (pMX-INV) based on the orientation of the RSS pairs just as in the endogenous antigen receptor loci. Additionally, they enable us to study both CJ and SJ formation in the context of a chromatinized environment. We have developed Southern blotting strategies to analyze rearrangement of these retroviral recombination substrates that enable us to not only detect products resulting from the normal repair of a RAG DNA DSB, but also aberrant repair products as well as V(D)J reaction intermediates as depicted in Fig 2a(107). Based on findings from initial studies utilizing chromosomal recombination

substrates in these transformed pre-B cell lines, we can go on to analyze rearrangement of the endogenous loci in these transformed cells or in primary cell cultures or bone marrow or thymic extracts. The complexity of the endogenous antigen receptor loci, however, remains an obstacle to the analysis of V(D)J recombination. We have circumvented this problem in some instances by utilizing mice with genetically modified antigen receptor loci(108, 276). The TCR SJα mouse has a TCRα locus containing a single functional Jα gene segment to which the Vα gene segments can recombine. This modified allele enables us to detect unrepaired Jα coding ends, but analyzing joints that do form is still limited by the number of possible Vα partners(108).

Specific materials and methods pertinent to each chapter are included below, but importantly have been published exactly as printed here.

Relevant to Chapter 3 (as published(276))

Cell lines and culture conditions: *Nbs1*$^{m/m}$ (lines 675.3 and 737.3), *Mre11*$^{ATLD1/ATLD1}$ (line 48.1), wild type (WT) (line A70.2), *Atm*$^{-/-}$ (lines Atm2E and Atm2F), *Artemis*$^{-/-}$ (lines 5.1, 0.1), *Atm*$^{-/-}$*:Artemis*$^{-/-}$ (line 0.1), *Nbs1*$^{m/m}$*:Artemis*$^{-/-}$ (lines 37.1, 37.3) and *Mre11*$^{ATLD1/ATLD1}$*:Artemis*$^{-/-}$ (lines 61.3, 64.1) v-abl-transformed pre-B cells were generated by culturing bone marrow of 3-5 week old mice with the pMSCV v-abl retrovirus, as described previously(107). All cells were generated from mice harboring the Eμ-Bcl-2 transgene(281). All Abl pre-B cells (10^6/mL) were transduced with retroviral recombination substrates by co-centrifugation at 1800 rpm for 90 minutes. Clonal populations of cells with single pMX-INV integrants were isolated by limiting dilution of *WT:INV* (A70.2-2 and -5), *Atm*$^{-/-}$*:INV* (Atm2E-26 and Atm2F-6), *Mre11*$^{ATLD1/ATLD1}$*:INV* (48.1-1 and -3) and *Nbs1*$^{m/m}$*:INV* (675.3-2 and 737.3-6) Abl pre-B cell lines. Cells were treated with 3μM STI571 (Novartis) for the indicated times at 10^6 cells/ml. KU-55933 (Sigma) was used at 15μM.

Southern blot and PCR analyses: Southern blot analyses were carried out on genomic DNA from cells harboring pMX-INV using the indicated restriction enzymes and the C4 probe, as previously described(107). Southern blot analyses of thymocytes from mice expressing the

TCRα^{sJ} allele were carried out using the *Stu*I restriction enzyme and the CαI probe, as reported previously(108, 282). Southern blot analyses for IgLκ locus Jκ coding ends was carried out on *Sac*I and *EcoR*I digested genomic DNA using the JκIII probe as previously described(270). pMX-INV coding joints were amplified using the pA and pB oligonucleotides and pMX-DEL^{SJ} signal joints were amplified used primers pB and pC oligonucleotides as previously described(107). Vδ5, Vβ14 and Vκ6-23 coding and hybrid joints, and the IL-2 gene, were amplified by PCR as previously described(107).

Western blot and EMSA analyses: Western blots were done on whole cell lysates using antibodies to mouse KAP-1 (GeneTex), phosphorylated KAP-1 (Bethyl Labs), Mre11 (Novus), and Nbs1 (Cell Signaling). The secondary reagents were horseradish peroxidase (HRP)-conjugated goat anti-mouse IgG (Zymed) or donkey anti-rabbit IgG (GE Healthcare). NFκB EMSA were run as described previously and were analyzed with a Li Cor Odyssey Infrared Scanner(270).

Immunofluorescent detection of γ-H2AX foci: Nuclear γ-H2AX foci were detected using standard protocols with minor modifications(105, 283). Briefly, cells were cyto-spun onto poly-L-lysine coated slides (Sigma), fixed in 4% paraformaldehyde for 10 min, washed in phosphate-buffered saline (PBS), permeabilized with 0.15% Triton X-100 in PBS, and blocked in PBS with 2% bovine serum albumin. Cells were incubated in anti γ-H2AX antibody (Upstate Biotechnology) at 1-2 µg/ml concentration for 3 hours at 37^{o}C in a moist chamber, washed with PBS, and further incubated with anti-mouse-FITC conjugate (Vector Labs) for 45 minutes. After washing with PBS slides were mounted in Vectashield mounting medium with DAPI (Vector Labs). Foci were observed and imaged as described before on Carl Zeiss Axioplan 2 microscope using Metasystems *In situ* Imaging System (ISIS) imaging software(283).

Relevant to Chapter 4

Southern blotting: Southern blot analysis of genomic DNA analyzing rearrangement of the pMX-DEL^{CJ} retroviral substrate was performed as described previously utilizing an EcoRV

restriction enzyme digest and the C4b probe(107). Southern blot analyses of coding ends generated during rearrangement of the IgL-κ locus was performed as described previously on genomic DNA digested overnight with SacI and for 5 hours with EcoRI utilizing the JκIII probe(270).

Urea-Agarose Gel Electrophoresis: The denaturing gels were run as described previously(284) with the following modifications: Briefly, 40ug of genomic DNA was digested overnight with EcoRV in a 400ul volume and concentrated to 30ul. The DNA was then re-suspended with the addition of 5 volumes 8M Urea, 1% NP-40, 1mM Tris pH 8.0 and 0.5 mg/ml bromophenol blue. This DNA solution was divided in two, with one half heated at 90 degrees Celsius for 8 min to denature while the other half was incubated on ice. After 8 min the heated DNA samples were placed on ice. All samples were ran on a 1.2% agarose gel made with 1X TAE with 1M urea at 50 volts for ~24hrs in at 4°C in TAE buffer also containing 1M urea.

TdT-assisted PCR: TdT-assisted PCR analysis of pMX-DEL^{CJ} coding ends was performed as described previously using the IRES REV5 oligo for the primary PCR reaction, the IRES REV4 oligo for the secondary PCR reaction and the I4 oligo as a probe(238). Primers IRESrev5 and T17 UNIV (Table 1) were used for the primary PCR reaction and 15 cycles of the PCR program described above were used. A secondary PCR was then carried out using primers IRESrev4 and UNIV (Table 1). 30 cycles were used for the secondary PCR. Conditions for PCR were as follows: 92° for 1 minute, 58° C for 1.5 min, and 72° C for 1.5 min. Similar conditions were used for PCR analyses of coding ends generated during rearrangement of the endogenous IgLκ locus, using the Jκ2 ds oligo for amplification and the Jκ oligo as a probe. IL2 gene PCR, which is provided as a DNA loading control, was performed as described previously(238).

Table 1. Oligos used in TdT assisted PCR.

IRES REV5	CTCGACTAAACACATGTAAAGC
IRES REV4	CCCTTGTTGAATACGCTTG
T17 UNIV	GTAAAACGACGGCCAGTCGAC-T_{17}
UNIV	GTAAAACGACGGCCAGTCGAC
IRES4 probe	TAAGATACACCTGCAAAGGCG
Jκ2 ds 200	CCACAAGAGGTTGGAATGATTTTC
Jκ2 probe	GTAGTCTTCTCAACTCTTGTTCACT

Western blotting: Western blotting was performed as described previously(276). Primary antibodies used were mouse monoclonal 14-1 (1:40)(285) and H2AX (1:3000) Millipore, Erk2 (1:2500) Santa Cruz and GAPDH (1:2500) Santa Cruz. Dilutions used are provided in parentheses. Secondaries were goat anti-mouse (Invitrogen) and donkey anti-rabbit F(ab')2 Fragment (Fisher).

Retroviral reconstitution and lentiviral knock-down: Reconstitution of *Artemis*$^{-/-}$*:H2AX*$^{-/-}$ and *Ligase IV*$^{-/-}$*:H2AX*$^{-/-}$ abl preB cells was performed by retroviral transduction with either empty retrovirus or retrovirus containing cDNAs encoding H2AX or H2AX^{S139A}. A cDNA encoding H2AX^{S139A} (serine 139 changed to alanine) was generated by PCR-based site-directed mutagenesis of WT H2AX cDNA. cDNAs encoding WT H2AX and H2AX^{S139A} were cloned into the pMX-PIE retroviral vector and cells were transduced by co-centrifugation as described previously. Cells expressing the retroviral construct were obtained by flow cytometric cell sorting of cells expressing GFP using a FACSVantage (BD Biosciences).

shRNA-mediated knockdown: Generation of lentiviral shRNAs vectors was carried using the previously described pFLRU:YFP lentiviral vector(286, 287). CtIP-specific and nontargeting(NT) shRNAs were cloned into the pFLRU:YFP lentiviral vector. Sequences targeted by the shRNA

are shown in Table 2. 4 μg of these PFLRU:shRNA:YFP vectors were individually co-transfected with 4 μg pHR'Δ8.2R packaging vector and 1 μg of pCMV-VSVg envelope plasmid into HEK293T cells plated at approximately 80% confluency in 6 cm^2 plates using Lipofectamine 2000 (Invitrogren). Media was replaced at 12 hours post-transfection. Supernatants were harvested 24 hours later. Transduction of abl pre-B cells was performed by co-centrifugation with viral supernatant at 1800 rpm for 90 min with polybrene added at 5 μg/mL. Cells expessing the pFLRU-shRNA vectors were obtained by flow cytometric cell sorting gating on cells expressing YFP using a FACSVantage (BD Biosciences).

Table 2. Target sequences for shRNA mediated knockdown.

CtIP shRNA target 6	GAGCAGACCTTTCTCAGTA
Non-targeting (NT) shRNA	GGTTCGATGTCCCAATTCTG

PCR Amplification of CJs: pMX-DEL^{CJ} coding joints were amplified using oligos pC and IRES REV5 flanking the coding joint as shown in Figure 21a. 300 ng of genomic DNA was used in the original amplification with serial 5-fold dilutions. Oligo IRES REV4 was used as a probe. Cloning and sequencing of pMX-DEL^{CJ} coding joints was performed as described previously(276). P-values were calculated by Student's t-test with Welsh's correction for unequal variances.

Table 3. Oligos used to PCR amplify pMX-DEL^{CJ} coding joints.

pC	GCACGAAGTCTTGAGACCT
IRES rev5	CTCGACTAAACACATGTAAAGC
IRES rev4	CCCTTGTTGAATACGCTTG
pA	CACAGGATCCCACGAAGTCTTGAGACCT
pB	ATCTGGATCCGTGCCGCCTTTGCAGGTGTATC
pD	AGACGGCAATATGGTGGA

Relevant to Chapter 5 (as published(270))

Cell culture: Three independently derived *RAG-2*$^{-/-}$ (R.1, R.2 and R.3), three independently derived *Artemis*$^{-/-}$ (A.1, A.2 and A.3), two independently derived *Artemis*$^{-/-}$*:Atm*$^{-/-}$ (AA.1 and AA.2) and individual Scid and *Ku-70*$^{-/-}$ v-abl-transformed pre-B cell lines containing the EμBcl-2 transgene were generated. The three Artemis$^{-/-}$:IκBα-ΔN cells (A.3ΔN1, A.3ΔN2, A.3ΔN3) were generated through standard transfection of the A.3 cells with a cDNA encoding an N-terminally truncated IκBα (IκBα-ΔN)(288). Expression of the IκBα-ΔN protein in these cells was confirmed by western blotting. STI571 treatments were carried out with 3μM STI571, as previously described(107). The KU-55933 Atm inhibitor (Sigma) was used at 15μM, the BAY-11-7085 inhibitor (Calbiochem) was used at 20μM. Irradiation was carried out with a Cs^{137} source, at doses of either 0.5 or 4 Gy.

Western blotting and EMSA: Western blotting was carried out as described previously, using an antibody to Pim-2 (Santa Cruz, 1D12)(276). The secondary reagent was horseradish peroxidase (HRP)-conjugated goat anti-mouse IgG (Zymed). EMSAs were run as described previously, and analyzed using a Li-Cor Odyssey Infrared scanner(289). Supershifts were performed using anti-p50 and anti-p65 antibodies (Santa Cruz, sc-114 X and sc-372 X).

Generation of the NFκB reporter: To generate pMSCV-NRE-GFP, the NFκB responsive elements and TATA box from pNF-κB-Luc (Stratagene) were amplified using the following oligonucleotides: pNRE-f: CCAAACTCATCAATGTATCTTATCATG; pNRE-r: TACCAACAGTACCGGAATGC. This PCR product was cloned upstream of a cDNA encoding enhanced GFP (Clontech) on the bottom strand of pMSCV containing an IRES upstream of the Thy1.2 cDNA.

Gene expression profiling: All Abl pre-B cells were harvested 48 hours following treatment with STI571. RNA was isolated using Qiagen RNeasy technology following the manufacturer's instructions. Gene expression analysis was conducted using Affymetrix Mouse Genome 2.0 GeneChip® arrays (Mouse 430 v2, Affymetrix, Santa Clara, CA). One μg of total RNA was

amplified as directed in the Affymetrix One-Cycle cDNA Synthesis protocol. Fifteen μg of amplified biotin-cRNAs were fragmented and hybridized to each array for 16 hours at 45°C in a rotating hybridization oven using the Affymetrix Eukaryotic Target Hybridization Controls and protocol. Array slides were stained with streptavidin/phycoerythrin utilizing a double-antibody staining procedure and then washed using the EukGE-WS2v5 protocol of the Affymetrix Fluidics Station FS450 for antibody amplification. Arrays were scanned in an Affymetrix Scanner 3000 and data was obtained using the GeneChip® Operating Software (GCOS; Version 1.2.0.037). Data pre-processing, normalization, and error modeling was performed with the Rosetta Resolver system (Version 6.0)(290).

In order to identify differentially expressed genes between the *RAG-2*$^{-/-}$ and *Artemis*$^{-/-}$ Abl pre-B cells, an error-weighted analysis of variance (ANOVA) utilizing the Benjamini Hochberg false discovery rate was performed using Rosetta Resolver (www.rosettabio.com). At p-value ≤ 0.05, this analysis yielded 1578 probe sets. Fold changes were generated in Resolver, based on the ratio of each individual cell line relative to the average of the three *RAG-2*$^{-/-}$ cells with 100-fold being the maximum change that Resolver can report. Of the 1578 probes found using the ANOVA analysis, only those that had a fold-change ≥ 2.0 (not including anti-correlated genes) in all ratios for a given genotype were considered for further analysis. A Venn diagram of the resulting ANOVA and fold-change data sets for each genotype comparison to *RAG-2*$^{-/-}$ was then used to determine which expression changes were dependent on ATM and NFκB.

For gene expression profiling of primary developing B cells, B220^{+} cells were isolated from *RAG-1*$^{-/-}$*:IgHtg* and *Art*$^{-/-}$*:IgHtg* bone marrow using Mouse Pan B (B220) Dynabeads from Invitrogen. RNA was isolated using the Qiagen RNeasy Mini Kit. Microarrays were treated as described above for the Abl pre-B cells. For the probe sets that were identified as being differentially regulated in response to RAG DSBs in the abl-pre-B cells, we compared the average expression in the two *RAG-1*$^{-/-}$*:IgHtg* samples to the each of the two *Art*$^{-/-}$*:IgHtg* samples. The probe sets that were not anti-correlated and changed ≥1.5-fold in the average of these comparisons were included.

Flow cytometry: Flow cytometric analyses were performed on a FACSCaliber (BD Biosciences) with the normalized geometric mean fluorescence intensity (MFI) calculated as the difference between the geometric mean fluorescence for the specific antibody and the isotype control. Flow cytometric cell sorting was performed using a FACSVantage (BD Biosciences). Flow cytometric analyses were performed using fluorescein isothiocyanate (FITC)-conjugated anti-CD45R/B220, allophycocyanin (APC)-conjugated anti-IgM, phycoerythrin (PE)-conjugated anti-CD40, PE-conjugated anti-CD62L, PE-conjugated anti-CD69, and the appropriate isotype controls (BD Biosciences).

Analysis of pMX-DEL^{CJ} rearrangement: PCR was carried out as described previously on 4-fold dilutions of genomic DNA(107). IL-2 PCR primers were IMR42 and IMR43, and the product was probed with IMR042-2, all of which have been described previously(107). Primer sequences for pMX-DEL^{CJ} are included above in Table 3.

RT-PCR gene expression analysis: Quantitative real-time PCR (RT-PCR) was performed using a Stratagene Mx3000P real-time PCR machine and Platinum® SYBR® Green qPCR SuperMix-UDG (Invitrogen). PCRs were carried out using the following program: 95°C, 30 sec; 55°C, 60 sec; 72°C, 30 sec; 40 cycles. Relative expression is calculated as the difference between beta-actin expression (C1) and expression of the gene of interest (C2), using the following equation: relative expression = $2^{-(C1-C2)}$. C is the PCR cycle where the product detection curve becomes linear.

Table 4. Primers used for RT-PCR.

Gene	Forward	Reverse
B-actin	AGTGTGACGTTGACATCCGTA	GCCAGAGCAGTAATCTCCTTCT
Bcl3	TCCAGAATAACATAGCCGCTGT	CATGCCAGGTGAATTGCAGTC
Cd40	GCTGGTCATTCCTGTCGTGAT	ACTGGAGCAGCGGTGTTATG
Cd69	TGGTGAACTGGAACATTGGA	CAGTGGAAGTTTGCCTCACA
IL12α	CTGTGCCTTGGTAGCATCTATG	GCAGAGTCTCGCCATTATGATTC
CD62L	TCTGGGAAATGGAACGATGACG	CCGTAATACCCTGCATCACAGAT
Pim-2	CGGGTGTGATACGCCTTCTTG	GCCCCTTCTCTGTGATATAGTCG
Swap70	ATGAGGGGGTTGAAAGACGAA	AGGTTATGGGAAAGGACCTTGA
Cd80	TCAAAAGAAGGAAAGAGGAACG	CGGAAGCAAAGCAGGTAATC

Chapter 3

A Requirement for MRN for the Proper Repair of RAG DNA DSBs

(reprinted with modification(276))

ATM-deficient mice and humans have a predisposition to lymphoid tumor formation including a subset resulting from the aberrant repair of RAG DNA DSBs during V(D)J recombination(111). Interestingly, mice with combined deficiencies in checkpoint pathways and DNA repair pathways develop lymphoid tumors while mice singly deficient in either do not exhibit the same frequency or onset of tumor generation(150, 248, 250). In lymphocytes, ATM is known to activate p53 in response to persistent DNA damage(73, 244). However, given the phenotype of increased lymphoid tumor formation, it seemed likely that ATM, in addition to promoting checkpoints and mediating apoptosis, might additionally play a direct role in repair of the RAG DSB.

In this regard, we have demonstrated that ATM-deficient cells have a defect in the repair of chromosomal RAG DNA DSBs with an increased frequency of aberrant hybrid joint (HJ) formation during rearrangements that occur by inversion and a decrease in the efficiency of coding joint (CJ) formation(107, 108). The unrepaired coding ends drift from one another in the absence of ATM and are frequently resolved as translocations(107). Taken together (as discussed later), these data suggest that ATM plays a role in the stabilization of the post-cleavage complex thereby facilitating repair of the break and preventing unrepaired ends from causing translocations. However, how ATM carries out this function is unknown. Most known functions of ATM including the promotion of repair, however, require its kinase activity(73, 107).

Interestingly, mice and patients with deficiencies in components of the MRN complex exhibit phenotypes similar to those deficient in ATM exhibiting a mild lymphopenia and sensitivity to ionizing radiation(117, 291-298). The MRN complex is recognized as a sensor of DNA damage as it has DNA binding abilities and functions to recruit ATM to the break site(70, 77, 90, 91, 104, 291, 299). ATM, in turn, phosphorylates all three components of the MRN complex(71, 300-302). Although the MRN complex is required for HR, until this point, no known role for the MRN complex in NHEJ during V(D)J recombination has been clearly defined(75, 76, 277, 299, 303, 304). However, we considered the possibility that MRN might play a role downstream of ATM in the repair of RAG DNA DSBs functioning to maintain un-repaired coding ends within the

post-cleavage complex via its unique DNA end alignment and tethering abilities(75, 76, 78, 81, 83, 86). To begin to address this hypothesis, we analyzed the repair of RAG DNA DSBs in MRN-deficient v-abl transformed pre-B cell lines and mice.

Generation of MRN-deficient v-abl transformed pre-B cell lines.

Mice with homozygous-null mutations at the Mre11, Nbs1, or Rad50 loci all exhibit early embryonic lethality(291, 296-298); thus, we were unable to generate Abl pre-B cells completely deficient in any of these proteins. However, we were able to generate Abl pre-B cell lines from mice homozygous for hypomorphic Mre11 (*Mre11*^{ATLD1}) and Nbs1 (*Nbs1*^{m}) alleles. The *Mre11*^{ATLD1} allele has a gene-targeted point mutation that generates a premature stop codon, resulting in a C-terminal truncation of the Mre11 protein, mimicking a mutation in that causes ataxia-telangiectasia–like disease (ATLD)(294). The Nbs$^{m/m}$ mice were generated by replacing exons 2 and 3 of the Nbs1 allele with a neomycin resistance gene generating the *Nbs1*^{m} allele, which encodes a truncated Nbs1 protein(292). Importantly, the three MRN components are thought to function only as a holocomplex; thus, deficiencies in any one component would impact the function of the entire complex(77). The Mre$^{ATLD1/ATLD1}$ and the Nbs$^{m/m}$ mice may be generally referred to here as MRN-deficient. We have additionally developed WT and *Atm*$^{-/-}$ Abl pre-B cell lines(107).

MRN-deficient cells have defects during rearrangement by inversion.

Atm-deficient pre-B cells have defects in repair during rearrangement by inversion with a decrease in overall recombination frequency and an increased formation of aberrant hybrid joints detectable in chromosomal recombination substrates as well as the endogenous IgL-κ and TCRβ and δ loci(107, 108). Given that MRN-deficient mice and patients have similar phenotypes as those deficient in ATM, we decided to assay for defects in rearrangement by inversion in the MRN-deficient cells. To this end, we introduced pMX-INV into the MRN-deficient Abl pre-B cells (*Mre*$^{ATLD1/ATLD1}$ Abl pre-B and *Nbs*$^{m/m}$ Abl pre-B) and assayed for recombination by Southern blotting. We purified populations containing pMX-INV integrants by sorting for the expression of human CD4 that is also encoded by the retrovirus. These bulk populations contain numerous

pMX-INV integrants at broadly heterogeneous locations thus eliminating potential contributions of integration effect on recombination. We also isolated clones from these bulk populations by limiting dilution that each contained a single integrant of the retroviral substrate. Work presented here is done on the clonal populations though we detected no difference in results of analyses in these clones and the original bulk populations.

We treated the Abl pre-B cells with STI to induce RAG expression, and this led to rearrangement of pMX-INV in all cell lines assayed. Analysis of EcoRV/Nco1-digested genomic DNA from WT Abl pre-B cells reveals a decrease in the 2 kb band representing un-rearranged substrate and an accumulation of a 3 kb species representing a normal coding joint (CJ) upon STI treatment (Figure 2a-b). In ATM-deficient Abl pre-B cells, we note an accumulation of CJs, but we also detect a 4 kb species representing an aberrant hybrid joint (HJ) following STI treatment (Figure 2a-b). This is in agreement with previously published work in the lab(107). In the MRN-deficient cells, we detect a similar accumulation of both HJs and CJs following STI treatment. Thus, MRN-deficient Abl pre-B cells also have a defect in repair by inversion when using recombination substrates with an increased production of aberrant hybrid joints (Figure 2b).

In ATM-deficient mice, we can also detect defects in rearrangement by inversion *in vivo* at the endogenous TCRδ and TCRβ loci as well as the endogenous IgLκ locus by PCR(107, 108). Specifically, we detected both CJ and aberrant HJ formation for rearrangements that occur between Vδ5 and DJδ1 and Vβ14 and DJβ2.7 in thymic DNA preparations (Figure 3a) and between Vκ6-23 and Jκ1 in splenic DNA samples (Figure 3b) from *Atm*$^{-/-}$ mice(107, 108). We isolated thymic and splenic DNA from the *Mre*$^{ATLD1/ATLD1}$ and *Nbs*$^{m/m}$ mice and used the same PCR-strategy to assay for *in vivo* defects in rearrangement by inversion. In all cases, we detect aberrant hybrid joints in the MRN-deficient cells that are also observed in *Atm*$^{-/-}$ cells but not observed in WT cells (Figure 3). Thus, we detect aberrant hybrid joint formation during the rearrangement of pMX-INV in our Abl pre-B cell lines but also in both primary B and T cells in the MRN-deficient mice.

Efficiency of CJ formation is decreased in MRN-deficient cells.

ATM-deficient cells also have a deficiency in CJ formation, and unrepaired coding ends are readily detectable in ATM-deficient cells undergoing V(D)J recombination at chromosomally integrated substrates as well as the endogenous antigen receptor loci(107, 108). We decided to assay for CE accumulation in the MRN-deficient cells as well. Whereas no coding end intermediates are detected in genomic DNA isolated from WT Abl pre-B cells (*WT:INV*) upon STI treatment, these reaction intermediates are readily detectable in samples from $Atm^{-/-}$ Abl pre-B cells and in $Mre^{ATLD/ATLD}$ and $Nbs^{m/m}$ Abl pre-B cells, although to a lesser extent (Figure 4). These coding ends are visualized by a 2.2 kb hybridizing fragment in EcoRV-digested genomic samples from pMX-INV rearrangement (Figure 2a and 4). Next, we wished to determine whether the MRN-deficient mice also exhibited defects in coding joint formation *in vivo*.

We have previously demonstrated that ATM-deficient mice have a defect in thymocyte development, more specifically a decrease in thymocyte counts with the most significant decrease in the number of CD4+ and CD8+ (single positive SP) thymocytes (Figure 5a)(108). Furthermore, we have demonstrated a decreased number of pre-selection αβ-TCR expressing (TCR-β intermediate) CD4+CD8+ (double positive, DP) thymocytes in $Atm^{-/-}$ mice(108). This defect is visualized by FACS analysis by staining for the surface expression of TCRβ; compared to wild-type mice, $Atm^{-/-}$ mice have decreased numbers of cells expressing intermediate and high levels of TCRβ (48% as compared to 9.5% of DP thymocytes) population (Figure 5b)(108). In characterizing the $Nbs^{m/m}$ mice, we note a similar, though less severe, decrease in total thymocyte number with the most significant decreases again in the numbers of CD4+ and CD8+ SP thymocytes (Figure 5a). Furthermore, we note the same block at the DP stage with only 21% of DP cells expressing intermediate levels of TCRβ (Figure 5b). This suggested to us that MRN-deficient mice likely have a similar defect in thymocyte development that we see in the ATM-deficient mice. Cells at the DP stage of thymocyte development are actively assembling their TCRα genes in an attempt to generate a functional αβ-TCR. Production of a successful TCR, that is, one that binds peptide-MHC with sufficient affinity to mediate positive selection, but does

not afford self-reactivity, is a rare occurrence(108). As such, it is rather advantageous that the TCRα allele is arranged such that it can undergo multiple rounds of recombination. Specifically, the locus has over 100 V gene segments and 61 J gene segments all of which undergo rearrangement by deletion. The initial rearrangements involve the most 3' V segments and most 5' J gene segments. If coding joint formation during this first attempt at rearrangement is not successful, additional rounds of rearrangement are possible utilizing an upstream V and a downstream J segment. The requirement for multiple rearrangements at this locus might explain the particular block in thymocyte development seen in the ATM- and MRN-deficient mice(108). Increasing the number of breaks that must be repaired to generate a functional antigen receptor would increase the chances that both alleles would be inactivated due to the aberrant repair of RAG DNA DSBs, and as a result, no αβ-TCR expressing DP thymocyte would develop. Thus, defects in coding joint efficiency might be manifested as a specific decrease in the number of αβ-TCR expressing DP thymocytes(108).

Similar to the endogenous kappa locus, the noted complexity of the endogenous TCRα locus prevents us from quantitatively determining the extent of a defect in CJ formation by Southern blotting. To detect a possible defect in CJ formation at the TCRα locus in the ATM- and MRN-deficient mice, we generated mice with a modified TCRα allele containing two rather than 61 Jα gene segments(108). While any of the 100 V gene segments can be utilized, all TCRα rearrangements must utilize one of two Jα gene segments, enabling us to detect the accumulation of unrepaired coding ends (Figure 6a)(108). To assay for the accumulation of unrepaired ends during recombination of this modified TCRα allele in ATM- and MRN-deficient mice, we developed *WT:TCR-α*$^{sJ/sJ}$, *Atm*$^{-/-}$*:TCRα*$^{sJ/sJ}$, Mre$^{A/A}$:TCRα$^{SJ/SJ}$ and *Nbs*$^{m/m}$*:TCRα*$^{SJ/SJ}$ mice, isolated thymic DNA, and performed Southern blot analyses as diagrammed in Figure 6a (Figure 6a). Southern blotting revealed a smattering of non-germline bands that are indicative of successful Vα to Jα rearrangement in these thymocytes (Figure 6b). However, in contrast to *WT:TCRα*$^{SJ/SJ}$ cells, the *Atm*$^{-/-}$*:TCR-α*$^{sJ/sJ}$, *Nbs1*$^{m/m}$*:TCR-α*$^{sJ/sJ}$, and *Mre11*$^{ATLD1/ATLD1}$*:TCRα*$^{sJ/sJ}$

thymocytes each have a distinct 5.9-kb band that represents unrepaired Jα56 coding ends(108). As observed in the Abl pre-B cells, however, the phenotype of the MRN-deficient cells was less severe than that of *Atm*$^{-/-}$ cells, as we detect more Jα-56 CEs in the *Atm*$^{-/-}$*:TCR-*$\alpha^{SJ/SJ}$ thymocytes than either the *Nbs1*$^{m/m}$*:TCR-α*$^{sJ/sJ}$ or the *Mre11*$^{ATLD1/ATLD1}$*:TCRα*$^{sJ/sJ}$ thymocytes. Importantly, equivalent levels of DNA were ran on the Southern as shown by the loading control (Figure 6b). Based on these data, we believe that the block in thymocyte development seen in the Nbs-deficient mice (Figure 5) is a result of a decrease in efficiency of CJ formation during rearrangement of the TCRα locus as previously demonstrated for ATM-deficient mice(108).

MRN-deficiency does not lead to global defects in ATM activation.

The observed defect in repair of RAG DNA DSBs in the MRN-deficient cells and mice is remarkably similar to that we described for ATM-deficient cells(107, 108). Given the role for MRN in recruiting ATM to the site of a DNA DSB and the ability of MRN to augment ATM activity *in vitro*, it was important to demonstrate that the phenotype of MRN-deficient cells was not simply due to decreased ATM-activity in these cells(77). We decided to assay for the phosphorylation of known substrates of ATM in response to DNA damage to determine whether or not ATM was capable of being activated in the absence of a functional MRN complex during V(D)J recombination.

We reasoned that the assays available to detect ATM activity would not be sensitive enough to detect signaling events following the induction of a small number of RAG DNA DSBs that are made and repaired quickly as they are in WT cells. Thus, to better assess signaling downstream of RAG DNA DSBs, we utilized cells deficient in components of the NHEJ-pathway. Specifically, we used *Artemis*$^{-/-}$ Abl pre-B cells. Artemis is the endonuclease required to open the hairpin-sealed coding ends during V(D)J recombination, and in its absence, coding ends accumulate unrepaired(150, 158, 161). As mentioned above, in our Abl pre-B cells, rearrangement at the endogenous IgLκ locus occurs upon STI treatment. Cleavage at the endogenous kappa locus in NHEJ-deficient cells generates four distinct Jκ coding ends that are readily detectable by Southern blotting providing evidence that RAG DNA DSBs are being made

but not repaired in these cells (Figure 7). To assess the status of ATM activity in the absence of a functional MRN-complex, we generated Abl pre-B cells from *Artemis*$^{-/-}$, *Artemis*$^{-/-}$*:Atm*$^{-/-}$, *Artemis*$^{-/-}$*:Mre*$^{ATLD1/ATLD1}$, and *Artemis*$^{-/-}$*:Nbs*$^{m/m}$ mice. Differences in the number of unrepaired coding ends could potentially lead to changes in the activation of ATM. Thus, it was important to demonstrate that all cells used in these assays had similar accumulation of unrepaired RAG DNA DSBs upon STI treatment as assayed by Southern blotting for Jκ coding ends (Figure 9a).

ATM, in response to DNA damage, phosphorylates a large number of proteins including histone variant H2AX and Kap1(71, 206, 305, 306). Furthermore, it is known to lead to NFκB activation (as further discussed in Chapter 5)(263, 270). We chose to assess ATM activity in the MRN-deficient cells using these particular substrates and ATM-dependent functions as readouts. In *Artemis*$^{-/-}$ Abl pre-B cells, we detect RAG dependent phosphorylation of H2AX as assayed by immunostaining of these cells with an antibody specific to the phosphorylated form of H2AX (γ-H2AX). We detect γ-H2AX foci formation in 60% of the *Artemis*$^{-/-}$ cells at 24 hours of STI treatment and less than 5% of the *Artemis*$^{-/-}$*:Atm*$^{-/-}$ cells (Figure 8a); thus, the phosphorylation of H2AX in response to persistent Rag DNA DSBs is predominantly mediated by ATM. We detect levels of H2AX phosphorylation in the *Artemis*$^{-/-}$*:Mre*$^{ATLD1/ATLD1}$ and *Artemis*$^{-/-}$*:Nbs*$^{m/m}$ cells similar to those deficient in Artemis alone; furthermore, incubating these cells with a kinase inhibitor of ATM decreases γ-H2AX foci formation demonstrating that ATM is active in these cells (Figure 9b). We also detect Kap1 phosphorylation by Western blotting in response to RAG DNA DSBs in *Artemis*$^{-/-}$ but not *Artemis*$^{-/-}$*:Atm*$^{-/-}$ cells (Figure 8b). Neither *Artemis*$^{-/-}$*:Mre*$^{ATLD1/ATLD1}$ nor *Artemis*$^{-/-}$*:Nbs*$^{m/m}$ exhibit a significant defect in Kap1 phosphorylation following RAG DNA DSBs (Figure 9c). Finally, we are able to detect activation of NFκB in response to RAG DNA DSBs in STI-treated *Artemis*$^{-/-}$ (as discussed in Chapter 5) Abl pre-B cells by EMSA which detects translocation of the active p50:p65 NFKB heterodimer to the nucleus (Figure 8c). NFκB similarly readily translocates to the nucleus following RAG DNA DSBs in the *Artemis*$^{-/-}$*:Mre*$^{ATLD1/ATLD1}$ and *Artemis*$^{-/-}$*:Nbs*$^{m/m}$ cells but not in the *Artemis*$^{-/-}$*:Atm*$^{-/-}$ cells (Figure 9D and Figure 8c). Each of these assays suggest that ATM is being activated in the absence of the MRN complex. Moreover, the addition of the ATM-

inhibitor to the MRN-deficient cells increases the severity of the joining phenotype discussed above leading to an increase in the amount of unrepaired coding ends and further demonstrating that ATM is active in these MRN-deficient cells (Figure 10). Thus, we conclude that ATM activity is not grossly defective in the absence of a fully functional MRN complex.

Conclusion

Here, we demonstrate that MRN-deficient cells exhibit a defect in repair by NHEJ during V(D)J recombination that is similar to the repair defect previously described for ATM with an increase in aberrant hybrid joint formation during rearrangement by inversion and a decrease in the efficiency of coding joint formation(107, 108). While we cannot rule out isolated defects in the phosphorylation of specific targets of ATM that might affect repair, we demonstrate that ATM is activated in these cells. These data suggest, then, that the MRN complex might have important roles downstream of ATM in these cells.

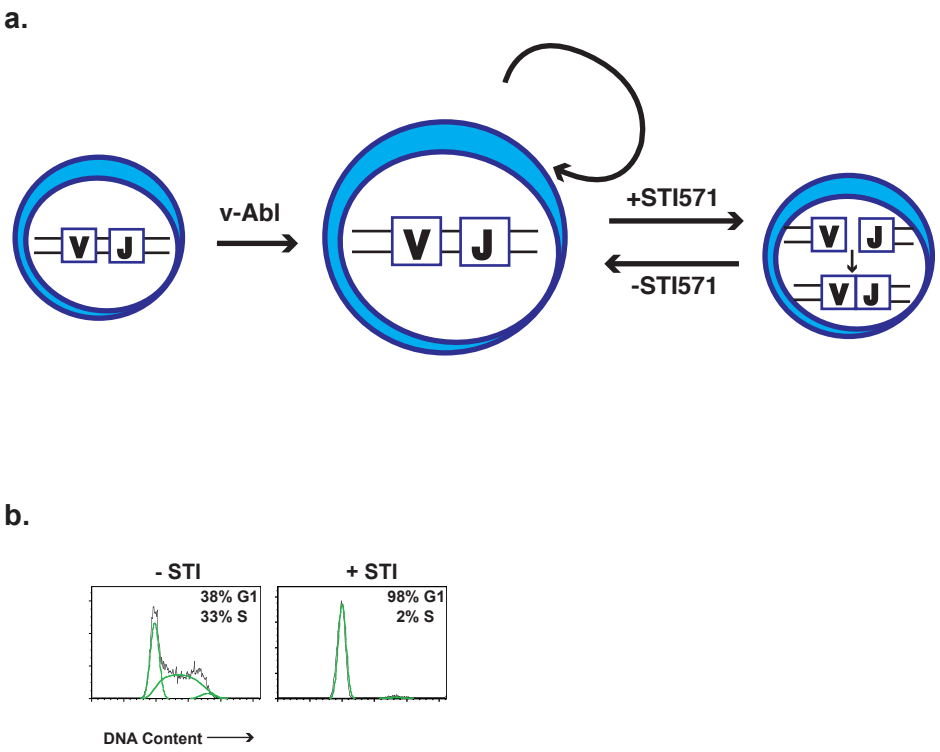

Figure 1. Assaying the repair of RAG DNA DSBs with Abl pre-B cells. (a) Schematic demonstrating the creation of Abl pre-B cell lines. Infection of BM samples with a retrovirus encoding the v-abl kinase transforms a pre-B cell population causing them to cycle rapidly. Upon STI treatment, these cells arrest in G1, express the Rag proteins and begin to undergo V(D)J recombination (as indicated by the deletion of the intervening sequence between the V and J gene segments and their subsequent joining). **(b)** FACS analysis of Abl pre-B cells before and after STI treatment demonstrating G1-arrest. Cells were either treated or not treated with STI571 for 48 hours and incubated with Hoechst dye to assay for DNA content. % of cells in G1 and S phase are indicated.

a.

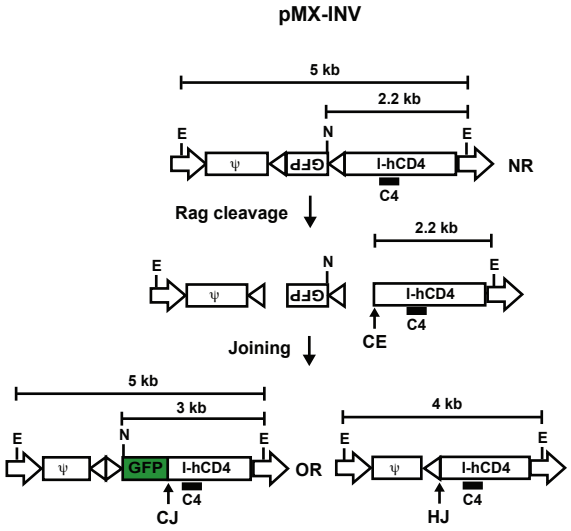

b.

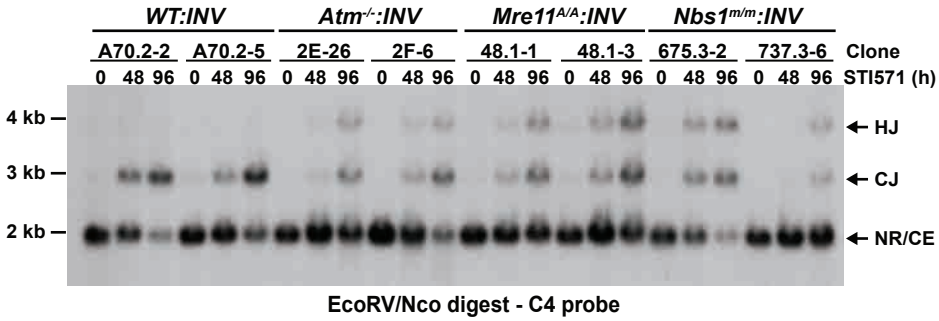

Figure 2. ATM- and MRN-deficient Abl pre-B cells have defects in rearrangement by inversion. (a) Schematic of the pMX-INV retroviral recombination substrate, rearrangement intermediates, and products. The retroviral packaging signal (ψ), GFP cDNA, and IRES-human CD4 (I-hCD4) cassette are labeled. The viral LTRs (open arrows) and the RSSs (open triangles) are shown. The non-rearranged (NR) pMX-INV and pMX-INV coding ends (CE), coding joint (CJ) and hybrid joint (HJ) are indicated. The relative position the C4 probe (bar) and EcoRV (E) and NcoI (N) endonuclease restriction sites are shown as are the expected sizes of hybridizing fragments. **(b)** Southern blot analysis of EcoRV/NcoI digested genomic DNA from wild type (*WT*), *Atm*$^{-/-}$, *Mre11*$^{ATLD1/ATLD1}$ (*Mre11*$^{A/A}$) and *Nbs1*$^{m/m}$ abl pre-B cell clones containing the pMX-INV (INV) retroviral recombination substrate that had been treated with STI571 for the indicated time (hours, h). The abl pre-B cell clones analyzed each have single pMX-INV integrants and were derived from parental lines as indicated (parental line – clone number). Expected sizes for bands generated by non-rearranged pMX-INV (NR), coding joints (CJ), hybrid joints (HJ) and coding ends (CE) are indicated.

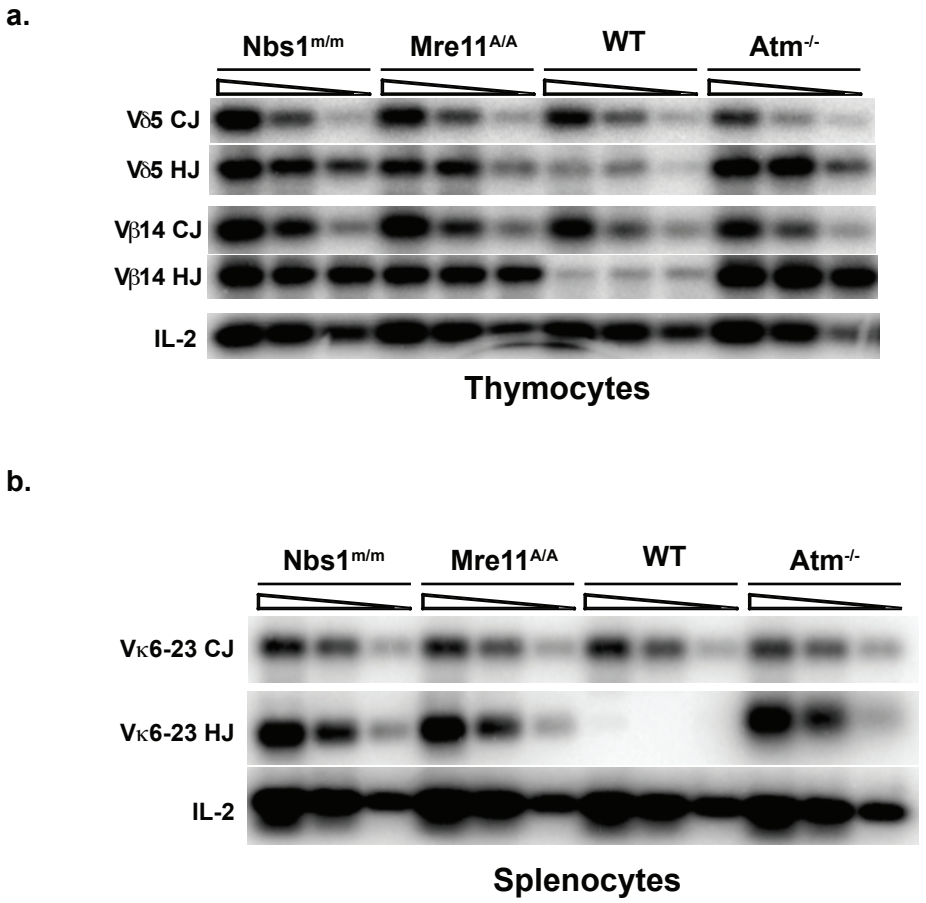

Figure 3. Defects in rearrangement by inversion at endogenous antigen receptor loci in ATM- and MRN-deficient mice. (a) PCR analysis of Vδ5DδJδ1 coding joints (Vδ5 CJ), Vδ5Dδ1 hybrid joints (Vδ5 HJ), Vβ14DβJβ2.7 coding joints (Vβ14 CJ) and Vβ14Dβ2 hybrid joints (Vβ14 HJ) in wild type (WT), *Atm*$^{-/-}$, *Nbs1*$^{m/m}$ *and Mre11*$^{ATLD1/ATLD1}$ thymocytes. **(b)** PCR analysis of Vκ6-23 to Jκ1 coding joints (Vκ6-23 CJ) and hybrids joints (Vκ6-23 HJ) in WT, *Atm*$^{-/-}$, *Nbs1*$^{m/m}$ and *Mre11*$^{ATLD1/ATLD1}$ splenocytes. The IL-2 gene PCR is shown as a DNA quantity control.

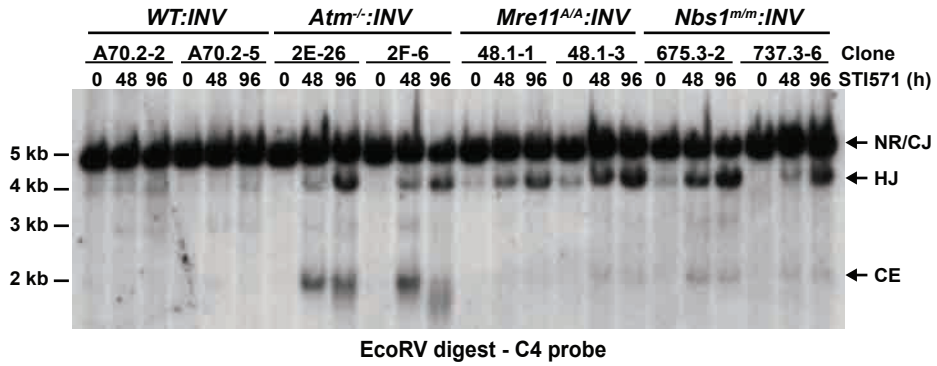

Figure 4. Defects in CJ formation in ATM- and MRN-deficient Abl pre-B cells. EcoRV digested genomic DNA from wild type (*WT*), *Atm*$^{-/-}$, *Mre11*$^{ATLD1/ATLD1}$ (*Mre11*$^{A/A}$) and *Nbs1*$^{m/m}$ abl pre-B cell clones containing the pMX-INV (INV) retroviral recombination substrate that had been treated with STI571 for the indicated time (hours, h). The abl pre-B cell clones analyzed each have single pMX-INV integrants and were derived from parental lines as indicated (parental line – clone number). Expected sizes for bands generated by non-rearranged pMX-INV (NR), coding joints (CJ), hybrid joints (HJ) and coding ends (CE) are indicated.

a.

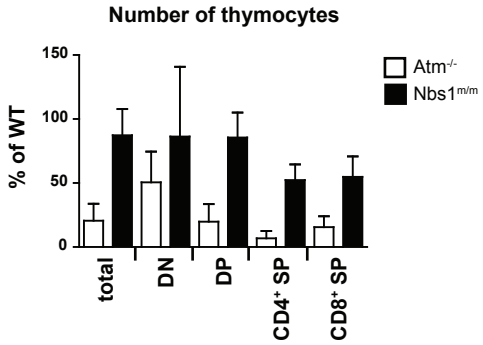

b.

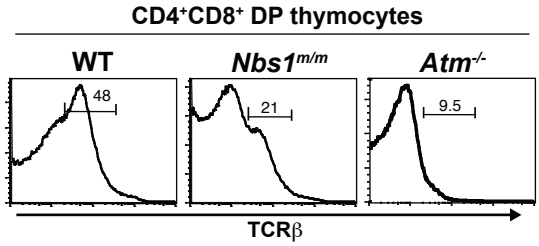

Figure 5. Block in thymocyte development in *Atm*$^{-/-}$ and *Nbs*$^{m/m}$ mice. (a) Number of thymocytes in *Atm*$^{-/-}$ (n=16) and *Nbs1*$^{m/m}$ (n=9) mice at the indicated stages of development expressed as a percentage of the number of thymocytes found at each stage in wild type *Atm*$^{+/+}$ (n=12) and *Nbs1*$^{+/+}$ (n=3) littermate controls. Calculations were done using mean numbers of thymocytes from mice of each genotype and propagated error. DN: $CD4^-CD8^-$ (double negative); DP: $CD4^+CD8^+$ (double positive); SP: single positive. **(b)** Representative flow cytometric analysis of TCRβ expression on $CD4^+CD8^+$ double positive thymocytes from wild type, *Nbs1*$^{m/m}$ and *Atm*$^{-/-}$ mice. Numbers indicate percentage of DP cells that are $TCR\beta^{int}$.

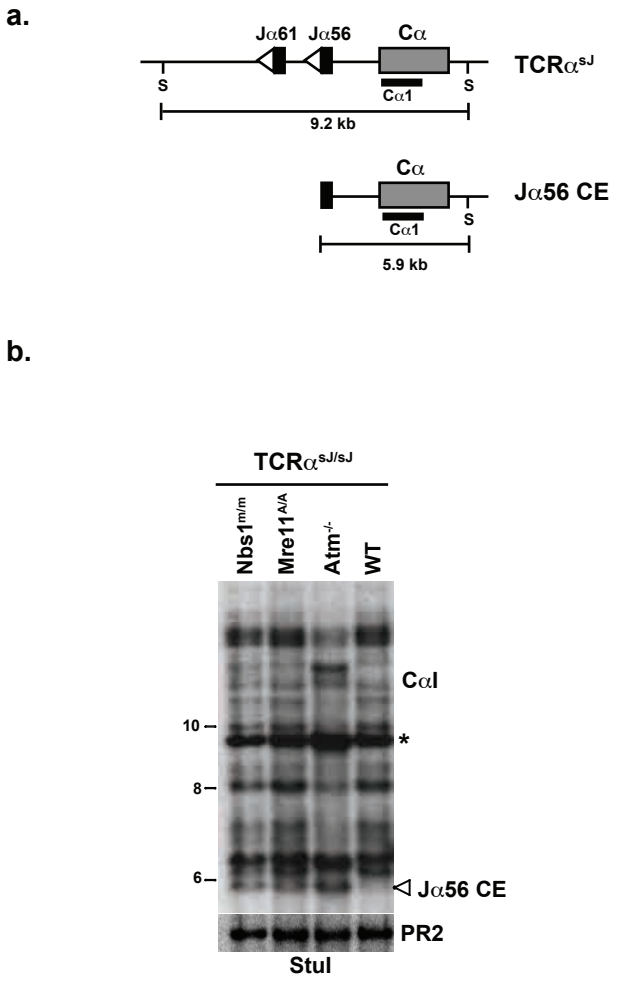

Figure 6. Accumulation of unrepaired TCRα coding ends in ATM- and MRN-deficient mice. (a) Schematic of Rag cleavage at the Jα56 gene segment on the TCRα^{sJ} allele. The gene segments are shown as black rectangles, RSSs are open triangles, and the Cα constant region is the grey rectangle. The StuI restriction sites (S) and the Cα1 probe (black bar) used for analysis are also shown. **(b)** Southern blot analysis of TCRα rearrangement in wild type, *Atm*$^{-/-}$, *Nbs1*$^{m/m}$ and *Mre11*$^{ATLD1/ATLD1}$ thymocytes, all on the TCRα$^{sJ/sJ}$ background. The expected sizes for germline TCRα^{sJ} allele (*) and Jα56 coding ends (Jα56 CE) are indicated. Genomic DNA was digested with StuI and probed with the Cα1 probe. Hybridization to a Rag-2 probe (PR2) is shown as a DNA loading control.

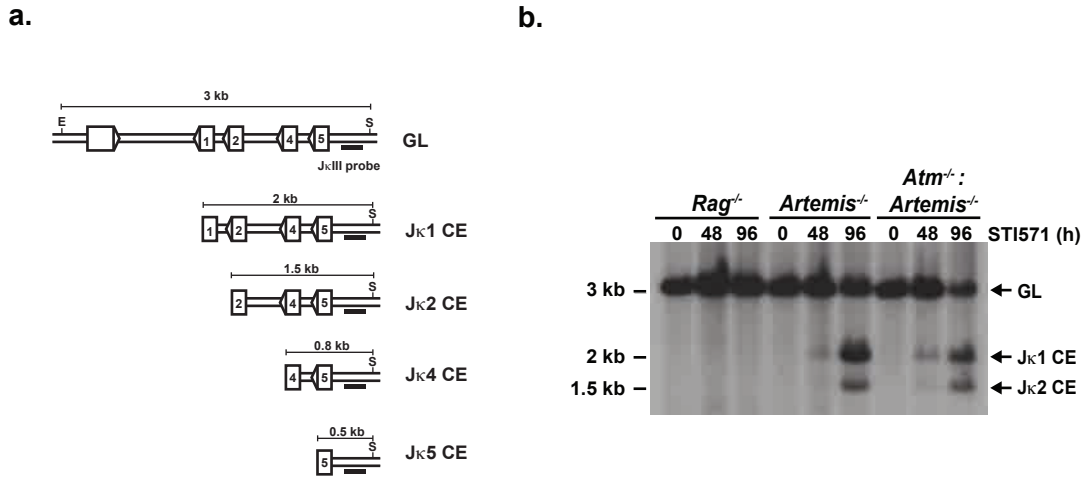

Figure 7. Accumulation of unrepaired coding ends at the endogenous kappa locus in NHEJ-deficient Abl pre-B cells. (a) Schematic of Southern blotting strategy for analysis of unrepaired coding ends generated in NHEJ-deficient cells at the endogenous IgL-kappa locus showing relative positions of the restriction sites (EcoRI and SacI) and the JκIII probe (black bar) used for analysis. Expected sizes for coding ends generated by cleavage at each of the 4 Jκ gene segments are shown. **(b)** Southern blot analysis showing Jκ1 and Jκ2 coding ends (CE) generated in *Rag2*$^{-/-}$, *Artemis*$^{-/-}$ and *Artemis*$^{-/-}$*:Atm*$^{-/-}$ abl pre-B cells treated with STI571 for the indicated times (hours, h). SacI and EcoRI digested genomic DNA was hybridized to the JκIII probe. The bands corresponding to the IgLκ locus in the germline configuration (GL) and Jκ1 and Jκ2 CEs are indicated.

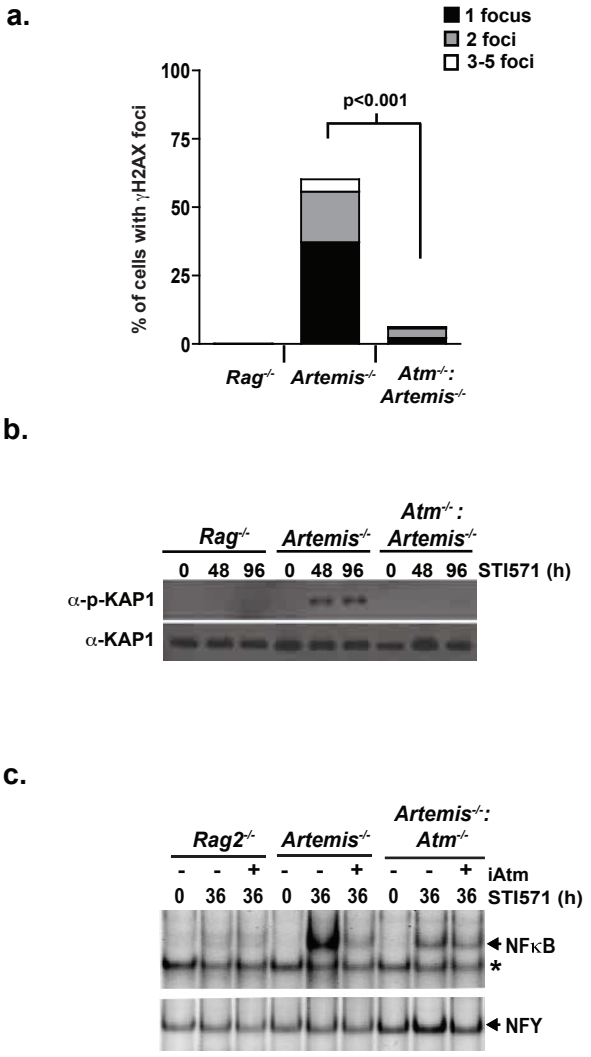

Figure 8. Evidence of ATM activation in NHEJ-deficient Abl pre-B cells. (a) Quantification of γ–H2AX nuclear foci following 24 hours of STI571 treatment. Shown is the percentage of cells containing 1, 2, or 3-5 foci γ–H2AX foci. Total number of cells analyzed for each genotype was 500 and p-values were calculated using a two-tailed Fischer's Exact test. Note that γ–H2AX foci were not detected in any of the STI571-treated Rag$^{-/-}$ abl pre-B cells. **(b)** Western blot analysis of phospho-KAP-1 (α-p-KAP-1) and KAP-1 (α-KAP-1) from STI571-treated cells shown. **(c)** NFκB EMSA of nuclear lysates from *Rag2*$^{-/-}$, *Artemis*$^{-/-}$ and *Artemis*$^{-/-}$*:Atm*$^{-/-}$ abl pre-B cells treated with STI571 for the indicated number of hours. NFY EMSA is shown as a control.

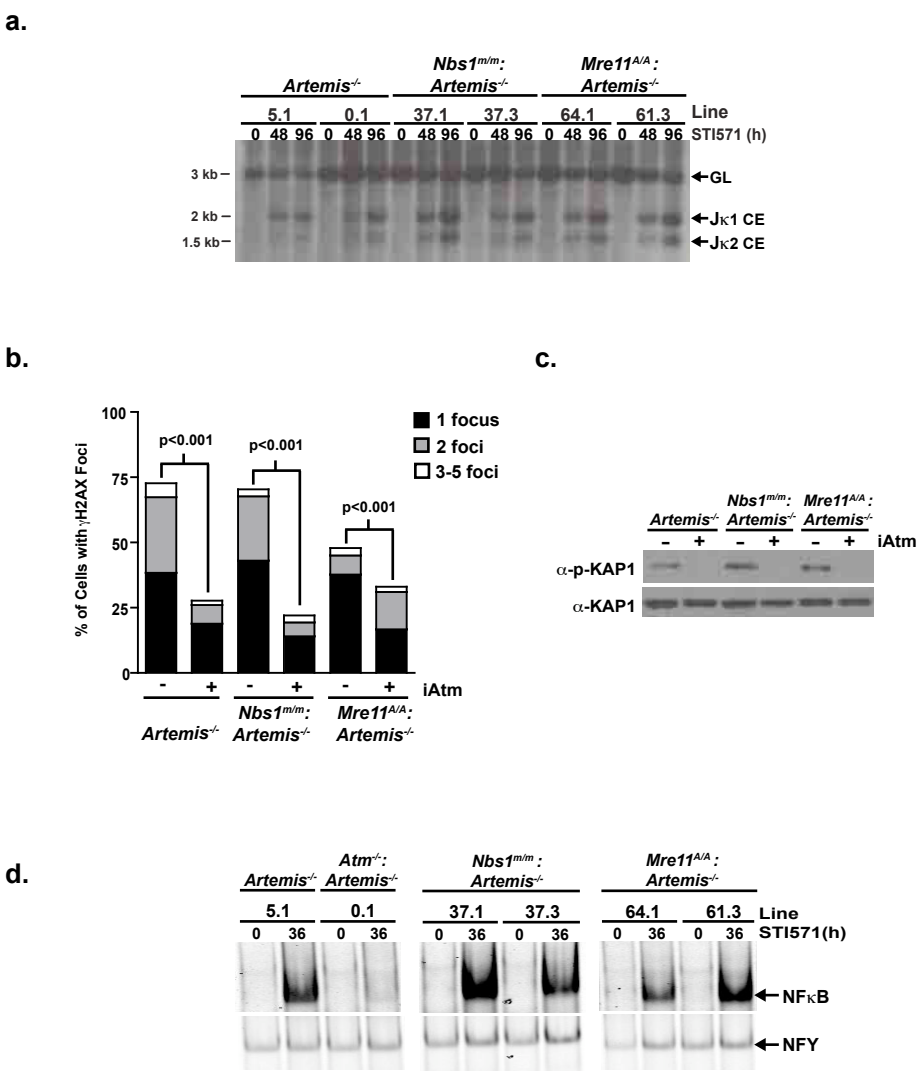

Figure 9. ATM is activated in MRN-deficient Abl pre-B cells. (a) Southern blot analysis showing Jκ1 and Jκ2 coding ends (CE) generated in *Artemis*$^{-/-}$, *Nbs1*$^{m/m}$*:Artemis*$^{-/-}$, and *Artemis*$^{-/-}$*:Mre*$^{A/A}$ abl pre-B cells treated with STI571 for the indicated times (hours, h). The bands corresponding to the IgLκ locus in the germline configuration (GL) and Jκ1 and Jκ2 CEs are indicated. **(b)** Percentage of *Artemis*$^{-/-}$, *Nbs1*$^{m/m}$*:Artemis*$^{-/-}$, and *Mre11*$^{ATLD1/ATLD1}$*:Artemis*$^{-/-}$ abl pre-B cells with 1, 2 or 3-5 nuclear γH2AX foci following treatment with STI571 for 24 hours and either DMSO (-) or the Atm inhibitor (iAtm) KU-55933 (+). Total number of cells analyzed for each genotype was 500 and p-values were calculated using a two-tailed Fischer's Exact test. **(c)** Western blot analysis for phospho-KAP-1 (α-p-KAP-1) and KAP-1 (α-KAP-1) in *Artemis*$^{-/-}$, *Nbs1*$^{m/m}$*:Artemis*$^{-/-}$, and *Mre11*$^{ATLD1/ATLD1}$*:Artemis*$^{-/-}$ abl pre-B cell lines treated with STI571 for 96 hours and either DMSO (-) or the Atm inhibitor (iAtm) KU-55933 (+). **(d)** NFκB EMSA of nuclear lysates from *Artemis*$^{-/-}$, *Atm*$^{-/-}$*: Artemis*$^{-/-}$, and two independent *Nbs1*$^{m/m}$ *:Artemis*$^{-/-}$ and *Mre11*$^{ATLD1/ATLD1}$*:Artemis*$^{-/-}$ abl pre-B cell lines treated with STI571 for 36 hours. NFY EMSA is shown as a control.

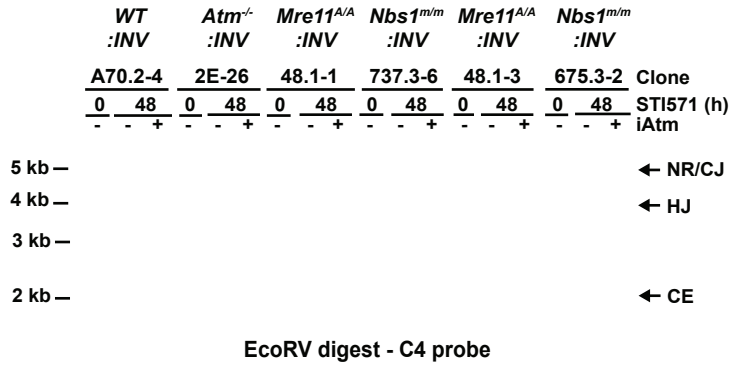

Figure 10. ATM functions during repair of Rag DNA DSBs in MRN-deficient cells. Atm inhibition in MRN-deficient cells leads to increased coding end accumulation. Southern blot analysis of EcoRV digested genomic DNA from wild type, *Atm*$^{-/-}$, and two Mre11$^{ATLD1/ATLD1}$ (labeled as *Mre11*$^{A/A}$) and *Nbs1*$^{m/m}$ abl pre-B clones containing pMX-INV. Cells were treated with STI571 for the indicated time (hours, h) and either DMSO (-) or the ATM inhibitor (iAtm) KU-55933 (+). Expected sizes for bands generated by non-rearranged substrate (NR), coding joints (CJ), hybrid joints (HJ) and coding ends (CE) are indicated.

Chapter 4

ATM Regulates the Processing of Persistent Coding Ends by Phosphorylating Histone H2AX

Previous work has demonstrated that ATM plays a critical role in the repair of RAG-mediated DNA DSBs by maintaining unrepaired ends in a post-cleavage complex thereby promoting their efficient joining, suppressing hybrid joint formation and preventing translocations(107). Furthermore, we show here that ATM may perform these functions via the phosphorylation of downstream substrates such as the MRN-complex. Interestingly, ATM also phosphorylates histone H2AX at the site of a RAG DNA DSB; we detect phosphorylation of H2AX in chromatin flanking the RAG DNA DSB up to 200 kb from the site of the break(211). The phosphorylation of H2AX is required for the accumulation of repair and signaling factors at the site of a break. Furthermore, H2AX-deficient mice have a mild defect in lymphocyte development and an increase in lymphoid tumors involving antigen receptor loci. Thus, we considered the possibility that H2AX might also play a critical role downstream of ATM in the repair of RAG DNA DSBs. However, in contrast to MRN-deficient cells, we and others have shown that there is no overt defect in V(D)J recombination in H2AX-deficient cells(233, 235, 243).

Millions of RAG DNA DSBs are generated each day. Although most RAG DNA DSBs are repaired efficiently, if even a fraction of those persist unrepaired, it could have significant deleterious effects on genomic stability. We reasoned that ATM might have additional roles in the response to or repair of DSBs that persist for some period of time. We reasoned that ATM might function in ensuring that the cells harboring these persistent breaks activate p53-mediated apoptosis rather than accessing alternative repair pathways that would lead to aberrant resolution and result in genomic instability. Furthermore, the substrates downstream of ATM that might carry out these functions might differ from those that are required for repair during V(D)J recombination. *H2AX*$^{-/-}$ mice have a high degree of genomic instability that is much increased in the absence of p53(234, 236); thus H2AX is a putative candidate for enabling this ATM-dependent effector function.

We considered the possibility that the phosphorylation of H2AX in response to persistent RAG DNA DSBs is required to prevent persistent coding ends from accessing aberrant repair pathways. As mentioned in the introduction, a key determinant in repair pathway choice is

whether and how the DNA ends are resected. Ends that are resected even a few base pairs are poor substrates for NHEJ, but end resection is required for homology mediated repair(140-142, 176). Therefore, we designed experiments to analyze the processing of persistent RAG DNA DSBs in the absence of H2AX.

Determining the outcome of unrepaired breaks in the absence of H2AX.

To determine whether H2AX affects the processing of persistent RAG DNA DSBs, we again made use of our Abl pre-B cell lines deficient in components of the NHEJ pathway; specifically, we generated cell lines deficient in Artemis or Artemis and H2AX and additionally lines deficient in DNA Ligase IV (Lig IV) or Ligase IV and H2AX and isolated clones containing single integrants of the pMX-DEL^{CJ} retroviral recombination substrate (*Artemis$^{-/-}$:DEL^{CJ}*, *Artemis$^{-/-}$:H2AX$^{-/-}$:DEL^{CJ}* and *Lig IV$^{-/-}$:DEL^{CJ}, Lig IV$^{-/-}$:H2AX$^{-/-}$:DEL^{CJ}*). Artemis is the endonuclease required to open hairpin-sealed coding end intermediates produced by RAG cleavage, while Ligase IV is the DNA ligase responsible for joining both SEs and CEs to form the SJ and CJ respectively. Deficiencies in Artemis lead to the accumulation of hairpin-sealed coding ends while deficiencies in Ligase4 lead to the accumulation of unrepaired SEs as well as hairpin-open coding ends. pMX-DEL^{CJ} differs from pMX-INV in the orientation of the RSSs such that rearrangement occurs by deletion of the intervening sequence with the coding joint being formed within the chromosomal context (Figure 2a and Figure 11a).

STI induction in *WT:DEL^{CJ}* cells leads to the robust rearrangement of pMX-DEL^{CJ}; this is evidenced by the presence of a 4 kb band on Southern blot, the size expected for a normal CJ (Figure 11). STI induction in the NHEJ-deficient cells leads to the accumulation of un-repaired coding ends with variable but low levels of CJ formation in the *Artemis$^{-/-}$:DEL^{CJ}* Abl pre-B cells but no accumulation of CJs in the *LigIV$^{-/-}$* Abl pre-B cells. The unrepaired coding ends in *Artemis$^{-/-}$:DEL^{CJ}* and *Lig IV$^{-/-}$:DEL^{CJ}* Abl pre-B cells are homogenous in size as depicted by the distinct 2.2 kb band detectable by Southern blotting (Figure 11). In striking contrast, coding ends in *Artemis$^{-/-}$:H2AX$^{-/-}$:DEL^{CJ}* and *Lig IV$^{-/-}$:H2AX$^{-/-}$:DEL^{CJ}* Abl pre-B cells are heterogenous in size with many significantly smaller (>1kb) than those in *Artemis$^{-/-}$:DEL^{CJ}* and *Lig IV$^{-/-}$:DEL^{CJ}* Abl pre-B cells

(Figure 11b and 11c). This demonstrates that unrepaired coding ends are aberrantly processed in the absence of H2AX. It additionally suggests that H2AX-deficiency permits hairpin-sealed coding ends to be opened and resected in an Artemis-independent manner, as we note degradation of the unrepaired coding ends in the *Artemis*$^{-/-}$*:H2AX*$^{-/-}$*:DEL*^{CJ} Abl pre-B cells but not the *Artemis*$^{-/-}$*:DEL*^{CJ} Abl pre-B cells.

Hairpin-sealed ends are aberrantly opened in the absence of H2AX.

To determine whether the hairpin-sealed coding ends in *Artemis*$^{-/-}$*:H2AX*$^{-/-}$*:DEL*^{CJ} Abl pre-B cells are being opened aberrantly, we needed to develop assays whereby hairpin-sealed coding ends can be distinguished from open coding ends. We developed two techniques, Southern blotting after denaturation and TdT-assisted PCR, that have enabled us to differentiate between these two recombination intermediates.

First, we decided to analyze DNA isolated from STI-treated *Artemis*$^{-/-}$*:H2AX*$^{-/-}$*:DEL*^{CJ} Abl pre-B cells by Southern blotting following denaturation. Denaturing an open hairpin forms two single-stranded fragments that migrate at a lighter molecular weight than the non-denatured duplex as evidenced by analysis of *Lig IV*$^{-/-}$ Abl pre-B cells, where hairpin-sealed coding ends are efficiently opened by the Artemis endonuclease (Figure 12a and b). In contrast, a denatured closed hairpin migrates similarly to the non-denatured duplex as evidenced by analysis of *Artemis*$^{-/-}$*:DEL*^{CJ} Abl pre-B cells where coding ends are predominantly hairpin-sealed (Figure 12a and b). Strikingly, denaturation of coding ends in *Artemis*$^{-/-}$*:H2AX*$^{-/-}$*:DEL*^{CJ} Abl pre-B cells revealed that 35-78% are open at early time-points after RAG induction (Figure 12a and b).

A second method developed in our lab to differentiate between hairpin-sealed and open coding ends is TdT-assisted PCR. This technique utilizes an enzyme, terminal deoxynucleotidyl transferase (TdT), an enzyme that adds nucleotides in a non-templated fashion to free 3'-hydroxyl groups but is unable to access hairpin-sealed coding ends. Briefly, we incubate genomic DNA with dATP and TdT; TdT then adds a string of adenosine molecules only to DNA ends with opened hairpins. This labeling step is followed by PCR using oligo-dT and substrate-specific primers as depicted in Figure 13a. Utilizing TdT PCR, we detect a robust Artemis-independent

opening of the hairpin-sealed DNA ends in the *Artemis*$^{-/-}$*:H2AX*$^{-/-}$*:DEL*^{CJ} Abl pre-B cells (Figure 13c). We conclude that hairpin-sealed coding ends in *Artemis*$^{-/-}$*:H2AX*$^{-/-}$ Abl pre-B cells are efficiently opened and resected by a nucleolytic pathway that cannot efficiently access these DNA ends in *Artemis*$^{-/-}$*:DEL*^{CJ} Abl pre-B cells.

H2AX prevents end processing in primary pre-B cell cultures.

To eliminate the possibility that this requirement for H2AX in regulating DNA end processing is unique to our Abl pre-B cell lines, we decided to perform the same analyses in primary pre-B cell cultures. Bone marrow cultures were generated from *Artemis*$^{-/-}$ and *Artemis*$^{-/-}$*:H2AX*$^{-/-}$ mice. Developing B lymphocytes in NHEJ-deficient mice normally do not progress to the pre-B cell stage as they are unable to undergo V(D)J recombination to form a heavy chain and a functional pre-B cell receptor. However, we introduced an IgH transgene (IgHtg) that drives the pro-B to pre-B transition. Thus, these cells are arrested at a pre-B cell stage where they will attempt rearrangement of the endogenous kappa locus. These cultures proliferate in the presence of IL-7, but upon withdrawal of IL-7, these cells arrest in G1 of the cell cycle, induce RAG and undergo recombination at the IgLκ locus (Figure 14b). In the NHEJ-deficient cells, just as we see in the Abl-pre B cells, induction of V(D)J recombination leads to the accumulation of unrepaired (Jκ) coding ends (Figure 14).

Withdrawal of IL-7 and the induction of RAG cleavage generates 4 distinct Jκ coding ends that are readily detectable by Southern blotting in the *Artemis*$^{-/-}$*:IgHtg* pre-B cells (Figure 14a and b). In *Artemis*$^{-/-}$*: H2AX*$^{-/-}$ *IgHtg* pre-B cells as compared to *Artemis*$^{-/-}$*:IgHtg* pre-B cells, we note that the ends are partially degraded as indicated by products of sizes intermediate to each of the four distinct coding end bands (Figure 15a). TdT-assisted PCR using primers downstream of Jκ2 corroborates this observation. We detect two bands corresponding to open coding ends produced from cleavage at either Jκ1 or Jκ2 in *Artemis*$^{-/-}$*:H2AX*$^{-/-}$*:IgHtg* pre-B cells but not *Artemis*$^{-/-}$*:IgHtg* pre-B cells (Figure 15b). Furthermore, we detect PCR products at sizes between the expected bands of Jκ1 and Jκ2 and some smaller than the product expected for cleavage at Jκ2 demonstrating that the hairpins are open and the ends are resected in the absence of H2AX

(Figure 15b). Thus, we note a requirement for H2AX in preventing hairpin-opening and resection of the unrepaired coding ends in *Artemis*$^{-/-}$*:H2AX*$^{-/-}$ in our Abl pre-B cell lines and in primary pre-B cell cultures.

The phosphorylation of H2AX and Mdc1 is required to prevent aberrant end processing.

During DNA damage responses, most H2AX-depndent processes are linked to its phosphorylation on serine 139 (forming γ-H2AX) in chromatin flanking DNA DSBs including those generated by RAG. To determine whether the phosphorylation of H2AX is required to prevent the opening and resection of persistent unrepaired coding ends, we reconstituted the *Lig IV*$^{-/-}$*:H2AX*$^{-/-}$*:DEL*^{CJ} and *Artemis*$^{-/-}$*:H2AX*$^{-/-}$*:DEL*^{CJ} Abl pre-B cells with either WT H2AX or H2AX mutated at Ser139 (S139A), the site known to be phosphorylated by ATM in response to DNA damage. We verified the expression of H2AX and equivalent levels of WT and H2AX^{S139A} mutants in these cells by Western blotting (Figure 16). We used an empty retrovirus as a control. We find that the reconstitution of *Lig IV*$^{-/-}$*:H2AX*$^{-/-}$*:DEL*^{CJ} or *Artemis*$^{-/-}$*:H2AX*$^{-/-}$*:DEL*^{CJ} Abl pre-B cells with wild type H2AX prevents coding end resection in these cells as we no longer see the degradation of coding ends by Southern blot that we see in the control cells (Figure 16). These ends are now distinct bands similar to what was observed in the *Lig IV*$^{-/-}$*: DEL*^{CJ} or *Artemis*$^{-/-}$*:DEL*^{CJ} Abl pre-B cells demonstrating that the end degradation we see is due to H2AX deficiency (Figure 11). However, reconstitution with the serine 139 to alanine mutant of H2AX (H2AX^{S139A}) does not prevent this resection (Figure 16). Thus, the function of H2AX in modulating DNA end resection in G1-phase lymphocytes relies on the formation of γ-H2AX.

Several DNA damage response proteins associate with γ-H2AX in chromatin flanking DNA breaks including Mdc1, which directly binds γ-H2AX through its BRCT domain, and functions to amplify DNA damage responses. To determine whether Mdc1 is also required to prevent hairpin-sealed coding ends from being opened and resected in an Artemis-independent fashion, we developed *Artemis*$^{-/-}$*:MDC-1*$^{-/-}$*:DEL*^{CJ} Abl pre-B cells. Upon STI treatment and the induction of RAG, we note that, similar to what was observed in the *Artemis*$^{-/-}$*:H2AX*$^{-/-}$*:DEL*^{CJ} Abl

pre-B cells, the unrepaired hairpin-sealed coding ends in the *Artemis*$^{-/-}$*:MDC-1*$^{-/-}$*:DEL*^{CJ} Abl pre-B cells are degraded (Figure 17).

ATM activates antagonistic pathways that regulate end processing.

As ATM is required to generate γ-H2AX in chromatin flanking RAG DSBs and MDC-1 amplifies DNA damage response signals, in part, by recruiting ATM to the site of a DSB, we reasoned that ATM would be required to prevent the nucleolytic resection of coding ends in G1-phase cells. To test this hypothesis, we treated the *Artemis*$^{-/-}$*:DEL*^{CJ} Abl pre-B cells with an inhibitor of ATM kinase activity (KU-55933). Interestingly, however, inhibition of ATM kinase activity did not lead to the resection of un-repaired coding ends in *Artemis*$^{-/-}$*:DEL*^{CJ} Abl pre-B cells (Figure 18a). This seemed at odds with our hypothesis as H2AX should not be phosphorylated in these cells and therefore, based on the evidence above, we would have predicted to see degradation of the unrepaired coding ends. We verified that the kinase inhibitor was working by assaying for NFκB activation in these cells as described in Chapter 3, and determined that it was, in fact, preventing ATM kinase activity. Additionally, we do not see degradation of unrepaired coding ends in the *Artemis*$^{-/-}$*:Atm*$^{-/-}$ cells although H2AX is abrogated in these cells (Figure 7b).

We therefore reasoned that ATM might also be required to promote this end processing. To test this hypothesis, we similarly treated the *Artemis*$^{-/-}$*:H2AX*$^{-/-}$*:DEL*^{CJ} Abl pre-B cells with KU-55933. This resulted in a near complete block in end resection (Figure 18a). Additionally, by analyzing these ends by Southern blotting following denaturation, we note that many of these DNA ends are now hairpin-sealed (Figure 18b). Thus, ATM is required to promote Artemis-independent hairpin-opening and end resection in the *Artemis*$^{-/-}$*:H2AX*$^{-/-}$*:DEL*^{CJ} Abl pre-B cells.

We conclude that ATM inhibits DNA end resection through the generation of γ-H2AX; however, ATM activity is also required to promote this resection. Thus, ATM activates antagonistic pathways to regulate the resection of un-repaired DNA ends in G1-phase cells.

Hairpin-opening and end resection are mediated by CtIP.

During HR, Mre11 and CtIP coordinate to regulate the end resection required to generate the 3' ssDNA overhang that is subsequently used for strand invasion. We demonstrate in

Chapter 3 that Mre11, as a component of the MRN complex, functions during V(D)J recombination. While CtIP activity is thought to be regulated at the level of protein abundance and CtIP levels are low in our G1-arrested cells, it is still expressed at a level detectable by Western. CtIP activity is also regulated by ATM, and we demonstrate that end resection in our cells is ATM-dependent. Finally, and perhaps most importantly, CtIP and Mre11 have hairpin-opening activity *in vitro*. Therefore, based on these data, we hypothesized that the Artemis-independent hairpin-opening in the absence of H2AX might be mediated by CtIP.

To investigate this possibility, we generated lentiviral shRNA constructs specific for CtIP and knocked down CtIP in *Artemis*$^{-/-}$*:H2AX*$^{-/-}$*:DEL*^{CJ} Abl pre-B cells. The knockdown in these cells was confirmed by Western blotting (Figure 19a). Analyses of un-repaired coding ends generated in cells depleted in CtIP revealed a dramatic reduction in DNA end resection as compared to cell lines transduced with a non-targeting shRNA (Figure 19a and b). Moreover, we analyzed these ends by Southern blotting following denaturation and show that many of the DNA ends in the *Artemis*$^{-/-}$*:H2AX*$^{-/-}$*:DEL*^{CJ} in which CtIP levels had been depleted are hairpin-sealed (Figure 19c). These data demonstrate that CtIP promotes the endonucleolytic opening and resection of hairpin-sealed coding ends in *Artemis*$^{-/-}$*:H2AX*$^{-/-}$ cells. Furthermore, depletion of CtIP similarly abrogates end resection in the *Lig IV*$^{-/-}$*:H2AX*$^{-/-}$*:DEL*^{CJ} Abl pre-B cells (Figure 20a and b). The low level of resection observed in the CtIP-deficient cells (both *Lig IV*$^{-/-}$*:H2AX*$^{-/-}$*:DEL*^{CJ} and *Artemis*$^{-/-}$*:H2AX*$^{-/-}$*:DEL*^{CJ}) might reflect the activity of additional nucleolytic pathways inhibited by H2AX or the activity of the residual CtIP in these cells (Figure 19a, b and 20). We conclude that H2AX prevents CtIP from efficiently promoting hairpin opening and resection of un-repaired DNA ends in G1-phase lymphocytes.

H2AX prevents homology-mediated joining in G1-phase cells.

Coding ends opened by CtIP in *Artemis*$^{-/-}$*:H2AX*$^{-/-}$ Abl pre-B cells DNA are not efficiently joined by NHEJ as evidenced by the abundance of unrepaired coding ends in these cells even at late time-points (Figure 11). This is surprising given that all core components of the NHEJ pathway are present in these cells, and Artemis is only required for the opening of the hairpin-

sealed end prior to joining and cells deficient in Artemis do not have a general defect in NHEJ as evidenced by normal SJ formation in *Artemis*$^{-/-}$ cells. The single strand overhangs generated by CtIP-dependent processing in S-G2-M are essential for homologous recombination; however, in G1, these ends would be poor substrates for classical NHEJ possibly explaining why we do not see robust levels of CJ formation in these cells following the opening of the hairpin-sealed end.

We reasoned, though, that if DNA ends processed by CtIP in G1-phase cells are joined efficiently primarily by homology-mediated pathways, then we might expect to find joints with significant deletions due to the use of homologous sequences in *cis* to promote joining. To address this possibility, we designed PCR primers to detect coding joints with significant deletions (≤ 600 bp) in our retroviral recombination substrate (Figure 21a). These analyses revealed that the coding joints formed in *Artemis*$^{-/-}$*:H2AX*$^{-/-}$*:DEL*^{CJ} Abl pre-B cells are heterogenous in size as compared to *Artemis*$^{-/-}$*:DEL*^{CJ} and *WT:DEL*^{CJ} Abl pre-B cells (Figure 21b). Sequence analyses confirmed that these coding joints have significant deletions (Figure 21c and Table 5).

While NHEJ does not require homologous sequences to join broken DNA ends, alternative pathways exist that do require varying degrees of homology to mediate end joining. We decided to clone and sequence individual CJs from *Artemis*$^{-/-}$*:H2AX*$^{-/-}$*:DEL*^{CJ}, *Artemis*$^{-/-}$*:DEL*^{CJ} and *WT:DEL*^{CJ} Abl pre-B cells to determine whether the CJs that form in the *Artemis*$^{-/-}$*:H2AX*$^{-/-}$*:DEL*^{CJ} Abl pre-B cells more frequently exhibit homologous sequences at the joint. These sequence analyses revealed that a higher fraction of the coding joints formed in *Artemis*$^{-/-}$*:H2AX*$^{-/-}$*:DEL*^{CJ} cells use microhomologies (≥ 1 base pairs) as compared to coding joints generated in *WT:DEL*^{CJ} and *Artemis*$^{-/-}$*:DEL*^{CJ} Abl pre-B cells (Figure 21d and Table 5). Moreover, coding joints formed in *Artemis*$^{-/-}$*:H2AX*$^{-/-}$*:DEL*^{CJ} Abl pre-B cells have generally longer tracts of microhomology (Figure 21d and Table 5).

Notably, the homologous LTR sequences that flank pMX-DEL^{CJ} could be used for homology-mediated joining if the 5' and 3' coding ends were resected as much as 1kb and 2kb, respectively (Figure 22a). We reasoned, that in the absence of H2AX, we might detect repair mediated by the homology of these repeats. To address this possibility, we determined the

location of the retroviral integration site for each of the cell lines. Then, we designed primers to genomic regions flanking the integration sites of pMX-DEL^{CJ} in these cells (Figure 22a). PCR with these primers revealed products of a size expected from LTR-LTR homology mediated joining. These products increased in abundance after RAG induction in an ATM-dependent manner in *Artemis*$^{-/-}$*:H2AX*$^{-/-}$*:DEL*^{CJ}, but not in *Artemis*$^{-/-}$*:DEL*^{CJ}, Abl pre-B cells (Figure 22b). These data further demonstrate that homology-mediated repair occurs more frequently in the *Artemis*$^{-/-}$*:H2AX*$^{-/-}$*:DEL*^{CJ} cells.

Conclusion

We demonstrate that, in G1-phase lymphocytes, the ATM-dependent formation of γ-H2AX inhibits the robust CtIP-dependent opening and resection of hairpin-sealed broken DNA (coding) ends generated by the RAG endonuclease. The DNA ends that have undergone aberrant CtIP-dependent processing are not efficiently joined by NHEJ. Furthermore, the joints that do form exhibit large deletions that would preclude the formation of a functional antigen receptor gene and usage of homology-mediated repair, which in G1-phase cells, would promote genomic instability and possibly lead to cellular transformation.

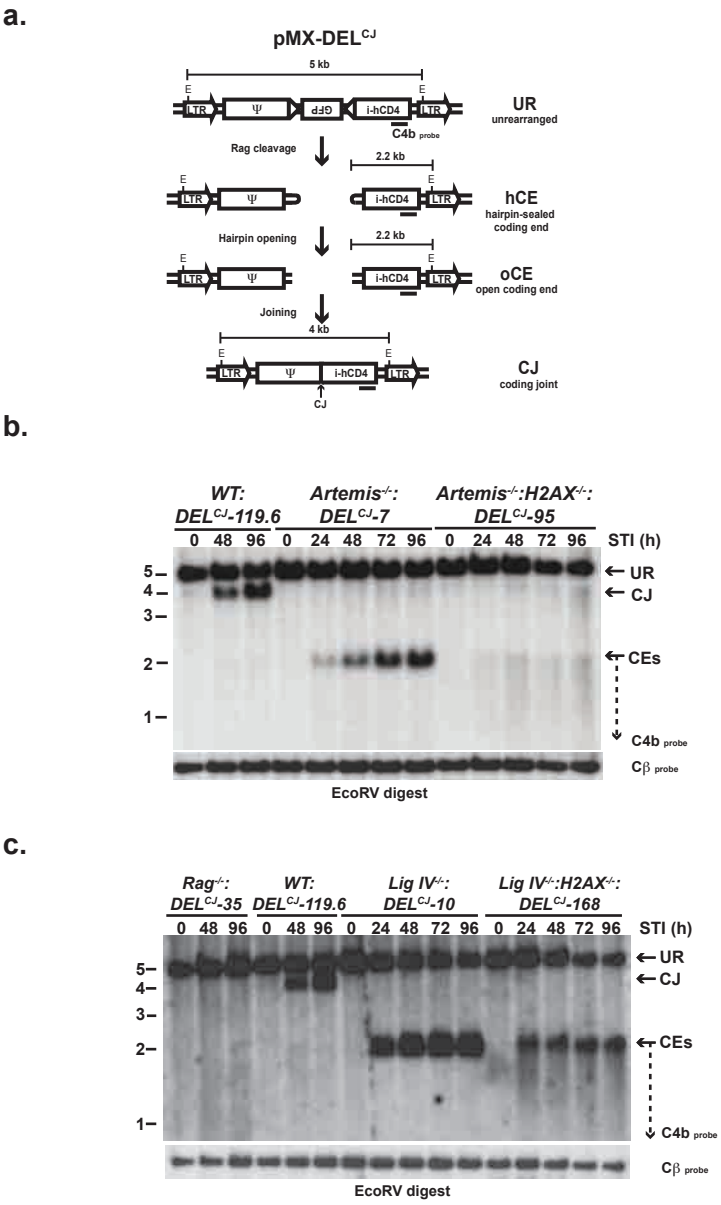

Figure 11. Aberrant processing of persistent coding ends in the absence of H2AX. **(a)** Schematic of the pMX-DEL^{CJ} retroviral recombination substrate. Shown are the un-rearranged substrate (UR), hairpin sealed (hCE) and open (oCE) coding end (CE) intermediates and coding joints (CJ). The RSs (open triangles), ψ sequence, IRES-hCD4 cDNA (i-hCD4) and the LTRs are indicated. Relative positions of EcoRV sites and the C4b probe (black bar) are shown. **(b)** Southern blot analysis of EcoRV-digested genomic DNA from *WT:DEL^{CJ}-119*, *Artemis$^{-/-}$:DEL^{CJ}-81* and *Artemis$^{-/-}$:H2AX$^{-/-}$:DEL^{CJ}-124* abl pre-B cells treated with STI571 for the indicated time. Bands reflecting pMX-DEL^{CJ} UR, CE and CJ are indicated. Cβ probe hybridization is shown as a DNA loading control and molecular weight markers (kb) are indicated. Dotted arrow indicates hybridization to resected CEs. **(c)** Southern blot analysis of pMX-DEL^{CJ} rearrangement on EcoRV-digested genomic DNA from *Rag$^{-/-}$:DEL^{CJ}-35*, *WT:DEL^{CJ}-119.6*, *LigIV$^{-/-}$:DEL^{CJ}-10* and *LigIV$^{-/-}$:H2AX$^{-/-}$:DEL^{CJ}-168* abl pre-B cell lines.

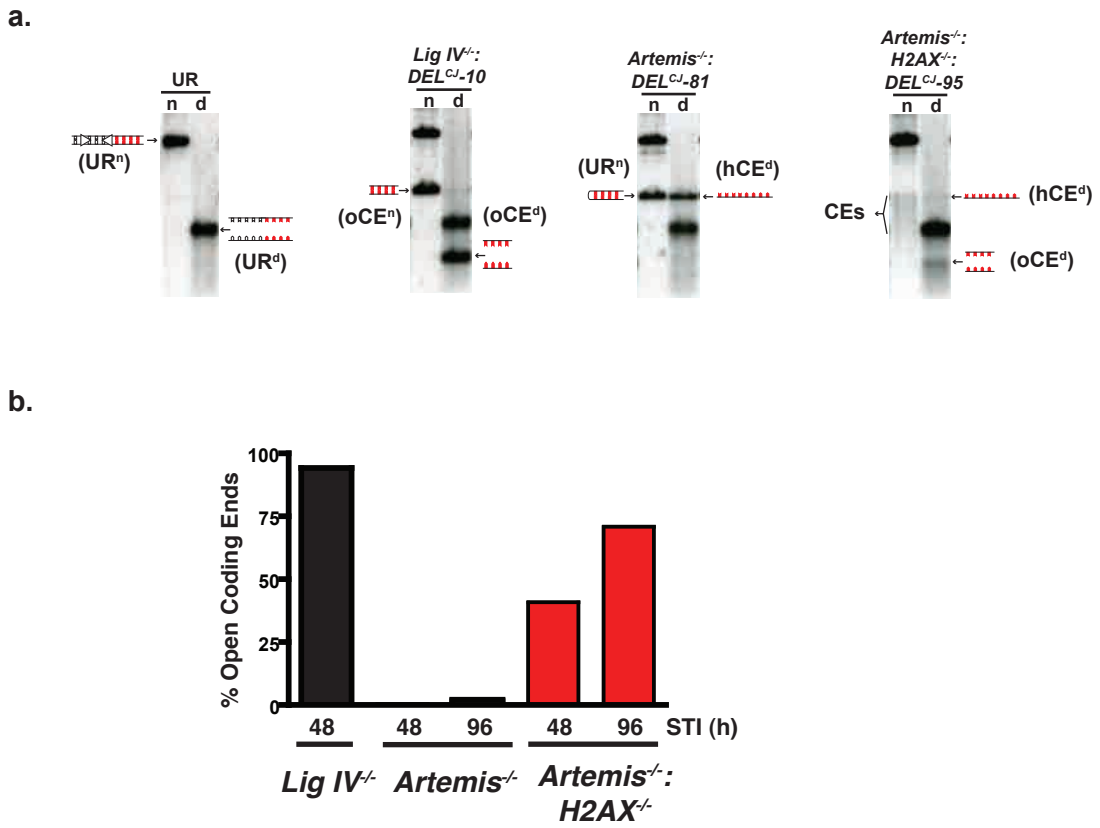

Figure 12. Persistent hairpin-sealed coding ends are opened in the absence of H2AX. **(a)** Southern blot analysis of non-denatured (n) or denatured (d) EcoRV-digested genomic DNA from *Lig IV*$^{-/-}$*:DEL*^{CJ}*-10*, *Artemis*$^{-/-}$*:DEL*^{CJ}*-81* and *Artemis*$^{-/-}$*:H2AX*$^{-/-}$*:DEL*^{CJ}*-95* abl pre-B cells treated with STI571 for 48 hours as well as from *Lig IV*$^{-/-}$*:DEL*^{CJ}*-10* abl pre-B cells not treated with STI. Hybridizing bands reflecting non-denatured hairpin-sealed CEs (hCE^{n}), denatured hairpin-sealed CEs (hCE^{d}), non-denatured open CEs (oCE^{n}), denatured open CEs (oCE^{d}), non-denatured UR (UR^{n}), denatured UR (UR^{d}), non-denatured CJ (CJ^{n}) and denatured CJ (CJ^{d}) pMX-DEL^{CJ} are indicated. **(b)** Quantification of denaturing Southern showing the percentage of coding ends that are open in *LigaseIV*$^{-/-}$*:DEL*^{CJ}, *Artemis*$^{-/-}$*:DEL*^{CJ}, and *Artemis*$^{-/-}$*:H2AX*$^{-/-}$*:DEL*^{CJ} treated with STI571 for 48 or 96 hours as indicated.

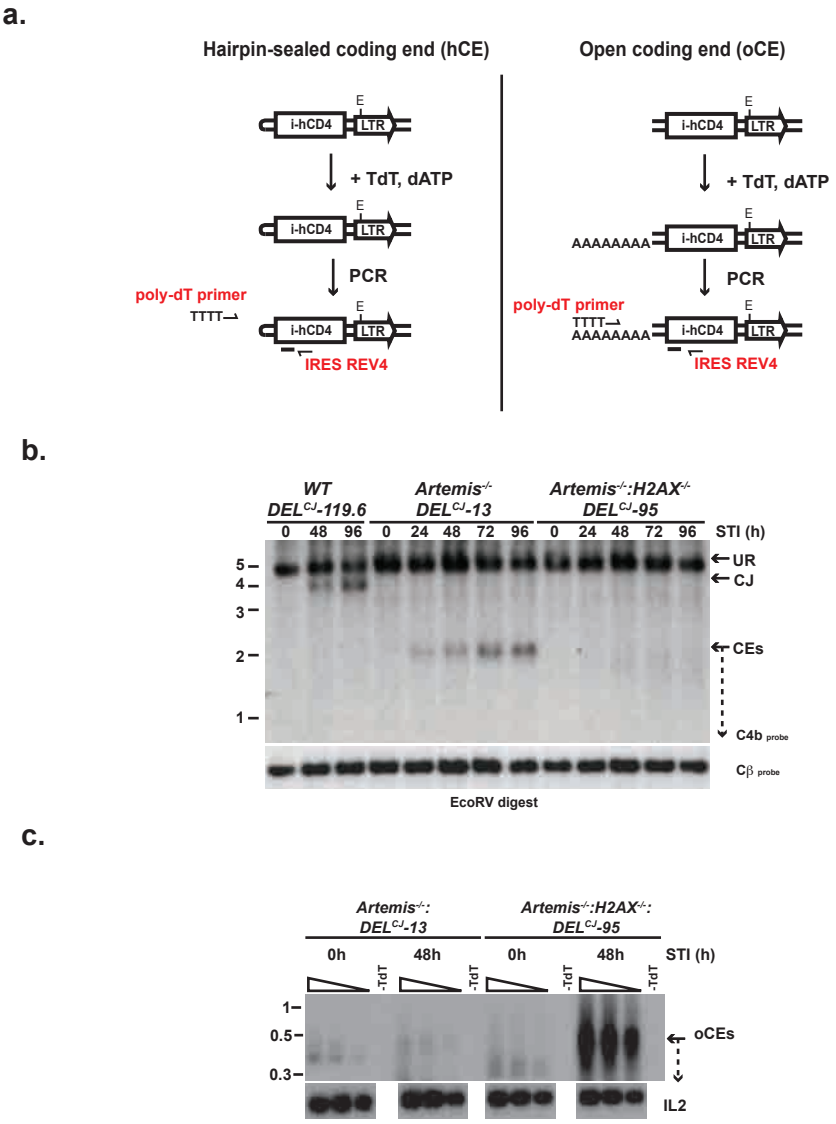

Figure 13. Detection of open coding ends by TdT-assisted PCR. (a) Schematic of Southern blotting strategy for TdT-assisted PCR for pMX-DEL^{CJ} rearrangement. Open coding ends have an accessible 3'-hydroxyl group and a series of adenosine residues will be added to the 3' end upon incubation with TdT and dATP. PCR with a poly-dT primer and a substrate specific primer will yield the PCR product shown. Relative position of oligo probe is also shown. Coding ends that are open and degraded will yield PCR products of smaller size. Hairpin-sealed ends are not accessible to TdT labeling and therefore, will yield no product. **(b)** Southern blot analysis of pMX-DEL^{CJ} rearrangement on EcoRV-digested genomic DNA from *WT:DEL^{CJ}-119*, *Artemis$^{-/-}$:DEL^{CJ}-13* or *Artemis$^{-/-}$:H2AX$^{-/-}$:DEL^{CJ}-95* abl pre-B cells treated with STI571 for the indicated amount of time. Southern blots were carried out as described in Figure 11 **(c)** Southern blot of PCR products from TdT-assisted PCR of pMX-DEL^{CJ} coding end intermediates from *Artemis$^{-/-}$* and *Artemis$^{-/-}$:H2AX$^{-/-}$* abl pre-B cells shown in (b) treated with STI571 for 0 or 48h. Arrow indicates the expected position of an un-processed open coding end. PCR products from samples not treated with TdT are shown as a negative control. IL2 is provided as a loading control.

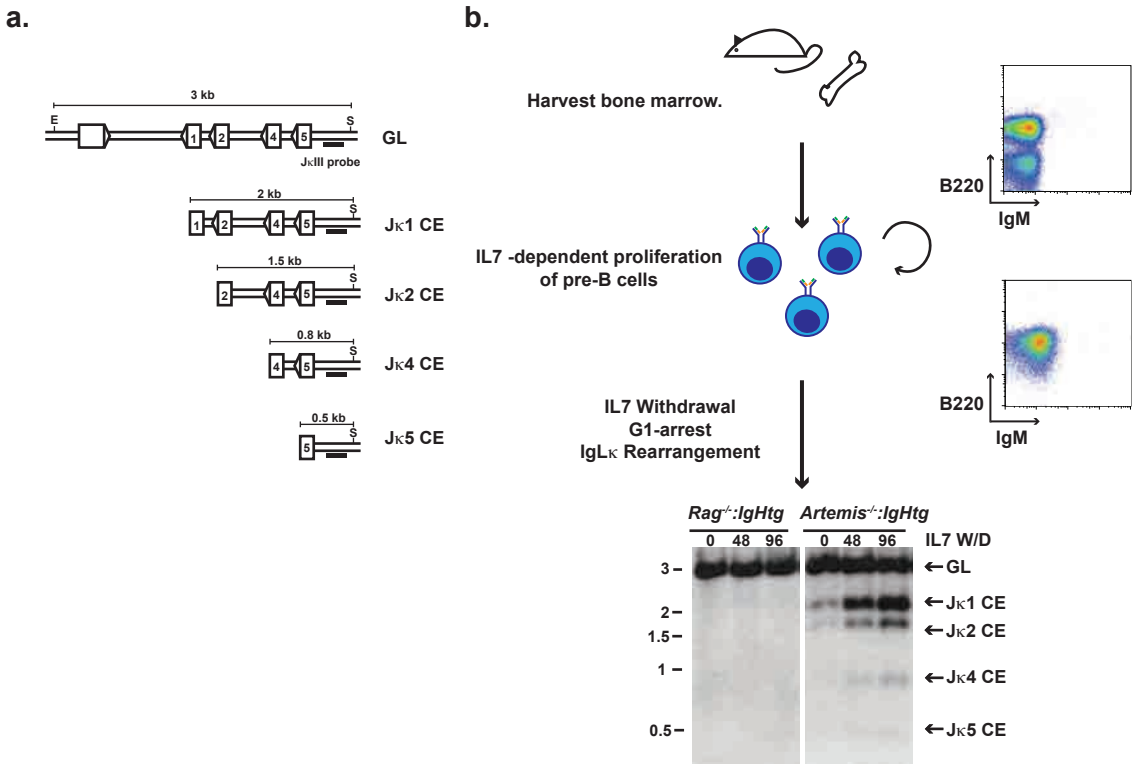

Figure 14. Utilizing IL7-dependent pre-B cell cultures to analyze V(D)J recombination. (a) Schematic demonstrating Southern blotting strategy for analyzing rearrangement at the endogenous IgL-κ locus. Shown is the un-rearranged or germline configuration (GL) as well as the four possible coding ends (CE) corresponding to cleavage at each of the four Jκ gene segments (Jκ1 CE, Jκ2 CE, Jκ4 CE, and Jκ5 CE). Gene segments are indicated by boxes and RSSs by triangles. The relative positions of the EcoRI and SacI restriction enzyme sites as well as the 3' Jκ probe used (JκIII) are shown. **(b)** Demonstration of usage of IL7 pre-B cell cultures. Bone marrow from *Rag*$^{-/-}$ or *Artemis*$^{-/-}$ mice harboring an IgH transgene that promotes development to the pre-B cell stage is harvested (B220^{+}, IgM^{-}). These cells preferentially proliferate in the presence of IL-7 and following 5-10 days in culture are the predominant cell type (see FACS plot). Upon withdrawal of IL7, these cells arrest in G1, express Rag and undergo rearrangement of the endogenous kappa light chain locus. Southern blot analysis of recombination at the IgL-κ locus in *Rag*$^{-/-}$*:IgHtg* and *Artemis*$^{-/-}$*:IgHtg* is provided demonstrating the accumulation of unrepaired coding ends following IL7 withdrawal in the *Artemis*$^{-/-}$ but not the *Rag*$^{-/-}$ cells.

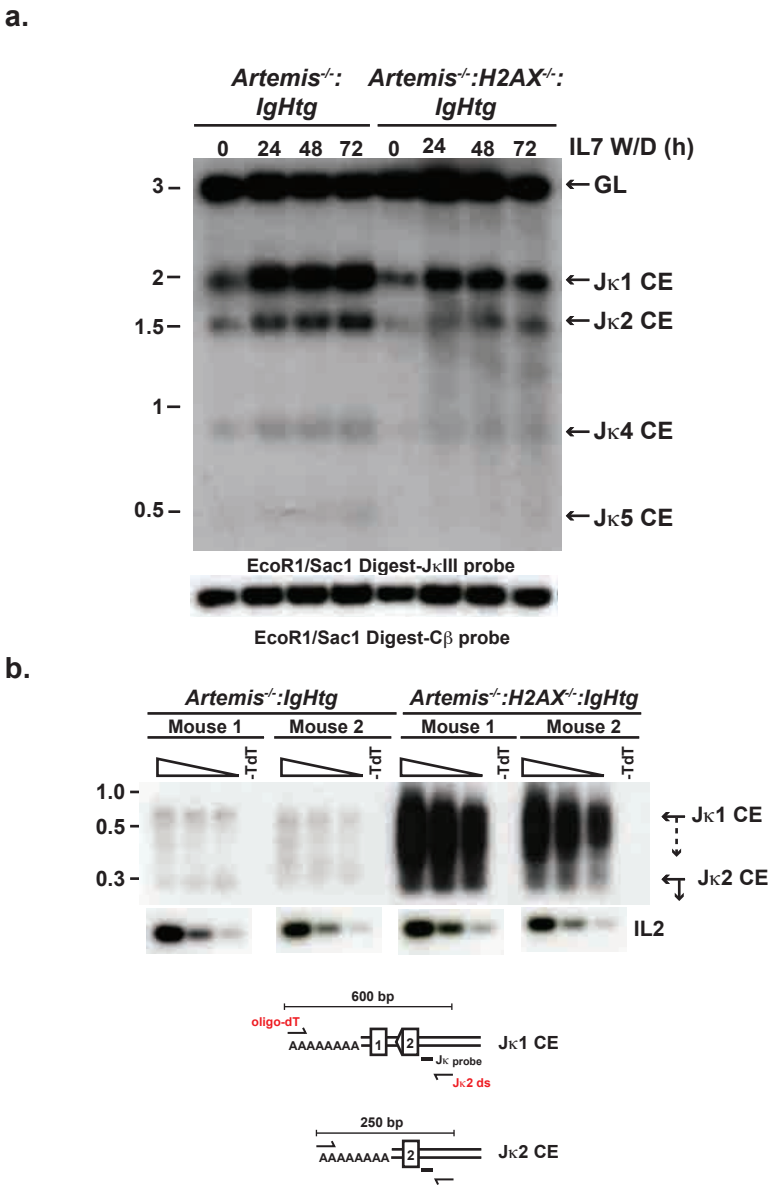

Figure 15. H2AX prevents resection of persistent coding ends in primary cells. **(a)** Southern blot analysis of recombination at the IgL-κ locus in *Artemis*$^{-/-}$*:IgHtg* and *Artemis*$^{-/-}$*:H2AX*$^{-/-}$*:IgHtg* IL7 pre-B cell cultures while in IL7 or following removal of IL7 for the indicated amount of time. **(b)** Southern blot of TdT-assisted PCR products of IgLκ CE intermediates in bone marrow pre-B cells from two *Artemis*$^{-/-}$*:IgHtg* and *Artemis*$^{-/-}$*:H2AX*$^{-/-}$*:IgHtg* mice 48 hours after IL-7 withdrawal. Expected products for Jκ1 and Jκ2 CEs are indicated. PCR products from samples not treated with TdT are shown as a negative control. IL2 gene PCR is provided as a DNA loading control.

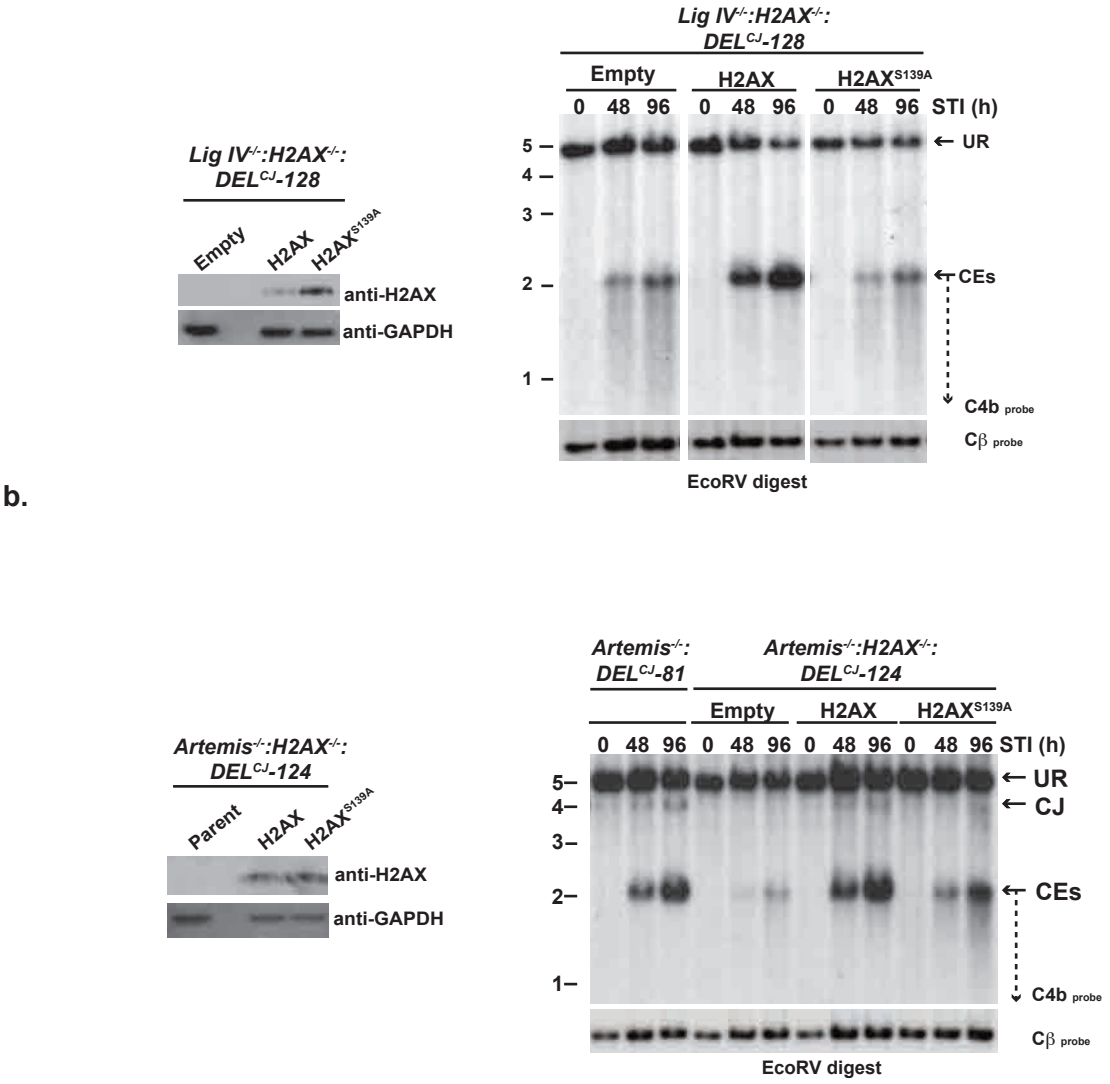

Figure 16. Phosphorylation of H2AX is required to prevent aberrant resection of persisten coding ends. (a) Western blot analysis showing H2AX levels in *LigIV$^{-/-}$:H2AX$^{-/-}$:DEL^{CJ}-128* abl pre-B cells reconstituted with WT (H2AX) or mutant H2AX (H2AX^{S139A}) and Southern blot analysis of pMX-DEL^{CJ} rearrangement in these cells. **(b)** As in (a) but for *Artemis$^{-/-}$:H2AX$^{-/-}$:DEL^{CJ}-124* reconstituted with WT (H2AX) or mutant H2AX (H2AX^{S139A}).

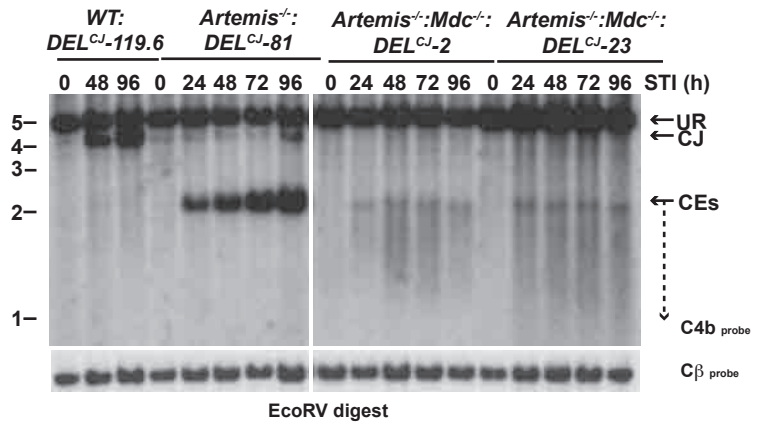

Figure 17. Mdc is required to prevent resection of persistent hairpin-sealed coding ends. Southern blot analysis of pMX-DEL^{CJ} rearrangement on EcoRV-digested genomic DNA from *WT:DEL^{CJ}-119.6*, *Artemis$^{-/-}$:DEL^{CJ}-81* and *Artemis$^{-/-}$:Mdc$^{-/-}$:DEL^{CJ}-2* and *-23* Abl pre-B cells treated with STI571 for the indicated amount of time. Southern blots were carried out as described in Figure 11.

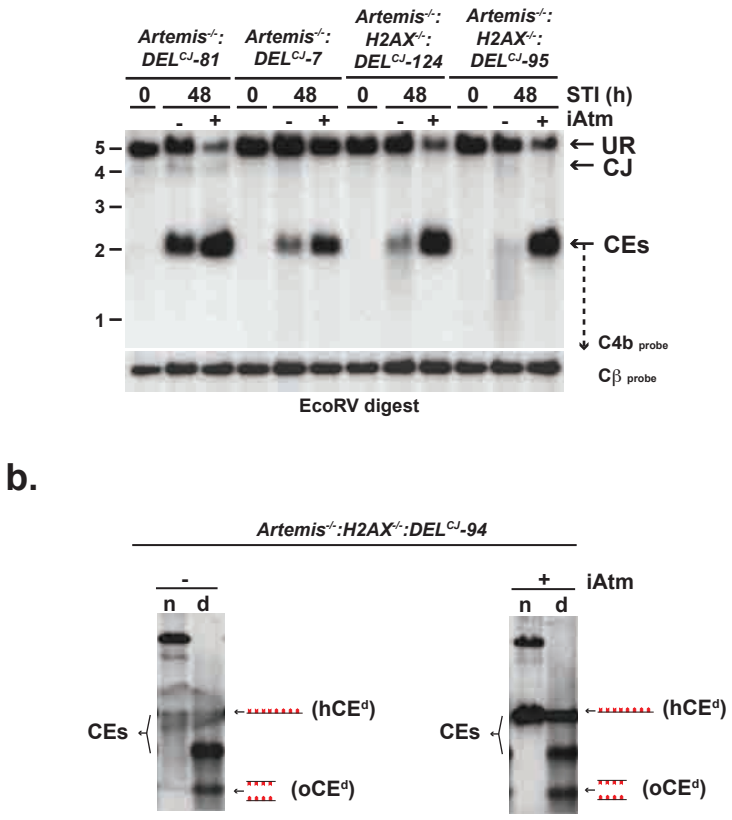

Figure 18. ATM activity is required to promote end resection. **(a)** Analysis of pMX-DEL^{CJ} rearrangement in two *Artemis*$^{-/-}$ (*Artemis*$^{-/-}$*:DEL*^{CJ}*-81* and *-7*) and two *Artemis*$^{-/-}$*:H2AX*$^{-/-}$ (*Artemis*$^{-/-}$*:H2AX*$^{-/-}$*:DEL*^{CJ}*-124* and *-95*) abl pre-B cells treated with STI571 for the indicated amount of time and treated with either the ATM-specific inhibitor KU55933 (+) or a DMSO vehicle control (-). **(b)** Southern blot analysis of pMX-DEL^{CJ} rearrangement on non-denatured (n) and denatured (d) EcoRV-digested genomic DNA samples from *Artemis*$^{-/-}$*:H2AX*$^{-/-}$*:DEL*^{CJ}*-94* Abl pre-B cells treated with STI571 for 48 hours.

a.

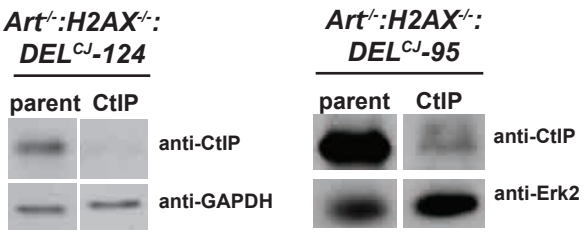

b.

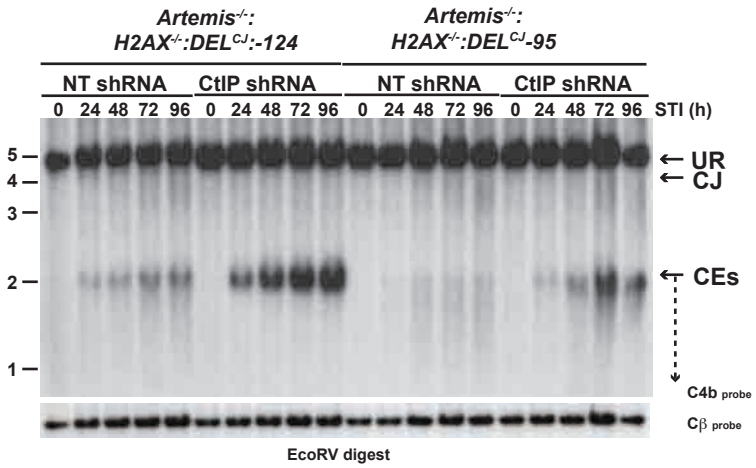

c.

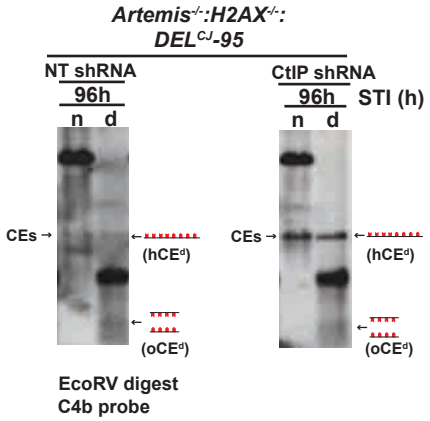

Figure 19. CtIP mediates opening and resection of persistent hairpin-sealed coding ends. (a) Western blot analysis of *Artemis*$^{-/-}$*:H2AX*$^{-/-}$*:DEL*^{CJ}*-124* and *-95* Abl pre-B cells expressing CtIP-specific shRNA. GAPDH or Erk2 are shown as loading controls. **(b)** Southern blot analysis of pMX-DEL^{CJ} rearrangement in *Artemis*$^{-/-}$*:H2AX*$^{-/-}$*:DEL*^{CJ}*-124* and *-95* Abl pre-B cells expressing either non-targeting (NT) or CtIP-specific (CtIP) shRNAs and treated with STI571 for the indicated amount of time. **(c)** Southern blot analysis of pMX-DEL^{CJ} rearrangement in *Artemis*$^{-/-}$*:H2AX*$^{-/-}$*:DEL*^{CJ}*-95* cells treated with STI571 for 48 hours. DNA was run under non-denaturing (n) and denaturing (d) conditions.

a.

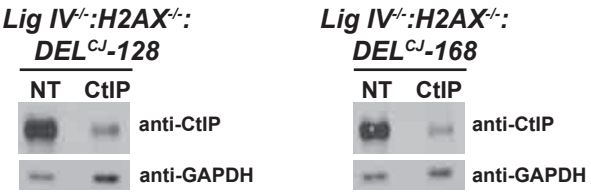

b.

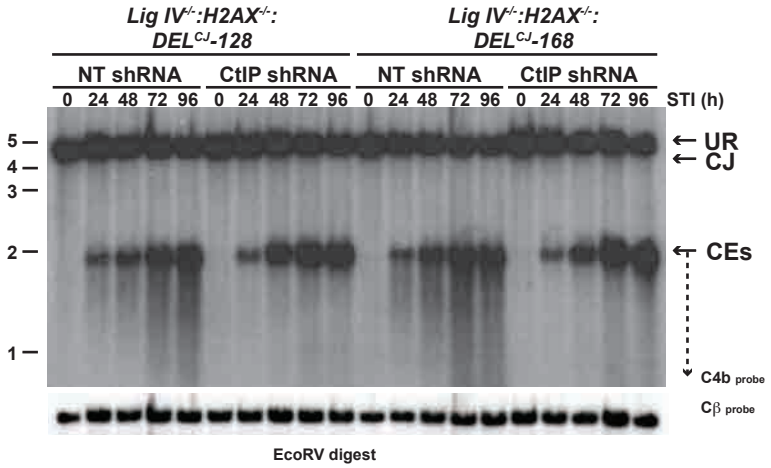

Figure 20. CtIP mediates resection of persistent open coding ends in the absence of H2AX. **(a)** Western blot analysis demonstrating CtIP knockdown for *LigIV$^{-/-}$:H2AX$^{-/-}$:DEL^{CJ}-128* and *-168* expressing CtIP-specific or non-targeting shRNA constructs. GAPDH is shown as a loading control. **(b)** Southern blot analysis of pMX-DEL^{CJ} rearrangement in *LigIV$^{-/-}$:H2AX$^{-/-}$:DEL^{CJ}-128* and *-168* expressing either non-targeting (NT) or CtIP-specific (CtIP) shRNAs and treated with STI571 for the indicated amount of time.

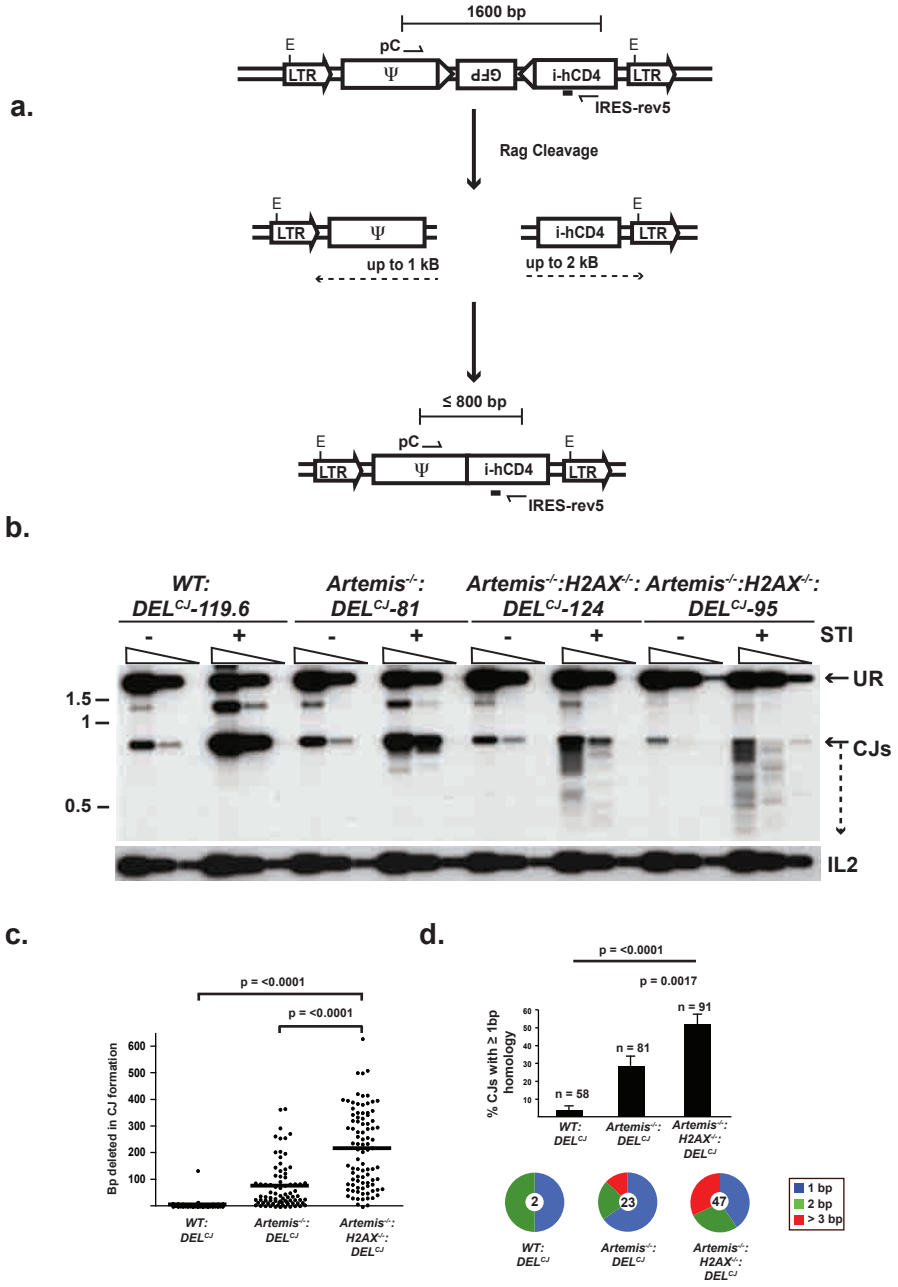

Figure 21. Coding joints formed exhibit significant deletions and usage of microhomologies. **(a)** Schematic of pMX-DEL^{CJ} showing relative positions of the oligonucleotides used to amplify aberrant pMX-DEL^{CJ} joints and the oligonucleotide used as a probe. **(b)** PCR of pMX-DEL^{CJ} coding joints in *WT:DEL^{CJ}-119.6*, *Artemis$^{-/-}$:DEL^{CJ}-81* and *Artemis$^{-/-}$:H2AX$^{-/-}$:DEL^{CJ}-124* and *-95* abl pre-B cells treated with STI571 for 0 (-) or 96 (+) hours using the pC and IRES REV5 oligonucleotides. PCR products were probed with the IRES REV4 oligonucleotide. Bands representing un-rearranged pMX-DEL^{CJ} substrate (UR) and an unprocessed coding joint (CJ) are indicated. Coding joints with deletion are visualized as hybridizing fragments lower in molecular weight than the CJ species. IL2 is shown as a loading control. **(c-d)** Nucleotide deletions **(c)** and microhomologies **(d)** in pMX-DEL^{CJ} coding joints formed in *WT:DEL^{CJ}*, *Artemis$^{-/-}$:DEL^{CJ}* and *Artemis$^{-/-}$:H2AX$^{-/-}$:DEL^{CJ}* Abl pre-B cells treated with STI571 .

a.

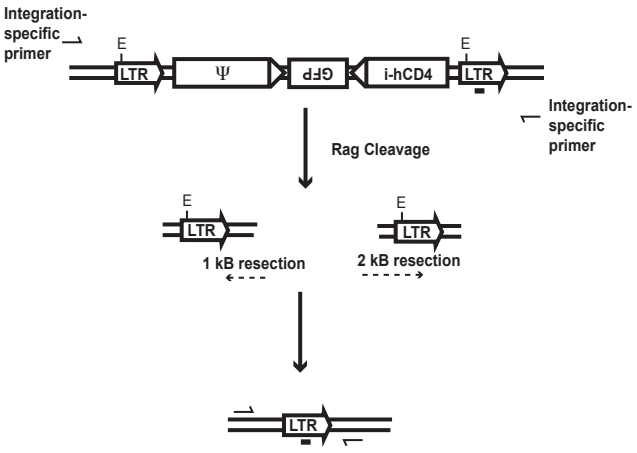

b.

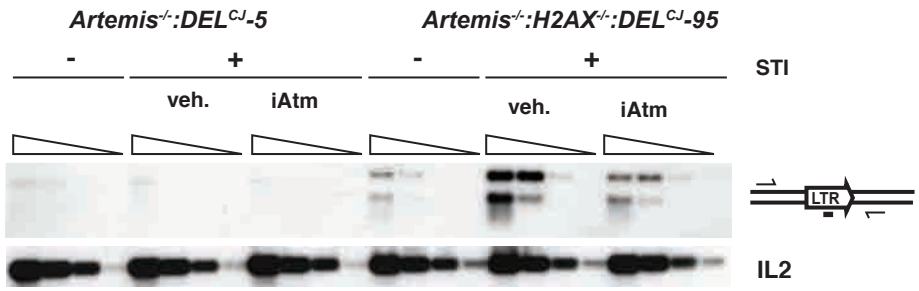

Figure 22. Detection of coding joint formation mediated by the homologous LTR sequences. (a) Schematic of pMX-DEL^{CJ} showing relative positions of the oligonucleotides used to amplify joints formed due to the homology of the LTRs and the oligonucleotide used as a probe. **(b)** PCR of pMX-DEL^{CJ} coding joints in *Artemis$^{-/-}$:DEL^{CJ}* and *Artemis$^{-/-}$:H2AX$^{-/-}$:DEL^{CJ}* abl pre-B cells not treated (-) or treated (+) with STI571 and vehicle or KU-55933 (iATM) using integration specific primers designed to detect homology-mediated joining that deletes pMX-DEL^{CJ} leaving a single LTR.

WT:DEL^{CJ}

# Lost	5' CE	N/P	3' CE	# Lost	
1	GAACGTCTG GAACGTCT		CAGCCTACAATTCC ACAATTCC	6	
4	TAGGAACGTCTG TAGGAACG		CAGCCTACAAT CCTACAAT	3	
2	GGAACGTCTG GGAACGTC		CAGCCTACAA GCCTACAA	2	
1	GAACGTCTG GAACGTCT		CAGCCTAC CAGCCTAC	0	
1	GAACGTCTG GAACGTCT		CAGCCTACA AGCCTACA	1	
0	AACGTCTG AACGTCTG		CAGCCTACAATTCC ACAATTCC	6	
0	AACGTCTG AACGTCTG		CAGCCTACAATTC TACAATTC	5	
2	GGAACGTCTG GGAACGTC		CAGCCTAC CAGCCTAC	0	
0	AACGTCTG AACGTCTG		CAGCCTACA AGCCTACA	1	
0	AACGTCTG AACGTCTG		CAGCCTAC CAGCCTAC	0	*13
0	AACGTCTG AACGTCTG	G	CAGCCTAC CAGCCTAC	0	
0	AACGTCTG AACGTCCG	CTG	CAGCCTAC CAGCCTAC	0	
0	AACGTCTG AACGTCTG	CCTTG	CAGCCTAC CAGCCTAC	0	
0	AACGTCTG AACGTCTG	A	CAGCCTACA AGCCTACA	1	
0	AACGTCTG AACGTCTG	G	CAGCCTACA AGCCTACA	1	
0	AACGTCTG AACGTCTG	C	CAGCCTACAA GCCTACAA	2	*3
0	AACGTCTG AACGTCTG	GG	CAGCCTACAA GCCTACAA	2	*4
0	AACGTCTG AACGTCTG	A	CAGCCTACAAT CCTACAAT	3	
0	AACGTCTG AACGTCTG	CA	CAGCCTACAAT CCTACAAT	3	
0	AACGTCTG AACGTCTG	AG	TACAATTCCGCCCC TCCGCCCC	11	
1	GAACGTCTG GAACGTCT	A	CAGCCTAC CAGCCTAC	0	
1	GAACGTCTG GAACGTCT	TG	CAGCCTAC CAGCCTAC	0	
1	GAACGTCTG GAACGTCT	ACCCCCT	CAGCCTAC CAGCCTAC	0	
1	GAACGTCTG GAACGTCT	A	CAGCCTACA AGCCTACA	1	
1	GAACGTCTG GAACGTCT	CCTTACG	CAGCCTACAA GCCTACAA	2	
1	GAACGTCTG GAACGTCT	C	CAGCCTACAAT CCTACAAT	3	
2	GGAACGTCTG GGAACGTC	G	CAGCCTAC CAGCCTAC	0	
2	GGAACGTCTG GGAACGTC	CTTG	CAGCCTAC CAGCCTAC	0	
2	GGAACGTCTG AGAACGTC	CCC	CAGCCTAC CAGCCTAC	0	*3
2	GGAACGTCTG GGAACGTC	GAGATG	CAGCCTAC CAGCCTAC	0	
2	GGAACGTCTG GGAACGTC	TGA	CAGCCTACA AGCCTACA	1	
2	GGAACGTCTG GGAACGTC	CGCG	CAGCCTACAA GCCTACAA	2	
2	GGAACGTCTG GGAACGTC	CA	GCCTACAATTCCCG AATTCCCG	8	
3	AGGAACGTCTG AGGAACGT	G	CAGCCTAC CAGCCTAG	0	
4	TAGGAACGTCTG TAGGAACG	GGTG	CAGCCTAC CAGCCTAC	0	*3
3	AGGAACGTCTG AGGAACGG	G	CAGCCTAC CAGCCTAC	0	
3	AGGAACGTCTG AGGAACGT	TG	CAGCCTAC CAGCCTAC	0	
3	AGGAACGTCTG AGGAACGT	CG	CAGCCTAC CAGCCTAC	0	
3	AGGAACGTCTG AGGAACGT	TTG	CAGCCTAC CAGCCTAC	0	
3	AGGAACGTCTG TAGGAACG	GTG	CAGCCTAC CAGCCTAC	0	
3	AGGAACGTCTG AGGAACGT	TTTG	CAGCCTAC CAGCCTAC	0	
3	AGGAACGTCTG AGGAACGT	CCCGTG	CAGCCTAC CAGCCTAC	0	
3	AGGAACGTCTG AGGAACGT	TTGAG	CAGCCTACAA GCCTACAA	2	
4	TAGGAACGTCTG TAGGAACG	G	CAGCCTAC CAGCCTAC	0	
4	TAGGAACGTCTG TAGGAACG	CCG	CAGCCTAC CAGCCTAC	0	
4	TAGGAACGTCTG TAGGAACG	CCCG	CAGCCTAC CAGCCTAC	0	
4	TAGGAACGTCTG TAGGAACG	CTTCTG	CAGCCTAC CAGCCTAC	0	
4	TAGGAACGTCTG TAGGAACG	GCTGG	CAGCCTACA AGCCTACA	1	
4	TAGGAACGTCTG TAGGAACG	GCTAAGG	CAGCCTACAAT CCTACAAT	3	
4	TAGGAACGTCTG TAGGAACG	G	CAGCCTACAATT CTACAATT	4	
4	TAGGAACGTCTG AACGTCTG	A	CAGCCTACAATTCC ACAATTCC	6	

# Lost	5' CE	N/P	3' CE	# Lost
4	TAGGAACGTCTG TAGGAACG	CCGC	AGCCTACAATTCCC CAATTCCG	7
4	TAGGAACGTCTG TAGGAACG	CCG	GCCTACAATTCCCG CAGCCTAC	8
4	TAGGAACGTCTG TAGGAACG	C	ACAATTCCGCCCCC CCGCCCCC	12
7	TATTAGGAACGTCT TATTAGGA	GAGTCT	CAGCCTAC CAGCCTAC	0
7	TATTAGGAACGTCT TAATAGGA	CGCTGCC	CAGCCTACAAT CCTACAAT	3
13	AAAAATATTAGGAA AAAAATAT	CCTGGGA	CAGCCTACAAT CCTACAAT	3
89	ACTGCCGGATCTCG ACTGCCGG	GTCTCGCGGCCGC GACTCTAGAATC	AAGCCGCTTGGAAT CTTGGAAT	46

Table 5. Coding joint sequences in *Artemis$^{-/-}$:H2AX$^{-/-}$* Abl pre-B cells show significant deletions and microhomologies . Coding joints sequences from *WT:DEL^{CJ}-119.6*, *Artemis$^{-/-}$:DEL^{CJ}-81* and *Artemis$^{-/-}$:H2AX$^{-/-}$:DEL^{CJ}-124* and *-95* abl pre-B cells treated with STI571 for 96 hours and amplified using the pB and pC oligonucleotides described in Chapter 4. PCR products were cloned and sequenced.

Artemis$^{-/-}$:*DEL*^{CJ}

# Lost	5' CE	N/P	3' CE	# Lost	
50	GAGCGCCGGTCGCT GAGCGCCG		TGGCCGAAGCCGCT AAGCCGCT	40	
210	GGAAAGGACCTTAC GGAAAGGA		CTTGGAATAAGGCC ATAAGGCC	49	
44	GTCGCTACCATTAC GTCGCTAC		CGTTACTGGCCGAA TGGCCGAA	32	
46	GCCGGTCGCTACCA GCCGGTCG		TGGCCGAAGCCGCT AAGCCGCT	40	
5	ATAGGAACGTCTG ATAGGAAC		CGTTACTGGCCGAA TGGCCGAA	34	
46	GCCGGTCGCTACCA GCCGGTCG		TGGCCGAAGCCGCT AAGCCGCT	40	
1	GAACGTCTG GAACGTCT		CAGCCTACAATTCC ACAATTCC	6	
1	GAACGTCTG GAACGTCT		CAGCCTACAATTCC ACAATTCC	6	
21	TGGTGTCAAAAATA TGGTGTCA		ACGTTACTGGCCGA CTGGCCGA	31	
14	CAAAAATAATAGGA CAAAAATA		CCCTAACGTTACTG CGTTACTG	26	
32	ACCAACTTGTCTGG ACCAACTT		CAGCCTACAATTCC ACAATTCC	6	
165	AGTAGACGGCATCG AGTAGACG		TGAATGTCGTGAAG TCGTGAAG	203	
4	TAGGAACGTCTG TAGGAACG		CAGCCTACAAT CCTACAAT	3	
1	GAACGTCTG GAACGTCT		TACAATTCCGCCCC TCCGCCCC	11	
0	AACGTCTG AACGTCTG		ATTCCGCCCCCCCC CCCCCCCC	15	
0	AACGTCTG AACGTCTG		CAGCCTACAAT CCTACAAT	3	
21	TCTGGTGTCAAAAA TCTGGTG T		CAGCCTACAATTCC ACAATTCC	6	
27	AACTTGTCTGGTGT AACTTGT C		CCCCCCCTAACGTT CTAACGTT	24	
133	GCCCACGTGAAGGC GCCCACGT		TGGAATAAGGCCGG AAGGCCGG	54	*2
50	AACTGAGCGCCGGT AACTGAGC		CGTTACTGGCCGAA TGGCCGAA	34	
206	AGGACCTTACACAG AGGACCTT		GTGCGTTTGTCTAT TTGTCTAT	69	
51	TGAGCGCCGGTCGC TGAGCGCC		CGTTACTGGCCGAA TGGCCGAA	35	
75	GGCCGCGACTCTAG GGCCGCGA		ATGCAAGGTCTGTT GGTCTGTT	190	
171	CCCTCAAAGTAGAC CCCTCAAA		GATTTTCCACCATA CCACCATA	87	
0	AACGTCTG AACGTCTG		AGCCTACAATTCCG CAATTCCG	7	
29	CCAACTTGTCTGGT CCAACTTG		CGCCCCCCCCCCTA CCCCCCTA	19	
8	ATAATAGGAACGTC ATAATAGG		CCCGCCCCCCCCCC CCCCCCCC	17	*2
41	TCGCTACCATTACC TCGCTACC		GCCGCTTGGAATAA TGGAATAA	48	
26	ACTTGTCTGGTGTC ACTTGTCT		AGCCTACAATTCCG CAATTCCG	7	
9	AATAATAGGAACGT AATAATAG		ACGTTACTGGCCGA CTGGCCGA	33	
10	AAATAATAGGAACG AAATAATA		CAGCCTACAATT CTACAATT	4	
0	AACGTCTG AACGTCTG		TTCCGCCCCCCCCC CCCCCCCC	16	
15	GTCAAAAATAATAG GTCAAAAA		ACAATTCCGCCCCC CCGCCCCC	12	
78	TCGCGGCCGCGACT TCGCGGCC		CCGGTGTGCGTTTG TGCGTTTG	64	
29	CCAACTTGTCTGGT CCAACTTG		GCCTACAATTCCGC AATTCCGC	8	
6	AATAGGAACGTCTG GATAGGAA		GTTACTGGCCGAAG GGCCGAAG	35	
62	AGAATTCCAACTGA AGAATTCC		CGCTTGGAATAAGG GAATAAGG	50	
0	AACGTCTG AACGTCTG		CAGCCTACA AGCCTACA	1	
0	AACGTCTG AACGTCTG		CAGCCTAC CAGCCTAC	0	*6
55	ACTGAGCGCCGGTC ACTGAGCG	GCTATTTGTT	TATGTGATTTTCCA ATTTTCC-	80	
55	ACTGAGCGCCGGTC ACTGAGCG	G	GTTTGTCTATATGT CTATATGC	71	
31	CCAACTTGTCTGGT CCAACTTG	G	TTTTCCACCATATT ACCATATT	87	
87	CCGGATCTCGCGGC CCGGATCT	GG	GCCGGTGTGCGTTT GTGCGTTT	61	
16	CCAACTTGTCTGGT CCAACTTG	AAACTG	TACAATTCCGCCCC TCCCGCCC	8	
161	CACGCCGCCCACGT CACGCCGC	TCACGTGAAGGC	CCGCTTGGAATAAG GGAATAAG	47	
124	GGCTGCCGACCCCG GGCCGCCG	CGGGAATAAGGC CGGTGCGCGTT	TCTATATGTCTATA TGTCTATA	76	
22	CTGGTGTCAAAAAA CTGGTGTC	G	CAGCCTACAATTCC ACAATTCC	6	
25	GTCTGGTGTCAAAA GTCTGGTG	CCCT	CAGCCTACAATTC TACAATTC	5	
13	AAAATAATAGGAAC AAAATAAT	CT	CAGCCTACAATT CTACAATT	4	
0	AACGTCTG AACGTCTG	CA	AATTCCGCCCCCCC GCCCCCCC	12	

# Lost	5' CE	N/P	3' CE	# Lost
0	AACGTCTG AACGTCTG	ATG	CAGCCTACAATT CTACAATT	4
40	CTACCATTACCAAC CTACCATT	G	GCCGAAGCCGCTTG GCCGCTTG	40
169	CTCAAAGTAGACGG CTCAAAGT	TCTTA	GGTCTGTTGAATGT TTGAATGT	197
0	AACGTCTG AACGTCTG	CG	CCCCCCCCCTAACG CCCTAACG	22
25	CTTGTCTGGTGTCA CTTGTCTG	CC	CAGCCTAC CAGCCTAC	0
2	GGAACGTCTG GGAACGTC	G	CCCCCCCCTAACGT CCTAACGT	23
2	GGAACGTCTG GGAACGTC	CCG	ACAATTCCGCCCCC CCGCCCCC	15
0	AACGTCTG AACGTCTG	CAGG	AATTCCGCCCCCCC GCCCCCCC	14
35	CCATTACCAACTTG CCATTACC	GACTTGTC	TACTGGCCGAAGCC CCGAAGCC	37
3	AGGAACGTCTG AGGAACGT	TG	CAGCCTAC CAGCCTAC	0
0	AACGTCTG AACGTCTG	AA	CAGCCTACA AGCCTACA	1
19	TGGTGTCAAAAATA TGGTGTCA	GGACCTA	TTCCGCCCCCCCCC CCCCCCCC	16
11	AAAATAATAGGAAC AAAATAAT	CT	ATTCCGCCCCCCCC CCCCCCCC	15
21	TCTGGTGTCAAAAA TCTGGTGT	CCGG	TGGCCGAAGCCGCT AAGCCGCT	40
8	ATAATAGGAACGTC ATAATAGG	GG	CGCCCCCCCCCCTA CCCCCCTA	19
20	CTGGTGTCAAAAAT CTGGTGTC	C	CAGCCTACAAT CCTACAAT	3
117	CCGACCCCGGGGGT CCGACCCC	TCG	CTCGCCAAAGGAA- AAAGGAAA	179
28	CAACTTGTCTGGTG CAACTTGT	GA	GATTTTCCACCATA CCACCATA	87
20	CTGGTGTCAAAAAT CTGGTGTC	G	GCCCCCCCCCCTAA GGCCGAAG	35
2	GGAACGTCTG GGAACGTC	CCG	ACAATTCCGCCCCC CCGCCCCC	12
87	TGCCGGATCTCGCG TGCCGGAT	TA	GGCCGGTGTGCGTT TGTGCGTT	62
40	TCGCTACCATTACC TCGCTACC	G	TGGAATAAGGCCGG AAGGCCGG	54
118	GCCGACCCCGGGGG GCCGACCC	GCC	AAGCCGCTTGGAAT CTTGGATT	46
69	CGACTCTAGAATTC CGACTCTA	AGT	TTCCGCCCCCCCCC CCCCCCCC	16
3	AGGAACGTCTG AGGAACGT	AGGCTG	CAGCCTAC CAGCCTAC	0
15	GTCAAAAATAATAG GTCAAAAA	G	CAGCCTAC GCCTACGA	3
121	GCTGCCGACCCCGG GCTGCCGA	AGGA	GTGATTTTCCACCA TTCCACCA	85
3	AGGAACGTCTG AGGAACGT	CCGCTG	CAGCCTAC CAGCCTAC	0
0	AACGTCTG AACGTCTG	A	CAGCCTACA AGCCTACA	1
6	AATAGGAACGTCTG AATAGGAA	TAGG	CCTACAATTCCGCCC TTCCGCCC	9
30	ACCAACTTGTCTGG ACCAACTT	T	CTTGGAATAAGGCCG TAAGGCCG	53

Table 5 cont.

Artemis$^{-/-}$:H2AX$^{-/-}$DEL^{CJ}

# Lost	5' CE	N/P	3' CE	# Lost
333	AGACCTCTGGCGGC AGACCTCT		CCCTCTCGCCAAAG CGCCAAAG	171
326	CTGGCGGCAGCCTA CTGGCGGC		TGCGGCCAAAAGCC CAAAAGCC	306
175	CCTCAAAGTAGACG CCTCAAAG		CCAAAGGAATGCGA GAATGCAA	178
168	AGTAGACGGCATCG AGTAGACG		TTGACGAGCATTCC AGCATTCC	145
40	ACCATTACCAACTT ACCATTAC		CGTTACTGGCCGAA TGGCCGAA	30
69	CGACTCTAGAATTC CGACTCTA		TGTCTATATGTGAT TATGTTAT	76
151	GCAGCTTGGATACA GCAGCTTG		TTCTTGACGAGCAT ACGAGCAT	146
177	CCACCGCCCTCAAA CCACCGCC		CTCGCCAAAGGAAT AAAGGAAT	177
35	CCAACTTGTCTGGT CCAACTTG		CGCTTGGAATAAGG GAATAAGG	48
26	TTGTCTGGTGTCAA TTGT CTGG		TACTGGCCGAAGCC CCGAAGCC	35
25	GTCTGGTGTCAAAA GTCTG GTG		AATGTGAGGGCCCG AGGGCCCG	113
178	ACCGCCCTCAAAGT ACCGCCCT		ATTCCTAGGGGTCT AGGGGTCT	155
134	GCCCACGTGAAGGC GCCCACGT		TGCCGTCTTTTGGC CTTTTGGC	101
75	CGGCCGCGACTCTA CGGCCGCG		TGTGCGTTTGTCTA TTTGTCTA	68
159	GCATCGCAGCTTGG GCATCGCA		AATGCAAGGTCTGT AGGTCTGT	187
153	TCGCAGCTTGGATA TCGCAGCT		GACCCTTTGCAGGC TTGCTGGC	265
24	TGTCTGGTGTCAAA TGTCTG GG		ACCTGGCCCTGTCT CCCTGTCT	132
37	TACCATTACCAACT TACCAT TA		GGAATAAGGCCGGT AGGCCGGT	54
3	AGGAACGTCTG AGGAACGT		GCCGGTGTGCGTTT GTGCGTTT	62
98	TCTAGACTGCCGGA TCTAGA CT		CAGCCTACAATTCC ACAATTCC	6
167	AAGTAGACGGCATC AAGTAGAC		GGAAACCTGGCCCT CTGGCCCT	129
133	CCACGTGAAGGCTG CCACGT GA		TGACGAGCATTCCT GCATTCCT	148
46	GCCGGTCGCTACCA GCCGGTCG		TGGCCGAAGCCGCT AAGCCGCT	40
165	AAGTAGACGGCATC AAGTAGAC		GGAAACCTGGCCCT CTGGCCCT	129
154	ATCGCAGCTTGGAT ATCGCA GC		TATTGCCGTCTTTT CGTCTTTT	99
71	CGACTCTAGAATTC CGACTC TA		ACGTTACTGGCCGA CTGGCCGA	31
56	AACTGAGCGCCGGT AACTGA GC		AGCCGCTTGGAATA TTGGAATA	49
90	CTGCCGGATCTCGC CTGCCG GA		GGCCGAAGCCGCTT AGCCGCTT	39
47	GCCGGTCGCTACCA GCCGGTC G		CCTAGGGGTCTTTC GGTCTTTC	160
47	GCCGGTCGCTACCA GCCGGTC G		GCAAGGTCTGTTGA TCTGTTGA	192
136	GCCGCCCACGTGAA GCCGCCC A		TTCCTAGGGGTCTT GGGGTCTT	159
212	CTGGAAAGGACCTT CTGGAAA G		GGAATGCAAGGTCT CAAGGTCT	188
5	ATAGGAACGTCTGC ATAGGAA C		CAGCCTACA AGCCTACA	1
24	TTGTCTGGTGTCAA TTGTCTG G		CCGAAGCCGCTTGG CCGCTTGG	43
26	ACTTGTCTGGTGTC ACTTGTC T		TAACGTTACTGGCC TACTGGCC	31
231	TAAGAACCTAGAAC TAAGAAC C		GAATGCAAGGTCTG AAGGTCTG	188
76	GCGCCCGCGACTCT GCGGCCG C		CCCCCCCCTAACGT CCTAACGT	23
23	TGTCTGGTGTCAAA TGTCTGG T		TACAATTCCGCCCC TCCGCCCC	11
86	GCCGGATCTCGCGG GCCGGAT C		GGCAGCGGAACCCC GGAACCCC	276
33	ATTACCAACTTGTC ATTACCA A		CTTGGAATAAGGCC ATAAGGCC	52
71	CGCGACTCTAGAAT CGCGACT C		CGAAGCCGCTTGGA CGCTTGGA	44
157	GGCATCGCAGCTTG GGCATCG C		GGGGTCTTTCCCCT TTT-CCCT	165
272	TACCGAGTCGGCGA TACCGAG T		GAGCATTCCTAGGG TCCTAGGG	153
202	CCTTACACAGTCCT CCTTACA C		AGGGCCCGGAAACC CGGAAACC	122
186	TGACCACCCCCACC TGACCAC C		GGAAGCAGTTCCTC AGTTCCTC	217
51	AGCGCCGGTCGCTA AGCGCCG G		CCGAAGCCGCTTGG CCGCTTGG	40
47	CCGGTCGCTACCAT CCGGTCG C		CCCCCCCCCTAACG CCCTAACG	18
226	AACCTAGAACCTCG AACCTAGA		GGTCTTTCCCCTCT TCCCCTCT	167
290	ACCGGTGGTACCTC ACCGGTGG		CAGTTCCTCTGGAA CTCTGGAA	222
161	CGGCATCGCAGCTT CGGCATCG		CCTCTCGCCAAAGG GCCAAAGG	176
57	TCCAACTGAGCGCC TCCAACTG		GAATAAGGCCGGTG GGCCGGTG	56

# Lost	5' CE	N/P	3' CE	# Lost
17	GTGTCAAAAATAAT GTGTCAAA		ATTCCGCCCCCCCC CCCCCCCC	16
94	TCTAGACTGCCGGA TCTAGACT		CCCTAACGTTACTG CGTTACTG	28
81	CTCGCGGCCGCGAC CTCGCGGC		TTGCCGTCTTTGA TCTTTTGA	99
18	GGTGTCAAAAATAA GGTGTCAA		AATTCCGCCCCCCC GCCCCCCC	14
189	TGCTGACCACCCCC TGCTGACC		TCTGTTGAATGTCG GAATGCCG	199
135	ACACGCCGCCCACG ACACGCCG		TGATTTTCCACCAT TCCACCAT	86
142	GTGAAGGCTGCCGA GTGAAGGC		GAATGTCGTGAAGG CGTGAAGG	205
195	CAGTCCTGCTGACC CTGTCCTG		CGCCAAAGGAATGC AGGAATGC	190
218	ACCTCGCTGGAAAG ACCTCGCT		CTCGCCAAAGGAAT AAAGC-AT	178
169	CAAAGTAGACGGCA CAAAGTAG		AAGGAATGCAAGGT TGCAAGGT	185
174	GCCCTCAAAGTAGA GCCCTCAA		GTCTGTTGAATGTC TGAATGTC	196
198	ACCGCCCTCAAAGT ACCGCCCT		GTTGAATGTCGTGA TGTCGTGA	202
187	CTGACCACCCCCAC CTGACCAC		TCTGCGGCCAAAAG GCCAAAAG	95
14	AAAAATAATAGGAA AAAAATAA		AACGTTACTGGCCG ACTGGCCG	30
4	TAGGAACGTCTG TAGGAACG		CCCCTAACGTTACT ACGTTACT	25
77	CGCGGCCGCGACTC CGCGGCCG		TTCCTAGGGGTCTT GGGGTCTT	160
125	GAAGGCTGCCGACC GAAGGCTG		TGGCAATGTGAGGG TGTGAGGG	112
149	AGCTTGGATACACG AGCTTGGA		CCCTCTCGCCAAAG CGCCAAAG	175
139	CACGCCGCCCACGT CACGCCGC		TTCCTAGGGGTCTT GGGTCTTT	160
0	AACGTCTG AACGTCTG		CAGCCTAC CAGCCTAC	0
304	GAACAACT GAACAACT	A	TCTGTTGAATGTCG GAATGTCG	199
222	AGAACCTAAAACAG AGAACCTA	AACCT	CTTTCCCCTCTCGC CCTCTCGC	168
173	CGCCCTCAAAGTAG CGCCCTCA	C	ATAAGGCCGGTGTG CCGGTGTG	82
59	ATTCCAACTGAGCG TTTCCAAC	CGA	GCCCCCCCCCCTAA CCCCCTAA	20
63	TAGAATTCCAACTG TAGAATTC	G	CGAGCATTCCTAGG TTCCTAGG	153
19	TGGTGTCAAAAATA TGGTGTCA	GA	CCCCCCCCCTAACG CCCTAACG	22
60	AATTCCAACTGAGC AATTCCAA	GG	ATGTGATTTTCCAC TTTTCCAC	83
10	AATAATAGGAACGT AATAATAG	GT	GGCCGAAGCCGCTT AGCCGCTT	41
121	GCTGCCGACCCCGG GCTGCCGA	GT	CCCTAACGTTACTG CGTTACTG	28
53	ACTGAGCGGCCGGTC ACTGAGCG	GT	CGCCCCCCCCCCCTA CCCCCCTA	20
100	CCATCCTCTAGACT CCATCCTC	CGG	GCCGAAGCCGCTTG GCCGCTTG	42
85	CCGGATCTCGCGGC CCGGATCT	G	TCTATATGTGATTT TGTTATTT	78
28	CAACTTGTCTGGTG CAACTTGT	GGG	ACGTTACTGGCCGA CTGGCCGA	33
113	CCCCGGGGGTGGAC CCCCGGGG	A	CCGTCTTTTGGCAA TTTGGCAA	104
106	GGTGGACCATCCTC GGTGGACC	CCA	CATTCCTAGGGGTC TAGGGGTC	158
184	ACCACCCCCACCGC ACCACCCC	AG	CGGAAACCTGGCCC CCTGGCCC	128
15	GTCAAAAATAATAG GTCAAAAA	C	GTTACTGGCCGAAG GGCCGAAG	35
0	AACGTCTG AACGTTTG	CAGC	CTACAATTCCGCCC TTCCGCCC	10
19	TGGTGTCAAAAATA TGGTGTCA	CACA	TACAATTCCGCCCC TCCGCCCC	11
127	GTGAAGGCTGCCGA GTGAAGGC	GTC	ACCTGGCCCTGTCT CCCTGTCT	133

Table 5 cont.

Chapter 5

ATM Activates a Broad Genetic Program in Response to RAG DNA DSBs

(reprinted with modification(270))

The relatively mild defect in the repair of RAG DNA DSBs during V(D)J recombination in ATM-deficient cells does not likely entirely account for the lymphopenia observed in ataxia telangiectasia. We considered the possibility that the more global effects of ATM activation in response to DNA damage, specifically its ability to activate gene transcription, might also affect lymphocyte development(73).

ATM, in response to genotoxic DNA damage, promotes cell cycle checkpoint activation and apoptosis through the activation of p53(244-247). It is known that ATM similarly activates p53 in response to persistent physiologic RAG DNA DSBs in developing lymphocytes, but whether it does so in response to all RAG DNA DSBs, including those in wild-type cells that are transient in nature, is not known(271). ATM also activates NFκB, a transcription factor with targets that promote survival, in response to genotoxic damage, and the balance of the NFκB and p53 pathways is thought to mediate cell outcome following genotoxic DNA damage(263, 264). If RAG DNA DSBs promote the ATM-mediated activation of p53, it is possible that ATM might simultaneously promote the transcription of pro-survival factors via the activation NFκB. The sum of these two pathways could be important for negotiating a balance between survival and apoptosis in the developing lymphocyte following a RAG DNA DSB, essentially affording the cell a window of opportunity in which to repair the break. Furthermore, while NFκB may solely be acting to promote the transcription of pro-survival factors, it is more likely that this multi-functional transcription factor would simultaneously modulate the expression of other genes that might be important for the developing lymphocyte.

Deficiencies in ATM, then, would eliminate the activation of these transcriptional programs and thereby potentially negatively impact lymphocyte development. We wished to determine whether ATM activates NFκB in response to transient RAG DNA DSBs and to fully characterize the transcriptional program initiated by ATM in response to these breaks.

Persistent RAG DNA DSBs activate NFκB via the classical pathway.

RAG DNA DSBs in a WT cell are transient in nature, and, as such, signals emanating from those breaks might also be transient in nature. As discussed in Chapter 3, we reasoned that the analysis of cells with persistent DSBs would increase our ability to detect the activation of transcriptional pathways in response to RAG DNA DSBs. We chose initially to compare the activation of NFκB in response to RAG DNA DSBs in cells deficient in components of the NHEJ-pathway, *Artemis*$^{-/-}$ Abl pre-B cells, where breaks are made but not repaired in response to STI treatment to similarly treated Rag$^{-/-}$ Abl pre-B cells where breaks are never made due to the lack of a functional RAG-holocomplex. NFκB activation was assessed by EMSA (electrophoretic mobility shift assays) wherein labeled oligo probes consisting of NFκB binding sites are incubated with nuclear extracts from the cells of interest and ran on a poly-acrylamide gel. If NFκB is activated in these cells, it should be present in the nucleus and will bind to the oligo probe. This binding will retard the flow of the oligo in the gel leading to a "shift" of the oligo probe(289). By EMSA, we detect robust NFκB activation in the *Artemis*$^{-/-}$ Abl pre-B cell lines but not the *Rag*$^{-/-}$ lines at 48 hours of STI treatment (Figure 23a). Importantly, this is at the same time that we see an accumulation of unrepaired Jκ coding ends in the *Artemis*$^{-/-}$ deficient cells (Figure 23b). Also, we do not see activation in cells deficient in both Artemis and ATM (Figure 23a) or in *Artemis*$^{-/-}$ cells treated with a small molecule inhibitor of ATM though breaks are clearly present in these cells (Figure 23b), demonstrating that ATM is mediating this DSB-dependent NFκB activation.

NFκB activation by ATM in response to genotoxic DNA damage occurs through the classical pathway in a manner dependent on the phosphorylation of NEMO(263). We carried out a number of tests to determine whether NFκB is similarly activated in response to RAG DNA DSBs. One way to characterize the activation of NFκB is to add antibodies specific for the two components of the classical NFκB heterodimer (p50:p65) to the nuclear extracts prior to EMSA. The binding of these antibodies to their respective proteins will cause a further retardation ("super-shift") of the oligo during PAGE(289). Indeed, we find that both p50 and p65 antibodies

cause a super-shift in the EMSA with lysates from the *Artemis*$^{-/-}$ cells. This is visualized as a disappearance of the band seen in the *Artemis*$^{-/-}$ lanes upon addition of antibodies specific for p50 or p65 and the detection of higher molecular weight species in these lanes (Figure 24a). Additionally, we find that NFκB activation, as read-out by EMSA, is completely blocked in *Artemis*$^{-/-}$ cells transfected with a N-terminally truncated dominant negative version of IκBα which primarily affects the classical pathway(307) (Figure 24b). Finally, incubating cells with a cell-permeable mutant NEMO binding domain peptide that prevents the association of NEMO with IKKα and IKKβ thereby preventing the activation of the IKK complex(308) inhibits NFκB activation by EMSA while a mutant peptide does not (Figure 24c). These data are all consistent with the idea that ATM activates NFκB via the classical pathway in response to RAG DNA-DSBs as it does in response to genotoxic DNA damage.

Characterizing RAG DNA DSB-dependent transcriptional changes by microarray analysis.

We wished to determine what genes are affected by the activation of NFκB in response to RAG DNA DSBs in the developing lymphocyte and whether ATM or other transducers might additionally activate other transcription factors in response to these physiologic breaks. Thus, we designed the microarray-based experiments described below to more fully characterize the transcriptional program(s) activated in response to these physiologic DNA DSBs.

As with the EMSA analyses, we began by comparing the transcriptional profiles of STI-treated *Artemis*$^{-/-}$ Abl pre-B cells to STI-treated *Rag*$^{-/-}$ Abl pre-B cells. The *Rag*$^{-/-}$ Abl pre-B cells serve as a critical control in our microarray analyses as STI is known to cause many changes in gene expression(280). By comparing the transcriptional profiles of similarly treated *Rag*$^{-/-}$ and *Artemis*$^{-/-}$ cells, we are able to distinguish STI-induced changes in transcription from those caused by the formation of RAG DNA DSBs.

ATM is thought to be the primary transducer of the DNA damage response in G1 of the cell cycle(73). However, we considered the possibility that other transducers might also activate pathways downstream of RAG DNA DSBs. To determine which of the transcriptional changes were dependent on ATM signaling, we compared the transcriptional response to RAG DNA DSBs

in STI-treated *Artemis*$^{-/-}$ Abl pre-B cells to those deficient in both Artemis and ATM. Finally, ATM in response to DNA damage is known to activate primarily p53 and NFκB(244-247, 263, 264). Considering that other transcriptional regulators such as Stat3 and FOXO-1 are also phosphorylated by ATM in response to DNA damage, it is likely that ATM modulates the activity of other transcriptional pathways as well(71). To begin to address this possibility, we transfected *Artemis*$^{-/-}$ cells with a dominant negative version of IκBα that is N-terminally truncated and functions as a dominant negative preventing activation of primarily the classical pathway(307). We simultaneously performed microarray analysis on these STI treated *Artemis*$^{-/-}$*:IkBα-ΔN* Abl pre-B cells.

All cell lines (*Rag*$^{-/-}$*, Artemis*$^{-/-}$*, Artemis*$^{-/-}$*:Atm*$^{-/-}$ *and Artemis*$^{-/-}$*:IκBα-ΔN*) were treated with STI for 48 hours prior to RNA isolation. Furthermore, we confirmed that all *Artemis*$^{-/-}$ cells used had similar level of breaks by Southern blot prior to microarray analysis to minimize differences in transcription due to the differential accumulation of un-repaired breaks. Three independently derived cell lines of each genotype were analyzed preventing us from inappropriately identifying differences in transcription due to cell line variation as RAG DNA DSB-dependent changes and furthermore to give us confidence in picking out any small but relevant changes in gene expression.

Results of the microarray analysis yielded a relatively concise cohort of genes (364) whose expression was modulated in response to RAG DNA DSBs, as they exhibited a ≥2-fold change in expression in all three *Artemis*$^{-/-}$ cell lines, as compared to the mean expression level in the three *RAG-2*$^{-/-}$ cell lines (Figure 25a). Of these, approximately half (189) of these genes depended on ATM as expression was diminished in the *Artemis*$^{-/-}$*:Atm*$^{-/-}$ Abl pre-B cells as compared to the *Artemis*$^{-/-}$ Abl pre-B cells (Figure 25a). Finally, 75 of the 364 genes exhibited transcriptional changes that were dependent on NFκB (Figure 25a). A large fraction of the microarray data was confirmed by qrtPCR and by protein analysis where possible (Figure 25b and Figure 26). Specifically, we note an increase in the expression of Bcl-3, Pim-2, CD40, CD62L, CD69 and common γ-chain upon STI treatment in the *Artemis*$^{-/-}$ but not *Rag-2*$^{-/-}$ or

Artemis$^{-/-}$*:Atm*$^{-/-}$, or *Artemis*$^{-/-}$*:IκBα-ΔN* (with the exception of CD62L) Abl pre-B cells (Figure 25b). Also, we detect increases in Pim-2 protein levels (all three isoforms) in *Artemis*$^{-/-}$ but not *Rag-2*$^{-/-}$ or *Artemis*$^{-/-}$*:Atm*$^{-/-}$ Abl pre-B cells upon STI treatment (Figure 26a). Finally, we note that the surface expression of CD40 and CD69 is similarly selectively increased in the *Artemis*$^{-/-}$ Abl pre-B cells in response to STI treatment (Figure 26b). Furthermore, we performed qrtPCR on Abl pre-B cells treated for varying amounts of time with STI to establish kinetic profiles of RAG-induced transcriptional changes (Figure 27). We noted that the transcription of each of these genes had different kinetic profiles. Interestingly, some like CD69 had a very transient increase in transcription and protein expression peaking at 48 hours and disappearing by 72 h even though the inciting stimulus (unrepaired RAG DNA DSB) was still present. Others like CD40 show slow and gradual increases in expression but hit a plateau near 48 hours and still others, like Pim-2 and Bcl-3, gradually increase throughout the 96-hour STI treatment.

It was important to confirm that these gene changes were not due to Artemis-deficiency alone. We analyzed the expression of a cohort of the genes in *Rag*$^{-/-}$*:Artemis*$^{-/-}$ cell lines (Figure 28a) reasoning that these cells, while deficient in Artemis would not make DNA DSBs. Importantly, we did not note significant changes in the expression of the RAG DNA DSB-dependent genes in these cells in upon STI treatment (Figure 28a). Secondly, we also analyzed the expression of this cohort of RAG DNA DSB-dependent genes in Abl pre-B cell lines derived from mice deficient in other components of the NHEJ pathway (*Ku80*$^{-/-}$ and *scid*). These cells contain unrepaired RAG DNA DSBs but contain a functional Artemis protein. Importantly, these cells do exhibit similar RAG-induced transcriptional changes (Figure 28b) as was seen in the *Artemis*$^{-/-}$ Abl pre-B cells. Thus, these genetic changes are not likely due to Artemis-deficiency *per se*.

These data demonstrate that, in response to RAG-induced DSBs, ATM activates NFκB but additionally other transcription factors that lead to the promotion of a broad transcriptional program. Notably, while some genes up-regulated in response to RAG DNA DSBs such as Pim-2 and Bcl-3 have known roles in promoting survival, many of the genes (CD40, CD69, Cd62L)

breaks have no known function in the canonical DNA damage response. Rather, the known functions of these gene products implicate them in lymphocyte development and function. For example, a number of genes belonging in this category have been implicated in migration and trafficking (Swap70(309), CD69(310, 311), L-Selectin(312)) in mature lymphocytes. Importantly, then, this program transcends the canonical DNA damage response, activating genes whose expression could have important ramifications for the developing lymphocyte.

Persistent RAG DNA DSBs activate a similar genetic program *in vivo*.

To determine whether a similar genetic program is activated by RAG DSBs *in vivo,* we isolated bone marrow from *Rag*$^{-/-}$*:IgHtg* and *Artemis*$^{-/-}$*:IgHtg* mice. As described in Chapter 4, lymphocyte development in these mice is arrested at the pre-B cell stage, being promoted to this stage by the immunoglobulin heavy chain transgene; however, as these cells are unable to undergo V(D)J recombination, they do not progress to the immature pre-B cell stage (Figure 29a). The *Rag*$^{-/-}$*:IgHtg* mice cannot initiate V(D)J recombination because they cannot make DNA DSBs, while the *Artemis*$^{-/-}$*:IgHtg* mice cannot complete V(D)J recombination because they cannot repair RAG DNA DSBs. We were able to isolate RNA from the bone marrow of these mice and submit it for microarray analysis just as was done for the Abl pre-B cells. In doing so, we determined that 109 of the 364 RAG DSB-responsive genes were also up-regulated at least 1.2 fold in the Artemis$^{-/-}$:*IgHtg* mice as compared to samples from *Rag*$^{-/-}$*:IgHtg* mice (Figure 29a). The asynchronous nature of RAG break induction in these cells *in vivo* likely explains the generally lower changes in gene transcription in these cells. However, and importantly, although these changes were less dramatic, they were confirmed by qrtPCR and additionally led to the expected relevant changes in protein expression with surface expression of CD40, CD69, CD62L and CD80 all significantly higher in the Artemis$^{-/-}$:*IgHtg* bone marrow pre-B cells as compared to *Rag*$^{-/-}$*:IgHtg* mice bone marrow pre-B cells (Figure 29b). Thus, we conclude that RAG DNA DSBs *in vivo* activate a similar genetic program.

Transient RAG DNA DSBs activate NFκB.

All data presented thus far supports the notion that persistent RAG DNA DSBs can activate a cohort of genes as all studies were performed in NHEJ-deficient cells. That these persistent DSBs might activate signaling pathways not generally activated during V(D)J recombination in WT cells where breaks are efficiently repaired was a distinct possibility. In this regard, we did not detect NFκB activation by EMSA in WT Abl pre-B cells that had been incubated with STI (Figure 30). For the gene changes we have identified to generally affect lymphocyte development, it is important that they be activated by all RAG DNA DSBs, not just those that persist unrepaired.

To determine whether transient RAG DNA DSBs can similarly activate NFκB and thus likely other components of this transcriptional program, we decided to introduce an NFκB reporter into WT cells that would enable us to detect NFκB activation on a cell-by-cell basis. Our reporter is a retrovirus containing 5-tandem NFκB-responsive elements driving the expression of GFP on the antisense strand. Thus, GFP would be produced only upon activation of NFκB. The production of GFP could be analyzed by FACS (Figure 31a). We further reasoned that, as these cells are arrested in G1 of the cell cycle, that any GFP produced would remain in that cell, and thus we could detect activation of NFκB that had occurred at any point in time even after the repair of the break (Figure 31b).

We began by introducing our retroviral reporter into a Rag-2 deficient cell Abl pre-B cell line (*RAG-2*$^{-/-}$ *NRE*, Figure 31b). We show that, in these lines, there is very little NFκB activation upon STI treatment in the absence of RAG proteins (Figure 31b, 32, and 33a). However, irradiation of these RAG-deficient lines, which induces a large number of DSBs, led to a robust GFP expression (Figure 32) demonstrating that this reporter enabled us to detect NFκB activation in response to DNA damage. GFP production in these cells is ATM- and NFκB dependent as it does not occur when these irradiated cells are treated with the ATM inhibitor or the BAY inhibitor that prevents the phosphorylation of IκBα thereby preventing NFκB activation(263).

At this point, confident that our reporter system was working, we retrovirally introduced Rag-2 back into the *RAG-2*$^{-/-}$ *NRE* cells thus creating a system wherein breaks could be made and repaired normally upon STI treatment (*RAG-2*$^{-/-}$ *NRE R2,* Figure 31b). Upon reconstitution of the RAG complex, STI treatment leads to DSB induction and efficient repair of the RAG DNA DSBs. A significant fraction of cells turn GFP+ indicating that transient RAG DNA DSBs that are repaired normally do activate NFκB (Figure 33a). Again, this GFP production was dependent on both ATM and NFκB as it was prevented by both the iATM and the BAY inhibitor (Figure 33a). Next, we sorted these GFP+ cells and GFP- cells by flow-cytometric assisted cell sorting. The GFP+ cells isolated had a 5-fold greater amount of CJ formation as compared to the GFP- population as assayed by PCR analysis, demonstrating that the cells that had activated NFκB had undergone rearrangement (Figure 33b and c). Furthermore, we detect changes in the expression of the RAG-dependent genes in the GFP+ cells as compared to the GFP- cells. Therefore, we conclude that RAG-DNA DSBs that are made and repaired normally do, in fact, activate the transcriptional program we had observed initially using the NHEJ-deficient Abl pre-B cells.

Further supporting the notion that transient breaks activate the described transcriptional program is our ability to detect significantly higher levels of CD40, CD69, and CD62L (genes known to be activated by ATM in response to persistent RAG DNA DSBs) on the surface of WT pre-B cells ($B220^+$:IgM^-) by FACS as compared to *Atm*$^{-/-}$ cells at a similar developmental stage (Figure 34). This $B220^+$:IgM^- population consists primarily of pre-B cells that would be actively rearranging the endogenous kappa locus. Thus, we have identified a RAG-DNA DSB dependent transcriptional program that includes genes with no known function in the canonical DNA DSB response. Furthermore, these changes are observed in WT cells, not just those with persistent DSBs.

Conclusion

Following a genotoxic insult, ATM activates transcriptional pathways that mediate the balance between cell survival and death, namely NFκB and p53. In response to RAG DSBs in

the developing lymphocyte (both WT and NHEJ-deficient cells), we demonstrate that ATM, through the activation of NFκB and other transcription factors, activates a broad genetic program that transcends this canonical DNA damage response and includes genes whose known functions are integral to lymphocyte development. We hypothesize that these signals emanating from a RAG DNA DSB are integrated with the numerous other cellular cues to overall guide lymphocyte development.

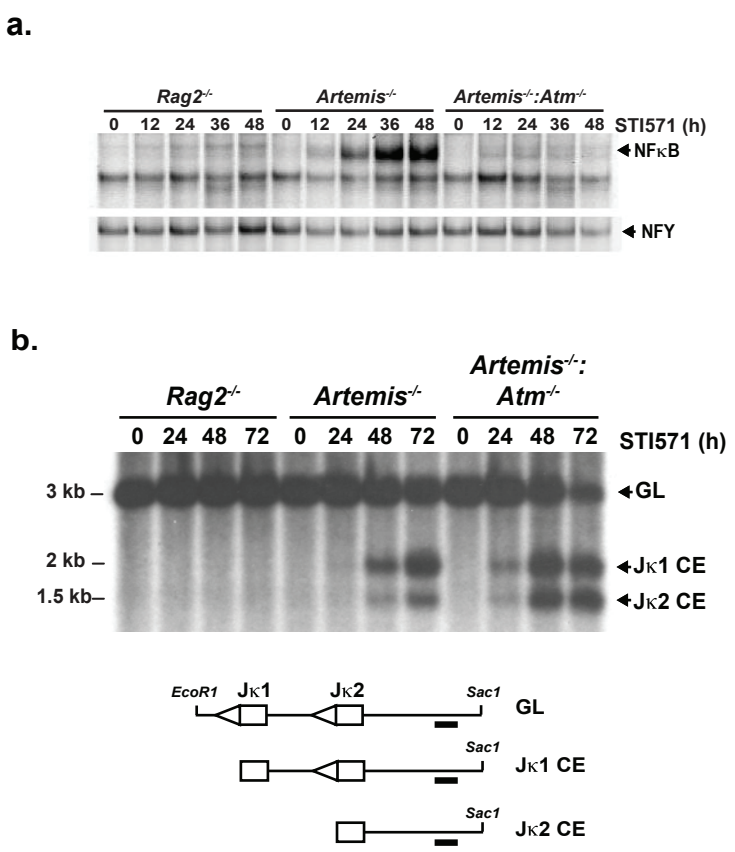

Figure 23. Persistent RAG DNA DSBs activate NFκB. (a) NFκB EMSA of nuclear lysates from *Rag2*$^{-/-}$, *Artemis*$^{-/-}$ and *Artemis*$^{-/-}$*:Atm*$^{-/-}$ abl pre-B cells treated with STI571 for the indicated number of hours. NFY EMSA is shown as a control. **(b)** Southern blot analysis of Rag DSBs (coding ends, CEs) generated at the Jκ gene segments in the IgLκ locus in cells treated with STI571 for the indicated number of hours. Bands generated by the germline (GL) IgL-κ locus and Jκ1 and Jκ2 CEs are indicated. The schematic of the products shows the relative positions of the restriction sites (EcoRI and SacI) and probe (filled rectangle) used for analysis.

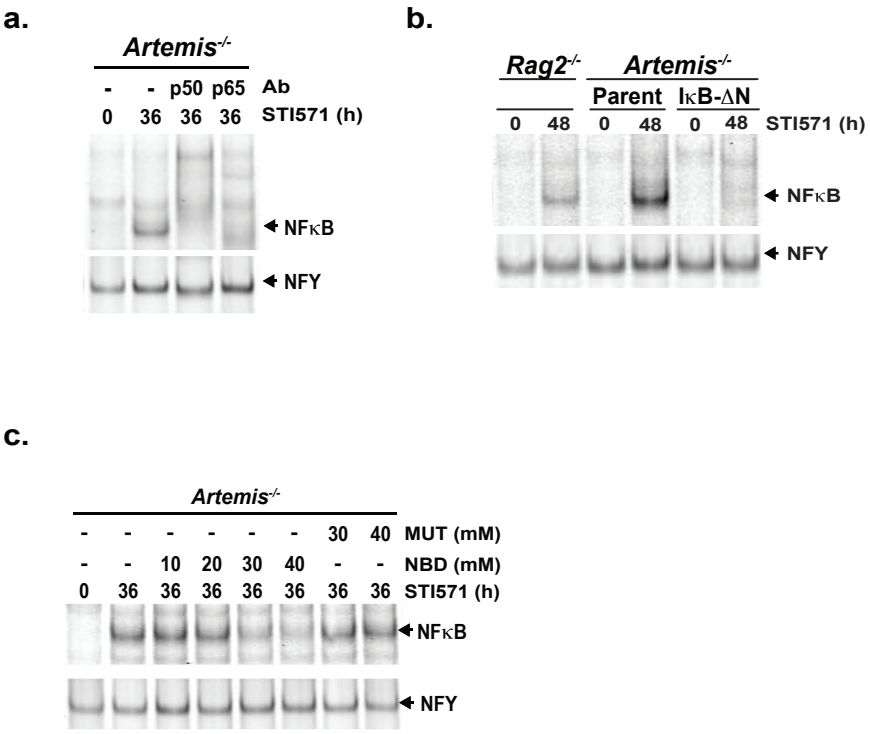

Figure 24. RAG DNA DSBs activate NFκB via the classical pathway. (a) NFκB supershift using antibodies to p50 or p65. **(b)** NFκB EMSA of nuclear lysates from *Artemis*$^{-/-}$ Abl pre-B cell lines that express an IκBα–dominant negative, IκBα-ΔN, generated by transfection of the parent *Artemis*$^{-/-}$ line as indicated treated with STI571 for either 0 or 48 h. **(c)** NFκB EMSA of nuclear lysates from *Artemis*$^{-/-}$ Abl pre-B cell lines treated with STI571 in the presence of increasing concentrations of either a cell-permeable NEMO binding domain peptide (NBD) or a control cell-permeable NBD mutant peptide (MUT). NFY EMSAs are shown as loading controls.

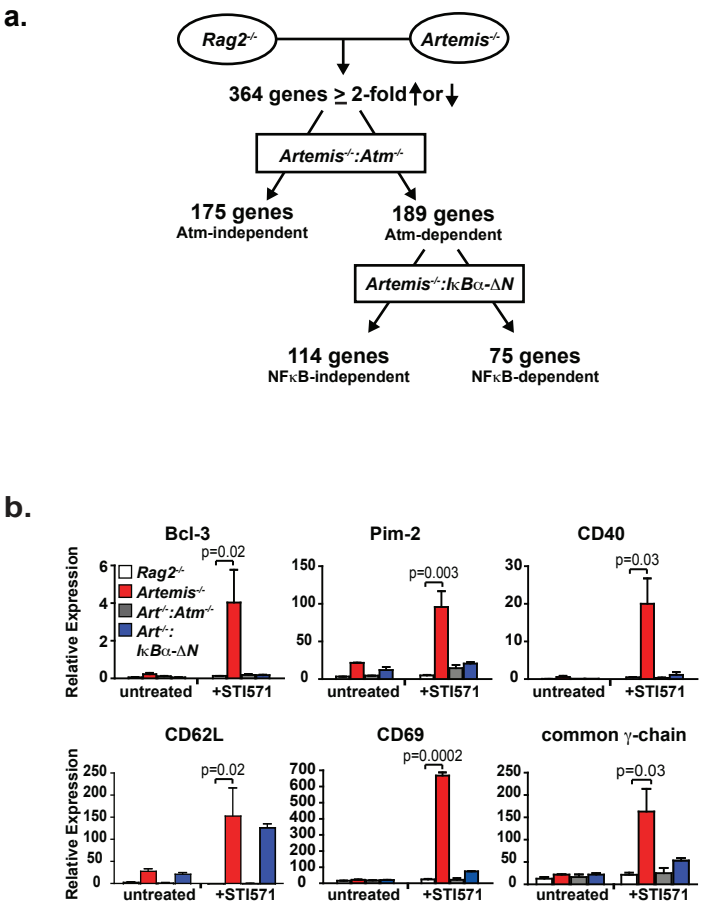

Figure 25. Global changes in gene expression in response to RAG DNA DSBs. (a) Schematic of gene expression changes in response to Rag DSBs by microarray analyses. **(b)** RT-PCR analysis of mRNA isolated from *Rag2*$^{-/-}$ (white bars), *Artemis*$^{-/-}$ (red bars), *Artemis*$^{-/-}$*:IkB*κ*-ΔN* (blue bars) and *Artemis*$^{-/-}$*:Atm*$^{-/-}$ (grey bars) abl pre-B cells treated with STI571 for 0 or 48 hours. Mean and standard deviation from two experiments. P values calculated using a one-tailed t-test.

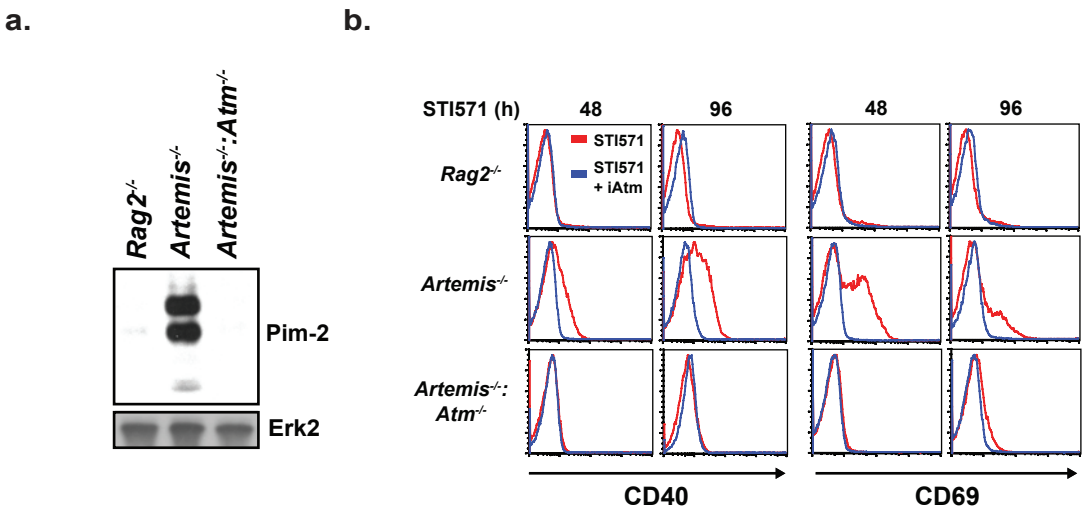

Figure 26. **RAG-dependent gene expression changes cause changes in protein expression. (a)** Western blot analysis of Pim-2 expression in abl pre-B cells treated with STI571 for 48 hours. The three isoforms of Pim-2 are shown. Erk2 is shown as a protein loading control. **(b)** Flow cytometric analysis of CD40 and CD69 protein expression on abl pre-B cells treated with STI571 for 48 or 96 h. Red histogram represents cells treated with STI571 alone; blue histogram represents cells treated with STI571 and KU-55933 (iATM).

Bredemeyer & Helmink et al. *Nature* 2008.

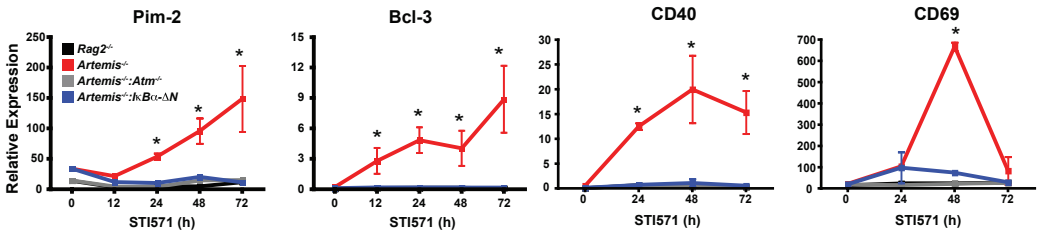

Figure 27. Time course of gene expression changes in response to RAG DNA DSBs. RT-PCR analysis of gene expression in abl pre-B cells treated with STI571 for different periods of time. Asterisks indicate that the difference between the *Rag2*$^{-/-}$ and *Artemis*$^{-/-}$ cell lines is significant ($p<0.05$).

a.

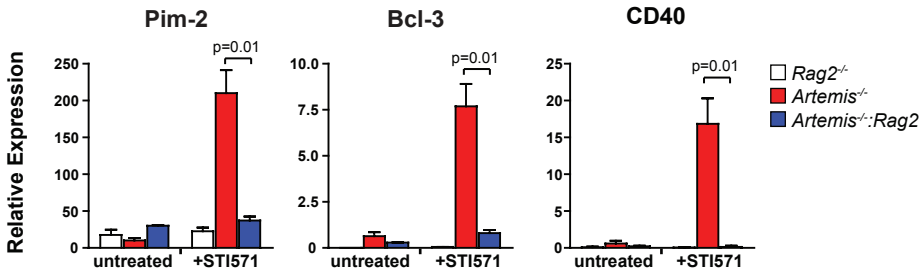

b.

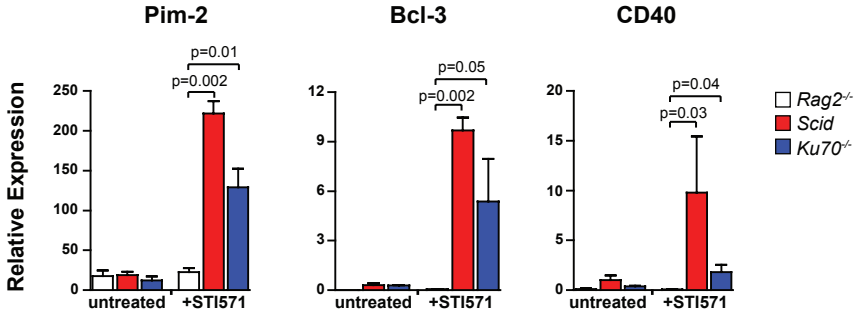

Figure 28. Gene expression changes are not a result of Artemis-deficiency *per se*. RT-PCR analysis of expression of the indicated genes in untreated and STI571-treated **(a)** *Rag2*$^{-/-}$, *Artemis*$^{-/-}$, and *Artemis*$^{-/-}$*:Rag2*$^{-/-}$ or **(b)** *Rag2*$^{-/-}$, *scid*, and *Ku70*$^{-/-}$ abl pre-B cells. Values are mean and standard deviation from two experiments. P values were calculated using a one-tailed t-test.

a.

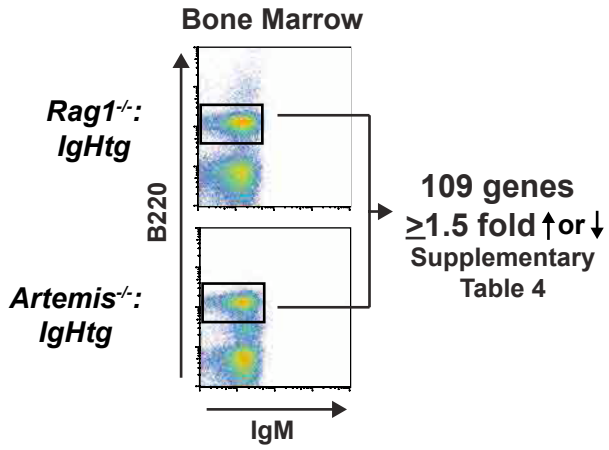

b.

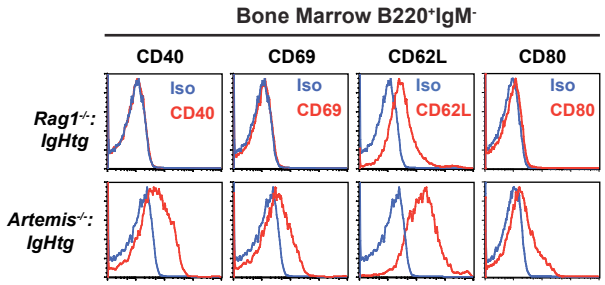

Figure 29. Gene expression changes downstream of RAG DNA DSBs in primary cells. (a) Schematic of gene expression analysis carried out on bone marrow pre-B cells. Gene expression profiling was carried out on RNA isolated from purified B220^{+}:IgM^{-} cells from the bone marrow of *Rag1*$^{-/-}$*:IgHtg* and *Artemis*$^{-/-}$*:IgHtg* mice. (b) Flow cytometric analyses of CD40, CD69, CD80 and CD62L expression by B220^{+}:IgM^{-} bone marrow B cells (primarily pre-B cells) from *Rag1*$^{-/-}$*:IgHtg* and *Artemis*$^{-/-}$*:IgHtg* mice (gated cells in a). Histograms for specific antibodies (red) and isotype controls (blue) are shown.

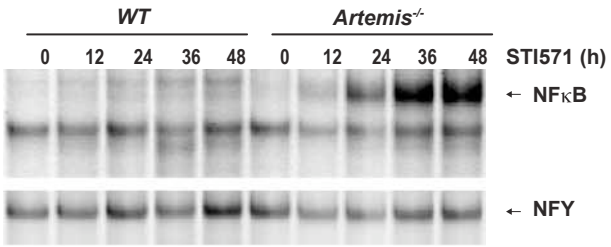

Figure 30. NFκB is not detectable in response to transient Rag DNA DSBs by EMSA. NFκB EMSA of nuclear lysates from wild type (*WT*) and *Artemis*$^{-/-}$ abl pre-B cells treated with STI571 for the indicated times. NFY EMSA is shown as a control.

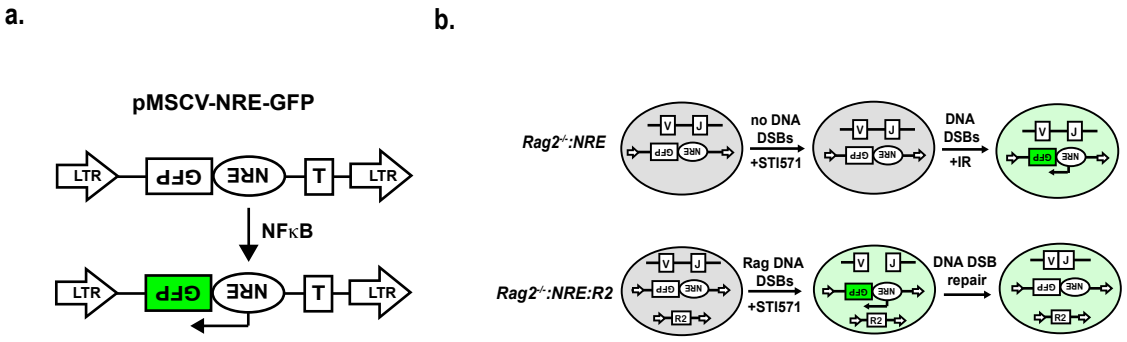

Figure 31. A reporter to detect NFκB activation in response to transient DNA DSBs. (a) Schematic of the pMSCV-NRE-GFP retrovirus, showing the Thy1 cDNA (T), the five tandem NFκB responsive elements (NRE), and the GFP cDNA in the anti-sense orientation. **(b)** Schematic of pMSCV NRE-GFP activation and GFP expression by treated and untreated *Rag2*$^{-/-}$*:NRE* and *Rag2*$^{-/-}$*:NRE:R2* cells. Transcription of the NRE-GFP cassette is indicated by the filled arrow from NRE and green shading of the GFP cDNA rectangle. The cessation of GFP transcription, as indicated by the white filled GFP cDNA rectangle, after repair of Rag-mediated DSBs is presumed. The presence of GFP in the cell is indicated by green shading of the cell. Rag DSBs are indicated by the discontinuity between the V and J gene segment, and a coding joint is indicated by the juxtaposition of the V and J gene segment. The retrovirally introduced Rag2 cDNA in *Rag2*$^{-/-}$*:NRE:R2* cells is shown (R2).

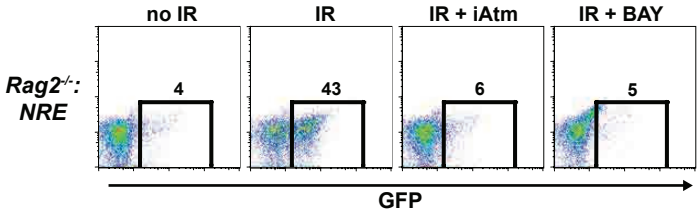

Figure 32. NFκB reporter detects activation of NFκB by genotoxic agents. *A*ctivation of NFκB in *Rag2*$^{-/-}$*:NRE* cells in response to IR induced DSBs. *Rag2*$^{-/-}$*:NRE* abl pre-B cells were treated with STI571 for 24 hours, then either not irradiated (no IR) or irradiated with 0.5 Gy (IR) and treated with vehicle alone, the Atm inhibitor KU-55933 (iAtm), or the inhibitor of IκB phosphorylation, BAY 11-7085 (BAY). Cells were analyzed for GFP expression from pMSCV-NRE-GFP by flow cytometry 12 hours post-irradiation.

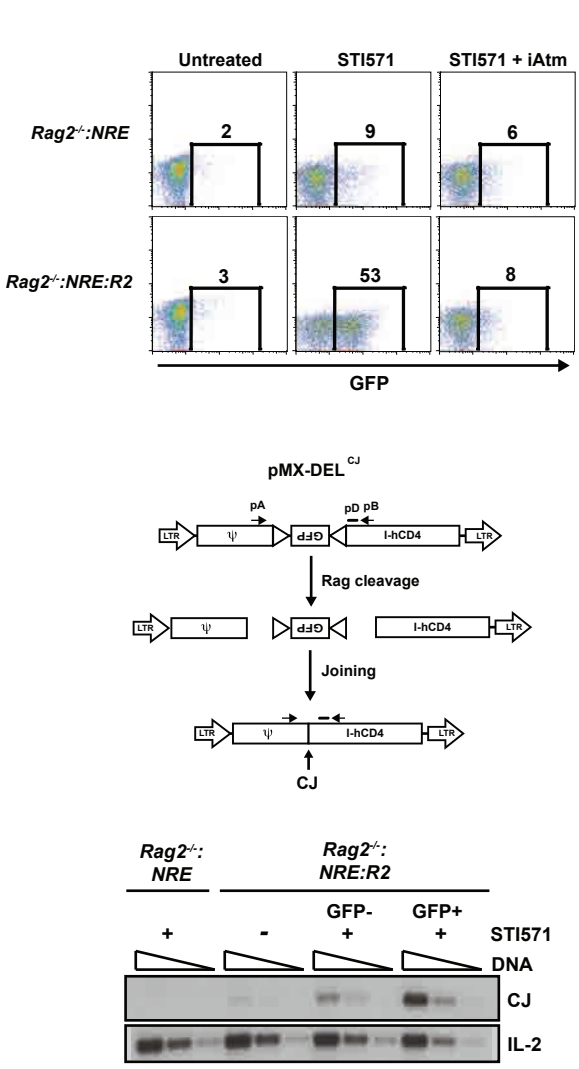

Figure 33. Transient Rag DNA DSBs activate NFκB. (a) Flow cytometric analysis of GFP expression in *Rag2*$^{-/-}$*:NRE* and *Rag2*$^{-/-}$*:NRE:R2* cells treated with STI571 for 48 hours in the presence or absence of the Atm inhibitor KU-55933 (iAtm). The percentage of GFP+ cells is indicated. **(b)** Schematic of the pMX-DEL^{CJ} retroviral recombination substrate. Shown is the GFP cDNA in the anti-sense orientation flanked by RSs (open triangles). Also shown are the IRES-human CD4 (I-hCD4) cassette, the long terminal repeats (LTRs), and the retroviral packaging sequence (ψ). The relative position of the pC and pB oligonucleotides (arrows) used for PCR analysis of coding joint (CJ) formation and the pD oligonucleotide (bar) used to probe the PCR products are also shown. **(c)** *Rag2*$^{-/-}$*:NRE* and *Rag2*$^{-/-}$*:NRE:R2* abl pre-B cells were un-treated (-) or treated with STI571 for 48 hours (+) and GFP+ and GFP- *Rag2*$^{-/-}$*:NRE:R2* abl pre-B cells isolated by flow cytometric cell sorting. Serial 4-fold dilutions of genomic DNA from all cells was assayed for pMX-DEL^{CJ} rearrangement by PCR.

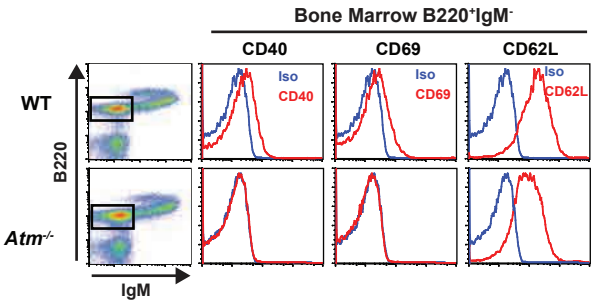

Figure 34. Transient breaks *in vivo* activate a broad genetic program. Flow cytometric analyses of CD40, CD69 and CD62L expression by $B220^{+}$:IgM^{-} bone marrow B cells (gated cells in dot plot) from *WT* and $Atm^{-/-}$ mice. Histograms for the specific antibodies (red) and isotype control (blue) are shown.

Chapter 6

Discussion

The generation of a functional antigen receptor gene in developing lymphocytes requires that the second exon be assembled through a process known as V(D)J recombination, which necessarily involves the generation and repair of DNA double-strand breaks made by the RAG endonuclease(1-3). Double strand breaks incurred during G1 of the cell cycle activate ATM, a PI3-kinase-like-kinase (PIKK) that, in response to genotoxic DNA damage, is known to phosphorylate hundreds of proteins with unique and diverse functions that coordinate the DNA damage response(71-73). Notably, deficiencies in ATM lead to ataxia-telangiectasia, a syndrome characterized by lymphopenia, genomic instability and a predisposition to tumors involving antigen receptor loci(99). These findings indicate that ATM plays a critical role downstream of RAG-mediated DNA DSBs during V(D)J recombination. The work presented here defines novel pathways activated by ATM in response to RAG DNA DSBs. Taken together with previous findings, the major ATM-dependent effector functions of the DNA damage response activated by RAG DNA DSBs include the following:

1—ATM promotes the efficient, proper repair of RAG DNA DSBs by maintaining coding ends in a stable post-cleavage complex through the MRN complex.

2—ATM promotes the activation of a broad genetic program that promotes the survival of cells actively undergoing V(D)J recombination but that also has potential diverse implications for lymphocyte development and function.

3—ATM activates p53-dependent apoptotic pathways in response to persistent unrepaired RAG DNA DSBs.

4—ATM phosphorylates H2AX to prevent resection of unrepaired coding ends and their aberrant resolution by homology-mediated pathways in G1 of the cell cycle.

Below I discuss how defects in each of these functions likely underlie the phenotypic manifestations of ATM-deficiency, namely lymphopenia and a predisposition to lymphoid tumors involving antigen receptor loci.

Lymphopenia of ATM-Deficiency

Lymphopenia caused by a defect in the repair of RAG DNA DSBs.

V(D)J recombination is the process by which the antigen receptors that are absolutely required for lymphocyte development are assembled. As such, defects in the generation or repair of RAG-induced DNA DSBs during V(D)J recombination can result in severe lymphopenia. As discussed above, SCID and RS-SCID patients harbor mutations in the RAG components that prevent DSB generation or in NHEJ factors that prevent the repair of the RAG-induced DSBs, respectively(65). Interestingly, A-T patients and ATM-deficient mice exhibit a phenotype that might be described as mild RS SCID. The patients and mice have a mild lymphopenia with reduced numbers of T cells primarily(111, 112). Furthermore, ATM-deficient mice are sensitive to ionizing irradiation, and AT patients have sensitivities to DSB-generating chemotherapeutic agents further suggesting that there may be a general defect in repair of DNA DSBs in the absence of ATM(122). Unlike the known core NHEJ-factors, however, we show that ATM is not absolutely required for V(D)J recombination and a majority of IR-induced breaks are repaired in the absence of ATM activity (122, 140). However, we reasoned that a non-absolute defect in the repair of RAG DNA DSBs could also impart radiosensitivity and cripple V(D)J recombination which would impact total lymphocyte numbers.

We demonstrate that ATM-deficient lymphocytes do, in fact, have a defect in the repair of RAG DNA DSBs characterized by an accumulation of unrepaired coding ends and an overall decrease in normal coding joint formation during rearrangement by both deletion and inversion(107, 108). Additionally, during rearrangement by inversion, ATM-deficient cells form aberrant hybrid joints with near equal kinetics as normal CJs(107).

How do we explain the decrease in normal CJ formation during rearrangement by deletion and inversion and the increase in HJ formation during rearrangement by inversion only? This defect is currently most aptly explained by a requirement for ATM in promoting the stability of the post-cleavage complex(107). One would predict that the loss of coding ends from this complex would lead to a decrease in CJ formation as ends that drift apart cannot be efficiently

joined. In fact, there is much redundancy amongst DNA repair factors that tether the broken DNA ends in many DNA repair pathways suggesting that keeping these broken ends in close physical proximity is absolutely required for efficient joining. Indeed, in our ATM-deficient cells, FISH analysis supported this hypothesis; unrepaired coding ends are more frequently separated from one another in *Atm*$^{-/-}$ cells as compared to *WT* cells(107). This defect would affect rearrangement by deletion and by inversion. Furthermore, instability of the post-cleavage complex might also explain the aberrant formation of hybrid joints only during rearrangement by inversion. During rearrangement by inversion, a decrease in the stability of the post-cleavage complex would allow the intervening sequence to escape from the complex. A resulting joint between the remaining coding end and signal end to form a HJ may reflect an act of desperation on the cell's behalf to maintain genomic integrity. During rearrangement by deletion, the intervening sequence is normally lost. Instability of the post-cleavage complex would not worsen this situation. In fact, hybrid joint formation during rearrangement by deletion would require that the intervening segment of DNA that is normally excised be inverted and maintained within the complex. Thus, we believe that the aberrant HJ formation during inversional rearrangement and the decrease in CJ formation during both deletional and inversional rearrangment can both be attributed to a decrease in the stability of the post-cleavage complex(107).

This activity of ATM during the repair of RAG induced DNA DSBs requires its kinase activity as treating wild-type cells with an ATM-specific kinase inhibitor leads to a phenotype similar to that of ATM deficiency(107). Presumably, then, ATM does not have a direct structural role in promoting post-cleavage complex stability. Rather, it may rely on the phosphorylation-dependent end stabilizing activities of an ATM substrate(s) at the break site. In this regard, the MRN complex is a potential candidate substrate. As discussed above, Mre11 can align two broken DNA ends and Rad50 can tether two broken DNA ends(75, 76, 78, 81, 83, 86). All three components of the MRN complex (Mre11, Rad50, and Nbs1) are phosphorylated by ATM(71, 300-302). Indeed, we demonstrate here that MRN-deficient cells have a similar, though milder,

repair defect as that characterized in the ATM-deficient cells. We note an increase in the number of HJs and a decrease in CJ efficiency.

Mice and patients deficient in any MRN component exhibit phenotypes that mimic ATM-deficiency(117, 291-298). Many have reasoned that the similarities in these phenotypes could simply reflect the role of the MRN complex as sensor in the DNA damage response in recruiting ATM and promoting ATM activity(70, 77, 90, 91, 104, 291, 299). Thus, the repair defect we see in the MRN-deficient cells may simply reflect an inability to fully activate ATM and the DNA damage response. That is, MRN may be acting upstream of ATM to promote the proper repair of RAG DNA DSBs. However, we do not see a global decrease in the phosphorylation of ATM substrates such as H2AX or the activation of ATM dependent DNA damage response pathways such as NFκB activation. These data suggest that MRN has important roles downstream of ATM in promoting the stability of the post-cleavage complex during the repair of RAG-mediated DSBs.

Does this repair defect observed in the ATM and MRN-deficient cells explain the lymphopenia observed in patients and mice with deficiencies in these factors? In both situations, T cell numbers are depleted moreso than B cell numbers(108, 292). In both ATM- and Nbs-deficient mice, we note a block in thymocyte development that results in decreased numbers of TCR-β intermediate DP thymocytes and partially explains the paucity of fully developed T cells(108). To reach this stage of development the thymocytes must rearrange the TCRα allele and the resulting TCR must be capable of positive selection(108). Often, a single round of V(D)J recombination does not produce a receptor that fulfill this requirements and successive rearrangements must take place. Failed repair at any juncture could result in thymocyte death(108). Thus, slightly attenuated efficiency of CJ formation during TCRα rearrangement could explain this block in thymocyte development(108). The repair defect of ATM- and MRN-deficiency may at least partially explain the T cell lymphopenia. However, we would note that the joining is likely similarly impaired in thymocytes at other stages of development and B cells undergoing V(D)J recombination but not manifested as a decrease in these populations as the antigen receptor loci rearranged in these cells at other developmental stages do not undergo

successive rearrangements to the same extent that T cells undergoing alpha rearrangement(108). Analysis of rearrangement of the TCRα locus and numbers of DP intermediates may simply be a more sensitive assay for defects in CJ formation in the endogenous loci.

We conclude that the described defect in the repair of RAG DNA DSBs contributes to the lymphopenia of ATM-deficient mice and humans as well as those deficient in MRN complex. We would note, however, that the described repair defect only leads to an ~50% reduction in CJ formation and is not likely to completely account for this aspect of the ATM-deficient phenotype(107, 108). Thus, we sought to identify other ways in which ATM might affect lymphocyte development.

Lymphopenia caused by defects in the RAG-dependent genetic program.

The canonical DNA damage response is largely concerned with promoting survival and cell cycle checkpoints during the repair of the break and initiating apoptosis in the event that the break cannot be repaired(73). In this regard, ATM activates p53 in cells with persistent RAG DNA DSBs(244). To this point, however, it was difficult to determine whether every RAG break or just those that remained unrepaired initiated the DNA damage response. Indeed, activating p53 in response to each RAG DNA DSB would be problematic because all lymphocytes must make and repair numerous RAG DNA DSBs during the course of development. The activation of p53, which initiates cell cycle checkpoints as well as apoptotic pathways, in response to each transient RAG DNA DSB, would significantly decrease the number of lymphocytes that successfully undergo V(D)J recombination. However, ATM might activate p53 in response to every RAG DNA DSB if it could simultaneously activate pro-survival pathways. The balance of these two pathways might determine cell survival. In this regard, ATM activates both p53 and NFκB in response to genotoxic DNA damage(244, 247, 269). Furthermore, inactivation of NFκB signaling leads to increased IR sensitivity, demonstrating that NFκB activation by ATM promotes cell survival following DNA damage(247). Similarly, we detect robust NFκB activation in response to persistent RAG DNA DSBs in NHEJ-deficient lymphocytes. Interestingly, we also detect NFκB

activation in response to transient RAG DNA DSBs in WT cells undergoing V(D)J recombination. Thus, it is likely that all RAG DNA DSBs activate the DNA damage response and result in transcriptional changes within the developing lymphocyte.

Lymphocytes with RAG DNA DSBs exhibit higher levels of pro-survival genes such as Pim-2 and Bcl-3 than observed in cells without RAG DNA DSBs. These transcriptional changes are dependent on both ATM and NFκB. Pim2 expression promotes the survival of lymphocytes following withdrawal of IL-7, a situation that mimics the environment of a lymphocyte undergoing V(D)J recombination; pre-B cells undergoing rearrangement of the kappa locus actively move away from IL-7 producing stromal cells(313). Thus, the ATM-dependent up-regulation of Pim-2 in response to RAG DNA DSBs might promote the survival of cells actively undergoing V(D)J recombination in an IL-7-depleted environment(J. Bednarski, unpublished). We conclude that the activation of NFκB by ATM in response to each RAG DNA DSB may promote the survival of cells undergoing V(D)J recombination and may be required to counteract the activation of p53 by the same DNA DSB. Defects in the activation and regulation of these pathways might lead to a disruption of the pro-life and pro-death balance in these developing lymphocytes and might also contribute to the lymphopenia observed in the setting of ATM-deficiency.

Lymphopenia caused by defects in the RAG-dependent genetic program.

We often think of the cellular response to DNA DSBs as a “damage” response. As discussed above, the canonical DNA damage response is known primarily to promote survival and cell cycle checkpoints during the repair of the break and initiating apoptosis in the event that the break cannot be repaired(244). In lymphocytes, however, RAG DNA DSBs are requisite intermediates in a process that is absolutely required for their proper development(1-3). Even transient RAG DNA DSBs can activate these DNA damage response pathways. As such, this “damage” response is likewise a part of normal development and the signaling pathways initiated in response to RAG-mediated DNA DSBs could affect lymphocyte development and/or function.

With these thoughts in mind, we decided to more fully characterize the transcriptional pathways activated by ATM in response to RAG DNA DSBs. Comparing the microarray analysis

data of lymphocytes with RAG DNA DSBs and those without DNA DSBs enabled us to globally determine the transcriptional changes afforded by the RAG DNA DSB. Analysis of this microarray data revealed that the transcriptional pathways activated by ATM in response to DNA DSBs are more numerous and diverse than previously thought; ATM activates a broad genetic program in response to RAG DNA DSBs. Only half of the ATM-dependent transcriptional changes caused by RAG DNA DSBs are mediated by NFκB. The others, we reason, are caused by transcription factors similarly directly or indirectly activated by ATM. It is notable that other transcription factors such as Stat3 and Foxo1 have SQ/TQ motifs that could be potentially modified by ATM(71).

A large fraction of this broad genetic program initiated by RAG DNA DSBs includes genes with no known function in the canonical DNA damage response. Rather, these are genes whose known functions implicate them in lymphocyte development and/or function. For example, a subset of these genes (L-selectin, Swap70, and CD69) have known roles in lymphocyte homing and migration(309-312). This suggests that RAG DNA DSBs might cause changes in the cell that somehow affect the localization of lymphocytes undergoing V(D)J recombination, perhaps through alterations in the expression levels of cell surface receptors. In support of this possibility, we find that lymphocytes harboring RAG dependent DNA DSBs partition differently between the peripheral blood and bone marrow than lymphocytes without breaks. The transcriptional changes, then, initiated by RAG DNA DSBs can have physiological consequences for the developing lymphocyte. While this is just one example, we believe that future work will elucidate additional developmental or functional consequences of the broad transcriptional program activated by ATM in response to RAG DNA DSBs. ATM influences lymphocyte development in ways not directly related to DNA repair or the survival of lymphocytes with breaks. Defects in this program might additionally contribute to the lymphopenia and immunodeficiency of ATM-deficient mice and humans.

Lymphopenia—A Combination of Two Distinct Defects

Based on the collected evidence, we propose that the lymphopenia observed in the setting of ATM-deficiency is caused by two primary factors. First, defects in the repair of RAG DNA DSBs lead to a smaller number of developing lymphocytes that successfully undergo V(D)J recombination to produce a functional antigen receptor gene. Second, ATM is required to activate a broad transcriptional program in response to RAG DNA DSBs. This program promotes the survival of cells actively undergoing V(D)J through the activation of NFκB. However, ATM also activates the transcription of genes that may affect lymphocyte development and/or function in additional and diverse ways.

A Predisposition to Lymphoid Tumors Involving Antigen Receptor Loci

In addition to lymphopenia, ATM-deficient mice and humans have a predisposition to lymphoid malignancies with translocations involving antigen receptor genes. The development of lymphoid malignancy requires a failure of the DNA damage response at multiple levels. Thus, just as defects in multiple ATM-dependent pathways can contribute to lymphopenia, the same is likely true for the development of lymphoid malignancies.

ATM deficiency causes a combined repair and checkpoint defect.

We have described a repair defect in ATM-deficient cells and mice that leads to an accumulation of unrepaired coding ends(107, 108). Notably, ATM is also required to promote p53 activation in response to DNA damage(244). Thus, in the absence of ATM, a single protein, we have essentially recapitulated the phenotype of mice deficient in both NHEJ and p53-dependent pathways that develop lymphoid malignancies at a young age(150).

It is thought that broken DNA ends form translocations primarily by joining with other broken DNA ends present in that particular cell(314). Cells arrested in G1-phase of the cell cycle generally have very few DNA DSBs besides RAG DNA DSBs. This is evidenced by the fact that we rarely see γ-H2AX foci in G1-arrested *Rag*$^{-/-}$ Abl pre-B cells(211, 276). While RAG DNA DSBs can occur outside the confines of the antigen receptor genetic loci, this is rare. Thus, unrepaired coding ends would not have ample opportunity to form translocations in G1. However, the

combined defect in repair and cell cycle checkpoint allows these ends to persist through multiple rounds of cell division(202, 272). During cell division, many DSBs are produced during DNA replication and other cellular processes. Thus, the persistence of these ends throughout the cell cycle would greatly increase the chance that they would form translocations(202, 272). The combined repair and checkpoint defect in ATM-deficient mice and humans likely contributes to the predisposition to lymphoid tumors with translocations involving antigen-receptor loci.

ATM actively prevents the aberrant resolution of persistent DNA ends.

However, we reasoned that ATM might play an additional active role in preventing unrepaired coding ends from accessing aberrant repair pathways, effectively shuttling cells that harbor these persistent breaks towards p53-mediated pathways. As discussed in the introduction, DNA repair pathway choice is determined at the level of end-resection(139). Even small amounts of end resection prevent NHEJ and commit the cell to repair through alternative homology-mediated pathways(140-142, 176). Cells undergoing V(D)J recombination are arrested in G1, where no sister chromatid is present; thus, repair by homology-mediated pathways would be particularly deleterious as it would lead to deletions and/or translocations. During HR, end resection is initiated through the cooperative action of Mre11 and CtIP(76, 129-136). Importantly, we have shown that Mre11 functions during V(D)J recombination as a component of the MRN complex and is present at RAG DNA DSB sites. Mre11 possesses both endo- and exo-nucleolytic activities but is not able to efficiently open the hairpin-sealed coding ends in *Artemis*$^{-/-}$ cells(77, 81). Thus, we know that end resection is tightly regulated during V(D)J recombination. We hypothesized that another ATM-dependent effector function of the DDR might be to ensure that persistent unrepaired DNA ends are not resected in a manner inappropriate to the stage of the cell cycle. Specifically, we predicted that unrepaired coding ends in the G1-phase of the cell cycle during V(D)J recombination are not resected.

We further reasoned that ATM would modulate end-processing pathways through the break-induced phosphorylation of one or more of substrates. In this regard, histone H2AX is phosphorylated in chromatin flanking DNA DSBs, including those generated by the RAG-

endonuclease forming γ-H2AX(206, 211). γ-H2AX is required for the maintenance of a host of repair and signaling proteins at the site of a DNA DSB(233). H2AX-deficient cells have a predisposition to genomic instability but no overt defect in the repair of RAG DNA DSBs, which is what we might expect if H2AX functions mainly in dealing with rare persistent RAG DNA DSB(233, 235, 243). Furthermore, while hairpin-sealed coding ends in *Artemis*$^{-/-}$ cells are rarely resolved as translocations, those in *Artemis*$^{-/-}$*:H2AX*$^{-/-}$ cells are more frequently resolved as translocations(243). The resolution of a hairpin-sealed coding end, at a minimum, would require end opening. Thus, we hypothesized that H2AX might regulate the processing of unrepaired coding ends and furthermore, that the phosphorylation of H2AX by ATM at the site of these RAG DNA DSBs might be required to facilitate end processing. Accordingly, we designed experiments to assess the integrity of unrepaired coding ends that accumulate in NHEJ-deficient cells in the presence and absence of H2AX.

We find that, in the absence of H2AX, unrepaired coding ends are robustly resected. We further demonstrate that the ATM-dependent phosphorylation of H2AX(forming γ-H2AX) and Mdc1, a factor that directly binds γ-H2AX, are both required to prevent this resection. Finally, we demonstrate that the end resection we see is mediated by CtIP, the mammalian homologue of yeast endonclease Sae2. The coding ends that have undergone aberrant CtIP-dependent processing are not efficiently joined by NHEJ. Furthermore, the joints that do form exhibit large deletions and usage of homology-mediated repair. The numerous implications of this novel role for γ-H2AX during DNA repair as well as additional thoughts regarding the resection and joining of these aberrantly processed ends are addressed below.

Regarding the End Resection

As discussed in the introduction, during HR, Mre11 and CtIP cooperate to initiate the resection of broken DNA ends that allows for the formation of a long 3' ssDNA overhang that permits strand invasion(76, 129-136). However, the activity of CtIP and Mre11 is normally restricted to post-replicative stages of the cell cycle. How, is it then, that H2AX prevents the CtIP-mediated opening and resection of persistent coding ends in *Artemis*$^{-/-}$*:H2AX*$^{-/-}$ and *Ligase IV*$^{-/-}$

:H2AX$^{-/-}$ cells that are arrested in G1 of the cell cycle? We hypothesize, based on known protein-protein interactions and crystallographic data, that the phosphorylation of H2AX may be required to exclude CtIP from the site of a persistent RAG DNA DSB in G1-phase cells. As demonstrated above, MRN functions during V(D)J recombination and Nbs1 has been demonstrated to localize at RAG DNA DSBs(105). We also know that MRN and CtIP directly interact in mammalian cells(89, 229, 230, 315). In fission yeast, Ctp1 (the homologue of CtIP) associates with the FHA domain of Nbs(88, 89, 229-231, 315). Interestingly, MDC-1 binds to that same FHA domain of mammalian Nbs1(89). In response to a DNA DSB, H2AX is rapidly phosphorylated and this phosphorylated H2AX is subsequently bound by Mdc1(206, 214, 228). Mdc1 then interacts with Nbs1 in a manner that is thought to potentiate ATM signaling(228, 316). However, in doing so, we hypothesize that it may competitively displace CtIP associated with the MRN complex at the break site. Such a model would be completely congruent with our findings as γ-H2AX and Mdc1 are both required to prevent end resection, and furthermore, we now know that the MRN complex functions during V(D)J recombination. We plan to test this hypothesis using ChIP assays to determine whether CtIP is associated with RAG DNA DSBs and whether that association is increased or altered in some manner in the absence of H2AX or Mdc1, perhaps explaining the aberrant end resection observed in H2AX-deficient cells.

ATM is required to generate γ-H2AX in chromatin flanking RAG DSBs(209-211). In turn, MDC-1 amplifies DNA damage response signals, in part, by recruiting ATM to the site of a DSB(228, 316). As such, we reasoned that ATM would be required to prevent the nucleolytic resection of coding ends in G1-phase cells. However, we do not detect degradation of coding ends in *Artemis*$^{-/-}$*:Atm*$^{-/-}$ Abl pre-B cells though γ-H2AX formation is largely disrupted in these cells. This seemed at odds with our data demonstrating that ATM-mediated phosphorylation of H2AX is required to prevent end resection. However, we subsequently show that ATM kinase activity is required to promote CtIP-mediated resection of persistent coding ends in the absence of H2AX. Inhibition of ATM kinase activity in *Artemis*$^{-/-}$*:H2AX*$^{-/-}$ cells completely abrogates the opening and resection of hairpin-sealed ends. Thus, ATM activates opposing pathways that

regulate resection of persistent coding ends. How ATM promotes CtIP activity, however, is still largely unknown. In Xenopus extracts that have characteristics of G1-phase cells, ATM activity is also required for CtIP activity, possibly through affecting its recruitment to a DNA DSB. In this system, CtIP is recruited to a DNA DSB after ATM and Nbs in a manner that requires MRN and ATM kinase activity(135). We know that CtIP is phosphorylated by ATM in response to DNA damage(71, 135, 317). However, in Xenopus extracts, mutation of all possible SQ/TQ sites in CtIP does not alter the localization of CtIP to a DNA DSB suggesting that ATM might affect the localization of CtIP indirectly(135). One possibility is that the ATM-dependent phosphorylation of another substrate might recruit CtIP to the site of a DNA DSB. We would like to test whether ATM kinase activity similarly alters the localization of CtIP in lymphocytes and whether the phosphorylation of CtIP in response to DNA damage alters its localization. It is also notable that CtIP has known functions as a transcriptional regulator, and the ATM-dependent phosphorylation of CtIP can lead to alterations in gene expression(317). CtIP associates with CtBP and they function together as a transcriptional co-repressor; interaction of CtIP and CtBP with BRCA1, for example, leads to decreased expression of BRCA1 target genes p21 and GADD45(317). Phosphorylation of CtIP by ATM causes its dissociation from BRCA1. This releases the repression and the cellular levels of both p21 and GADD45 transcripts increase(317). Thus, the ATM-dependent end resection of the persistent coding ends in *Artemis*$^{-/-}$*:H2AX*$^{-/-}$ and *Ligase IV*$^{-/-}$*:H2AX*$^{-/-}$ cells could also be a consequence of indirect effects of CtIP on gene transcription. For example, phosphorylation of CtIP may activate (de-repress) the transcription of a nuclease that can promote the degradation of persistent coding ends.

While it is likely that Mre11 and CtIP cooperate to cause the resection of persistent coding ends in the *Artemis*$^{-/-}$*:H2AX*$^{-/-}$ and *Lig4*$^{-/-}$*:H2AX*$^{-/-}$ cells, it is possible that CtIP is directly modulating the activity of another nuclease. Though no nuclease activity of CtIP has been formally demonstrated, CtIP contains a domain structurally similar to the catalytic domain of the budding yeast endonuclease Sae2(135, 137). *In vitro*, CtIP can alter the nuclease activity of Mre11(318). It is also notable that while Mre11 and CtIP are required to initiate resection during

HR, other nucleases (Dna2/Sgs1 and Exo1 for example) are thought to cause the formation of the ssDNA strand(137, 139). Thus, the degradation that we see may actually be a result of the nuclease activity of Mre11 or potentially other cellular nucleases. Additional evidence from our laboratory suggests that other nucleases play a role in the resection of unrepaired coding ends during V(D)J recombination. Consistent with this possibility, the coding ends that escape from the post-cleavage complex in *Atm*$^{-/-}$ cells are degraded at late time-points as are unrepaired coding ends in *Lig IV*$^{-/-}$*:Atm*$^{-/-}$ cells; this end resection is not CtIP-mediated as we now know that ATM is required to promote robust CtIP activity. However, this resection could also be regulated by H2AX as H2AX phosphorylation is largely abrogated in the absence of ATM. In addition to the CtIP- and ATM-dependent resection of open coding ends in *Ligase IV*$^{-/-}$*:H2AX*$^{-/-}$ Abl pre-B cells, we note a delayed ATM-independent resection of these ends. Finally, we observe residual end resection upon knockdown of CtIP in both the *Artemis*$^{-/-}$*:H2AX*$^{-/-}$ and *Ligase IV*$^{-/-}$*:H2AX*$^{-/-}$ cells. While the latter could be due to residual CtIP in these cells, it could also indicate that other nucleases act on persistent RAG DNA DSBs. Together, these data suggest that the activity of other nucleases must also be regulated during V(D)J recombination. By knockdown of candidate nucleases, specifically those known to function during HR with CtIP and Mre11, we may be able to further dissect components of the end processing pathways that collectively regulate the outcome of unrepaired ends. These future experiments may also provide insight into whether CtIP itself promotes end resection or does so by regulating the activity of other cellular nucleases.

Given the near normal repair of RAG DNA DSBs during V(D)J recombination in H2AX-deficient cells but the profound effect of H2AX-deficiency on persistent coding ends, we propose that the phosphorylation of H2AX might be especially important to protect coding ends when they are not joined efficiently. We predict that H2AX deficiency, when combined with defects that decrease the efficiency of RAG DNA DSB repair would lead to dramatic defects in V(D)J recombination. XLF or Cernunnos is a recently discovered NHEJ-component with an undetermined role in V(D)J recombination(152, 319, 320). In other settings, however, XLF associates with XRCC4 and Lig4 to alter the activity of this complex, increasing the efficiency of

joining and also enhancing the diversity of DNA ends that can be ligated by this complex(152, 155, 157). Intriguingly, while H2AX and XLF alone have no demonstrable defect in the repair of chromosomal RAG DNA DSBs in developing lymphocytes, a combined deficiency causes a profound defect in coding joint formation, with unrepaired coding ends exhibiting robust resection (unpublished data, Fred Alt lab). These findings support our hypothesis that H2AX is especially important for cells in which breaks are not efficiently repaired; that is, XLF may cause a decrease in joining efficiency that necessitates end protection by H2AX. Furthermore, XLF and H2AX may serve a redundant function in preventing the resection of unrepaired ends since end degradation in double mutants is greater than seen in the *Artemis*$^{-/-}$*:H2AX*$^{-/-}$ or *Ligase IV*$^{-/-}$*:H2AX*$^{-/-}$ Abl pre B cells alone. Furthermore, combined deficiency of H2AX and NHEJ-component XLF leads to embryonic lethality ((278, 321) and unpublished communication), suggesting that their cooperative action has additional roles for other types of DNA DSB repair. Determining how H2AX and XLF cooperate to promote repair and prevent end resection is, thus, a high priority.

Finally, it remains puzzling that *H2AX*$^{-/-}$ mice exhibit such profound genomic instability that is increased even further with genotoxic DNA damage but still lack an overt defect in the repair of RAG DNA DSBs(233, 235, 243). This may indicate that H2AX-deficiency impacts the resolution of DNA DSBs generated by genotoxic agents moreso than those generated by the RAG endonuclease. Importantly, RAG DNA DSBs are initiated by an enzymatic reaction that includes a hairpin-sealed intermediate(1). RAG-generated DNA ends are maintained in a post-cleavage complex that would presumably insulate them from the effects of cellular nucleases(198). In contrast, broken DNA ends resulting from irradiation or other genotoxic agents are diverse; many of these ends incorporate modified bases that must be processed prior to joining, thus increasing the amount of time they persist(322). Furthermore, these ends are not maintained in a post-synaptic complex. Thus, the ATM-dependent phosphorylation of H2AX at such damage sites may be especially important in preventing end resection. We propose that the lack of a significant defect in V(D)J recombination in *H2AX*$^{-/-}$ mice may reflect these unique features of physiologic RAG DNA DSBs.

Regarding the joints formed in *Artemis$^{-/-}$:H2AX$^{-/-}$:DEL^{CJ}* Abl pre-B cells.

Our observation that open resected ends in *Artemis$^{-/-}$:H2AX$^{-/-}$* cells are not efficiently joined by NHEJ was especially surprising given that all requisite NHEJ components are present. This finding suggests that the nature of resected end prevents joining in G1 of the cell cycle, perhaps due to specific DNA end modifications or the generation of a significant ssDNA overhang. Even small ssDNA overhangs can prevent Ku-binding to a DNA end, thereby inhibiting NHEJ(140-142, 176). During HR, the combined activity of Mre11 and CtIP initiates a process that results in a long ssDNA structure(76, 129-136). Therefore, we hypothesize that the combined activities of Mre11 and CtIP might similarly generate a ssDNA fragment during the processing of unrepaired coding ends in the absence of H2AX. This would preclude joining by NHEJ during G1 where these cells are arrested and may explain the persistent open coding ends we observe in the *Artemis$^{-/-}$:H2AX$^{-/-}$* Abl pre-B cells. Elucidating the structure of DNA ends generated in Artemis-deficient cells that also lack H2AX will be an important goal of future studies.

It is notable that a low level of coding joints are formed successfully in our G1-arrested *Artemis$^{-/-}$:H2AX$^{-/-}$* Abl pre-B cells. However, PCR and sequence analyses of these joints reveal significant deletions (>1 kB). During V(D)J recombination, deletions such as these would preclude the formation of a functional antigen receptor gene. It is also possible this observation may have uncovered a potential source of the general genomic instability observed in *H2AX$^{-/-}$* mice. Similar deletions at joints formed throughout the genome following genotoxic DNA damage could cause genomic instability and possibly lead to malignant transformation. While chromosomal instability is often thought of in terms of whole chromosome loss or translocation, small deletions are frequent contributors to oncogenic transformation. In this regard, small deletions in Brca-1 genes have been associated with breast and ovarian cancer; likewise, deletions in p53 are observed in a wide variety of tumors(323-325). Thus, maintaining the integrity of broken DNA prior to joining is crucial. Interestingly, H2AX may protect the genome from small cancer-causing deletions during DNA DSB repair. It has been described that small deletions in p53 led to a reduced latency of disease, specifically thymic lymphomas, in *H2AX$^{-/-}$*

:p53$^{+/-}$*:RAG-2*$^{-/-}$ mice as compared to *p53*$^{+/-}$*:RAG-2*$^{-/-}$ mice(326). This noted predisposition to small deletions during other types of DNA DSB repair may be due to the role of γ-H2AX in preventing the resection of broken DNA ends as demonstrated herein.

Coding joints that form in *Artemis*$^{-/-}$*:H2AX*$^{-/-}$ may derive from a subset of ends whose processing does not generate a significant ssDNA overhang. As such, these ends could be joined by classical NHEJ. Alternatively, these ends may be processed in ways that produce structures incompatible with NHEJ. In this case, the low level of joints we observe may form via an alternative homology-mediated pathway which is active but not efficient during G1. In support of this notion, we demonstrate that the ends that are joined in the *Artemis*$^{-/-}$*:H2AX*$^{-/-}$ Abl pre-B cells more frequently use microhomologies (up to 50% of joins in *Artemis*$^{-/-}$*:H2AX*$^{-/-}$ as compared to less than 5% in WT cells) and the tracts of homology are generally longer. Importantly, the number of joints with microhomology that we detect are likely an underestimate of the true numbers since TdT is present and active in these cells. TdT adds nucleotides to DNA ends in a non-templated fashion, and, in doing so, could create microhomologies that facilitate joining. However, these joints would not be classified as microhomology-mediated as these sequences would not be present in the germ-line. Thus, the addition of non-templated nucleotides by TdT would obscure joining that does actually occur by homology. We are currently generating *Artemis*$^{-/-}$*:H2AX*$^{-/-}$*:TdT*$^{-/-}$ mice and cell lines that will enable us to more accurately assess whether joins made in the *Artemis*$^{-/-}$*:H2AX*$^{-/-}$ cells preferentially engage homology mediate repair pathways to resolve unrepaired coding ends during G1. Importantly, the joining of unrepaired ends in a homology-mediated manner during G1 is particularly dangerous as there is no sister chromatid available to be used as a template for repair. These ends might use regions of homologous DNA sequence on the same or other chromosomes to mediate joining, leading to larger chromosomal deletions and/or translocations that could likewise cause genomic instability. We conclude that this aberrant resection and joining, could, in addition to the described combined repair and checkpoint defect, predispose ATM-deficient mice and humans to lymphoid tumors with translocations involving the antigen receptor loci.

Summary (see model in Figure 35)

Based on the work described here, we propose the following model for the functions of ATM during normal lymphocyte development. ATM contributes to V(D)J recombination in two main ways to generate normal numbers of functional lymphocytes. First, ATM maintains coding ends within a stable post-cleavage complex to promote efficient and proper repair of RAG DNA DSBs and enable developing lymphocytes to produce a functional antigen receptor gene. Second, ATM, through the activation of NFκB and other transcription factors, induces the activation of a broad genetic program that promotes the survival of lymphocytes while they rearrange their antigen receptor loci. Moreover, this program includes gene products that are required for proper lymphocyte development and/or function. In the event that RAG DNA DSBs persist unrepaired, ATM activates p53 to ensure that cells harboring these breaks undergo apoptosis. Additionally, ATM, through the phosphorylation of H2AX, actively prevents unrepaired ends from being processed in ways that enable their aberrant resolution and effectively shuttles the cells harboring these breaks towards apoptotic pathways. Together, these functions of ATM downstream of RAG DNA DSBs explain the lymphopenia and predisposition to lymphoid tumors observed in the absence of ATM.

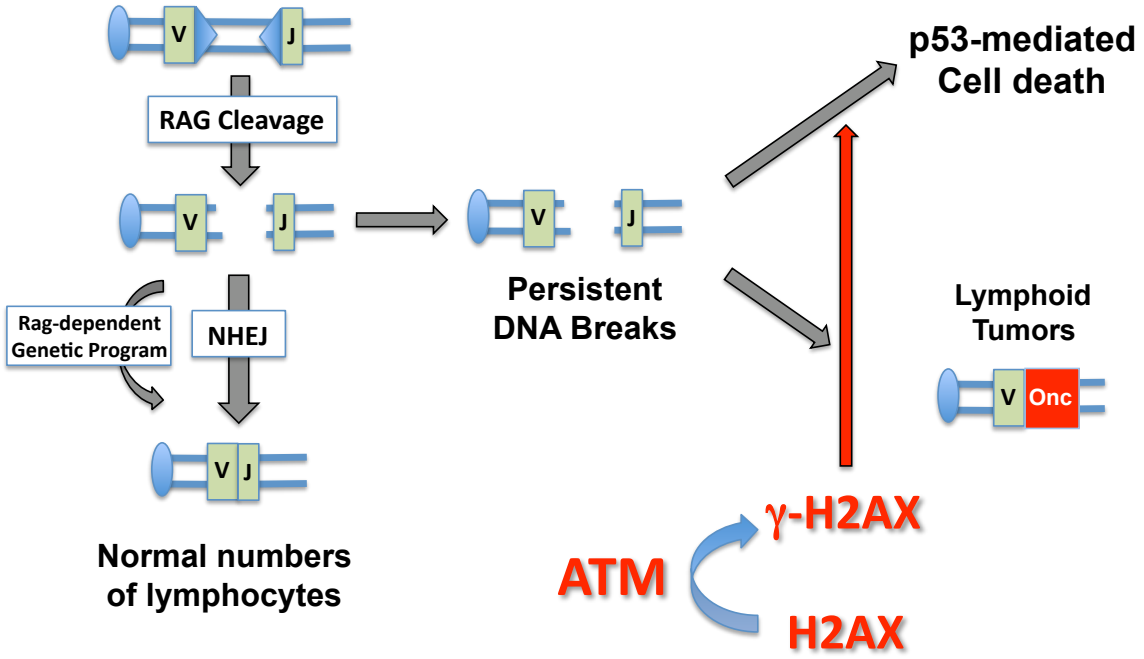

Figure 35. Functions of ATM during V(D)J recombination.

References:

1. Bassing CH, Swat W, Alt FW. 2002. The mechanism and regulation of chromosomal V(D)J recombination. *Cell* 109 Suppl: S45-55
2. Tonegawa S. 1983. Somatic generation of antibody diversity. *Nature* 302: 575-81
3. Hesslein DG, Schatz DG. 2001. Factors and forces controlling V(D)J recombination. *Adv Immunol* 78: 169-232
4. Polo SE, Jackson SP. 2011. Dynamics of DNA damage response proteins at DNA breaks: a focus on protein modifications. *Genes Dev* 25: 409-33
5. Jackson SP, Bartek J. 2009. The DNA-damage response in human biology and disease. *Nature* 461: 1071-8
6. Zhou BB, Elledge SJ. 2000. The DNA damage response: putting checkpoints in perspective. *Nature* 408: 433-9
7. Oettinger MA, Schatz DG, Gorka C, Baltimore D. 1990. RAG-1 and RAG-2, adjacent genes that synergistically activate V(D)J recombination. *Science* 248: 1517-23
8. Schatz DG, Oettinger MA, Baltimore D. 1989. The V(D)J recombination activating gene, RAG-1. *Cell* 59: 1035-48
9. Lee J, Desiderio S. 1999. Cyclin A/CDK2 regulates V(D)J recombination by coordinating RAG-2 accumulation and DNA repair. *Immunity* 11: 771-81
10. Mizuta R, Mizuta M, Araki S, Kitamura D. 2002. RAG2 is down-regulated by cytoplasmic sequestration and ubiquitin-dependent degradation. *J Biol Chem* 277: 41423-7
11. Desiderio S, Lin WC, Li Z. 1996. The cell cycle and V(D)J recombination. *Curr Top Microbiol Immunol* 217: 45-59
12. van Gent DC, Hiom K, Paull TT, Gellert M. 1997. Stimulation of V(D)J cleavage by high mobility group proteins. *EMBO J* 16: 2665-70
13. Sawchuk DJ, Weis-Garcia F, Malik S, Besmer E, Bustin M, Nussenzweig MC, Cortes P. 1997. V(D)J recombination: modulation of RAG1 and RAG2 cleavage activity on 12/23 substrates by whole cell extract and DNA-bending proteins. *J Exp Med* 185: 2025-32
14. Swanson PC. 2002. Fine structure and activity of discrete RAG-HMG complexes on V(D)J recombination signals. *Mol Cell Biol* 22: 1340-51
15. Schatz DG, Oettinger MA, Schlissel MS. 1992. V(D)J recombination: molecular biology and regulation. *Annu Rev Immunol* 10: 359-83
16. Gellert M. 1997. Recent advances in understanding V(D)J recombination. *Adv Immunol* 64: 39-64
17. Swanson PC, Kumar S, Raval P. 2009. Early steps of V(D)J rearrangement: insights from biochemical studies of RAG-RSS complexes. *Adv Exp Med Biol* 650: 1-15
18. De P, Rodgers KK. 2004. Putting the pieces together: identification and characterization of structural domains in the V(D)J recombination protein RAG1. *Immunol Rev* 200: 70-82
19. Schatz DG, Ji Y. 2011. Recombination centres and the orchestration of V(D)J recombination. *Nat Rev Immunol* 11: 251-63
20. Matthews AG, Kuo AJ, Ramon-Maiques S, Han S, Champagne KS, Ivanov D, Gallardo M, Carney D, Cheung P, Ciccone DN, Walter KL, Utz PJ, Shi Y, Kutateladze TG, Yang W, Gozani O, Oettinger MA. 2007. RAG2 PHD finger couples histone H3 lysine 4 trimethylation with V(D)J recombination. *Nature* 450: 1106-10
21. Liu Y, Subrahmanyam R, Chakraborty T, Sen R, Desiderio S. 2007. A plant homeodomain in RAG-2 that binds Hypermethylated lysine 4 of histone H3 is necessary for efficient antigen-receptor-gene rearrangement. *Immunity* 27: 561-71
22. Ramon-Maiques S, Kuo AJ, Carney D, Matthews AG, Oettinger MA, Gozani O, Yang W. 2007. The plant homeodomain finger of RAG2 recognizes histone H3 methylated at both lysine-4 and arginine-2. *Proc Natl Acad Sci U S A* 104: 18993-8
23. Fugmann SD, Schatz DG. 2001. Identification of basic residues in RAG2 critical for DNA binding by the RAG1-RAG2 complex. *Mol Cell* 8: 899-910

24. Landree MA, Wibbenmeyer JA, Roth DB. 1999. Mutational analysis of RAG1 and RAG2 identifies three catalytic amino acids in RAG1 critical for both cleavage steps of V(D)J recombination. *Genes Dev* 13: 3059-69
25. Kim DR, Dai Y, Mundy CL, Yang W, Oettinger MA. 1999. Mutations of acidic residues in RAG1 define the active site of the V(D)J recombinase. *Genes Dev* 13: 3070-80
26. Fugmann SD, Villey IJ, Ptaszek LM, Schatz DG. 2000. Identification of two catalytic residues in RAG1 that define a single active site within the RAG1/RAG2 protein complex. *Mol Cell* 5: 97-107
27. van Gent DC, Mizuuchi K, Gellert M. 1996. Similarities between initiation of V(D)J recombination and retroviral integration. *Science* 271: 1592-4
28. McBlane JF, van Gent DC, Ramsden DA, Romeo C, Cuomo CA, Gellert M, Oettinger MA. 1995. Cleavage at a V(D)J recombination signal requires only RAG1 and RAG2 proteins and occurs in two steps. *Cell* 83: 387-95
29. Schlissel M, Constantinescu A, Morrow T, Baxter M, Peng A. 1993. Double-strand signal sequence breaks in V(D)J recombination are blunt, 5'-phosphorylated, RAG-dependent, and cell cycle regulated. *Genes Dev* 7: 2520-32.
30. Roth DB, Menetski JP, Nakajima PB, Bosma MJ, Gellert M. 1992. V(D)J recombination: broken DNA molecules with covalently sealed (hairpin) coding ends in scid mouse thymocytes. *Cell* 70: 983-91.
31. Swanson PC, Desiderio S. 1999. RAG-2 promotes heptamer occupancy by RAG-1 in the assembly of a V(D)J initiation complex. *Mol Cell Biol* 19: 3674-83
32. Akamatsu Y, Oettinger MA. 1998. Distinct roles of RAG1 and RAG2 in binding the V(D)J recombination signal sequences. *Mol Cell Biol* 18: 4670-8.
33. Nagawa F, Kodama M, Nishihara T, Ishiguro K, Sakano H. 2002. Footprint analysis of recombination signal sequences in the 12/23 synaptic complex of V(D)J recombination. *Mol Cell Biol* 22: 7217-25
34. Difilippantonio MJ, McMahan CJ, Eastman QM, Spanopoulou E, Schatz DG. 1996. RAG1 mediates signal sequence recognition and recruitment of RAG2 in V(D)J recombination. *Cell* 87: 253-62.
35. Swanson PC, Desiderio S. 1998. V(D)J recombination signal recognition: distinct, overlapping DNA-protein contacts in complexes containing RAG1 with and without RAG2. *Immunity* 9: 115-25.
36. Eastman QM, Schatz DG. 1997. Nicking is asynchronous and stimulated by synapsis in 12/23 rule-regulated V(D)J cleavage. *Nucleic Acids Res* 25: 4370-8
37. Yu K, Lieber MR. 2000. The nicking step in V(D)J recombination is independent of synapsis: implications for the immune repertoire. *Mol Cell Biol* 20: 7914-21
38. Curry JD, Geier JK, Schlissel MS. 2005. Single-strand recombination signal sequence nicks in vivo: evidence for a capture model of synapsis. *Nat Immunol* 6: 1272-9
39. Fugmann SD, Lee AI, Shockett PE, Villey IJ, Schatz DG. 2000. The RAG proteins and V(D)J recombination: complexes, ends, and transposition. *Annu Rev Immunol* 18: 495-527
40. Bassing CH, Alt FW, Hughes MM, D'Auteuil M, Wehrly TD, Woodman BB, Gartner F, White JM, Davidson L, Sleckman BP. 2000. Recombination signal sequences restrict chromosomal V(D)J recombination beyond the 12/23 rule. *Nature* 405: 583-6
41. Dudley DD, Chaudhuri J, Bassing CH, Alt FW. 2005. Mechanism and control of V(D)J recombination versus class switch recombination: similarities and differences. *Adv Immunol* 86: 43-112
42. Jones JM, Gellert M. 2002. Ordered assembly of the V(D)J synaptic complex ensures accurate recombination. *Embo J* 21: 4162-71
43. Mundy CL, Patenge N, Matthews AG, Oettinger MA. 2002. Assembly of the RAG1/RAG2 synaptic complex. *Mol Cell Biol* 22: 69-77
44. van Gent DC, McBlane JF, Ramsden DA, Sadofsky MJ, Hesse JE, Gellert M. 1995. Initiation of V(D)J recombination in a cell-free system. *Cell* 81: 925-34

45. Yancopoulos GD, Alt FW. 1985. Developmentally controlled and tissue-specific expression of unrearranged VH gene segments. *Cell* 40: 271-81
46. Cobb RM, Oestreich KJ, Osipovich OA, Oltz EM. 2006. Accessibility control of V(D)J recombination. *Adv Immunol* 91: 45-109
47. Abarrategui I, Krangel MS. 2009. Germline transcription: a key regulator of accessibility and recombination. *Adv Exp Med Biol* 650: 93-102
48. Hesslein DG, Pflugh DL, Chowdhury D, Bothwell AL, Sen R, Schatz DG. 2003. Pax5 is required for recombination of transcribed, acetylated, 5' IgH V gene segments. *Genes Dev* 17: 37-42
49. Fuxa M, Skok J, Souabni A, Salvagiotto G, Roldan E, Busslinger M. 2004. Pax5 induces V-to-DJ rearrangements and locus contraction of the immunoglobulin heavy-chain gene. *Genes Dev* 18: 411-22
50. Zhang Z, Espinoza CR, Yu Z, Stephan R, He T, Williams GS, Burrows PD, Hagman J, Feeney AJ, Cooper MD. 2006. Transcription factor Pax5 (BSAP) transactivates the RAG-mediated V(H)-to-DJ(H) rearrangement of immunoglobulin genes. *Nat Immunol* 7: 616-24
51. Golding A, Chandler S, Ballestar E, Wolffe AP, Schlissel MS. 1999. Nucleosome structure completely inhibits in vitro cleavage by the V(D)J recombinase. *EMBO J* 18: 3712-23
52. Kwon J, Morshead KB, Guyon JR, Kingston RE, Oettinger MA. 2000. Histone acetylation and hSWI/SNF remodeling act in concert to stimulate V(D)J cleavage of nucleosomal DNA. *Mol Cell* 6: 1037-48
53. Abarrategui I, Krangel MS. 2006. Regulation of T cell receptor-alpha gene recombination by transcription. *Nat Immunol* 7: 1109-15
54. Skok JA, Gisler R, Novatchkova M, Farmer D, de Laat W, Busslinger M. 2007. Reversible contraction by looping of the Tcra and Tcrb loci in rearranging thymocytes. *Nat Immunol* 8: 378-87
55. Roldan E, Fuxa M, Chong W, Martinez D, Novatchkova M, Busslinger M, Skok JA. 2005. Locus 'decontraction' and centromeric recruitment contribute to allelic exclusion of the immunoglobulin heavy-chain gene. *Nat Immunol* 6: 31-41
56. Sayegh CE, Jhunjhunwala S, Riblet R, Murre C. 2005. Visualization of looping involving the immunoglobulin heavy-chain locus in developing B cells. *Genes Dev* 19: 322-7
57. Jhunjhunwala S, van Zelm MC, Peak MM, Murre C. 2009. Chromatin architecture and the generation of antigen receptor diversity. *Cell* 138: 435-48
58. Kosak ST, Skok JA, Medina KL, Riblet R, Le Beau MM, Fisher AG, Singh H. 2002. Subnuclear compartmentalization of immunoglobulin loci during lymphocyte development. *Science* 296: 158-62
59. Ji Y, Resch W, Corbett E, Yamane A, Casellas R, Schatz DG. The in vivo pattern of binding of RAG1 and RAG2 to antigen receptor loci. *Cell* 141: 419-31
60. Raghavan SC, Lieber MR. 2006. DNA structures at chromosomal translocation sites. *Bioessays* 28: 480-94
61. Raghavan SC, Swanson PC, Wu X, Hsieh CL, Lieber MR. 2004. A non-B-DNA structure at the Bcl-2 major breakpoint region is cleaved by the RAG complex. *Nature* 428: 88-93
62. Matthews AG, Oettinger MA. 2009. Regulation of RAG transposition. *Adv Exp Med Biol* 650: 16-31
63. Mombaerts P, Iacomini J, Johnson RS, Herrup K, Tonegawa S, Papaioannou VE. 1992. RAG-1-deficient mice have no mature B and T lymphocytes. *Cell* 68: 869-77
64. Shinkai Y, Rathbun G, Lam KP, Oltz EM, Stewart V, Mendelsohn M, Charron J, Datta M, Young F, Stall AM, et al. 1992. RAG-2-deficient mice lack mature lymphocytes owing to inability to initiate V(D)J rearrangement. *Cell* 68: 855-67
65. de Villartay JP. 2009. V(D)J recombination deficiencies. *Adv Exp Med Biol* 650: 46-58
66. Villa A, Santagata S, Bozzi F, Giliani S, Frattini A, Imberti L, Gatta LB, Ochs HD, Schwarz K, Notarangelo LD, Vezzoni P, Spanopoulou E. 1998. Partial V(D)J recombination activity leads to Omenn syndrome. *Cell* 93: 885-96

67. Corneo B, Moshous D, Gungor T, Wulffraat N, Philippet P, Le Deist FL, Fischer A, de Villartay JP. 2001. Identical mutations in RAG1 or RAG2 genes leading to defective V(D)J recombinase activity can cause either T-B-severe combined immune deficiency or Omenn syndrome. *Blood* 97: 2772-6
68. Sobacchi C, Marrella V, Rucci F, Vezzoni P, Villa A. 2006. RAG-dependent primary immunodeficiencies. *Hum Mutat* 27: 1174-84
69. Ciccia A, Elledge SJ. 2010. The DNA damage response: making it safe to play with knives. *Mol Cell* 40: 179-204
70. Uziel T, Lerenthal Y, Moyal L, Andegeko Y, Mittelman L, Shiloh Y. 2003. Requirement of the MRN complex for ATM activation by DNA damage. *Embo J* 22: 5612-21
71. Matsuoka S, Ballif BA, Smogorzewska A, McDonald ER, 3rd, Hurov KE, Luo J, Bakalarski CE, Zhao Z, Solimini N, Lerenthal Y, Shiloh Y, Gygi SP, Elledge SJ. 2007. ATM and ATR substrate analysis reveals extensive protein networks responsive to DNA damage. *Science* 316: 1160-6
72. Kastan MB, Lim DS. 2000. The many substrates and functions of ATM. *Nat Rev Mol Cell Biol* 1: 179-86
73. Shiloh Y. 2003. ATM and related protein kinases: safeguarding genome integrity. *Nat Rev Cancer* 3: 155-68
74. Rouse J, Jackson SP. 2002. Interfaces between the detection, signaling, and repair of DNA damage. *Science* 297: 547-51
75. Stracker TH, Theunissen JW, Morales M, Petrini JH. 2004. The Mre11 complex and the metabolism of chromosome breaks: the importance of communicating and holding things together. *DNA Repair (Amst)* 3: 845-54
76. D'Amours D, Jackson SP. 2002. The Mre11 complex: at the crossroads of dna repair and checkpoint signalling. *Nat Rev Mol Cell Biol* 3: 317-27
77. Williams RS, Williams JS, Tainer JA. 2007. Mre11-Rad50-Nbs1 is a keystone complex connecting DNA repair machinery, double-strand break signaling, and the chromatin template. *Biochem Cell Biol* 85: 509-20
78. de Jager M, van Noort J, van Gent DC, Dekker C, Kanaar R, Wyman C. 2001. Human Rad50/Mre11 is a flexible complex that can tether DNA ends. *Mol Cell* 8: 1129-35
79. Hopfner KP, Karcher A, Craig L, Woo TT, Carney JP, Tainer JA. 2001. Structural biochemistry and interaction architecture of the DNA double-strand break repair Mre11 nuclease and Rad50-ATPase. *Cell* 105: 473-85
80. Rass E, Grabarz A, Plo I, Gautier J, Bertrand P, Lopez BS. 2009. Role of Mre11 in chromosomal nonhomologous end joining in mammalian cells. *Nat Struct Mol Biol* 16: 819-24
81. Williams RS, Moncalian G, Williams JS, Yamada Y, Limbo O, Shin DS, Groocock LM, Cahill D, Hitomi C, Guenther G, Moiani D, Carney JP, Russell P, Tainer JA. 2008. Mre11 dimers coordinate DNA end bridging and nuclease processing in double-strand-break repair. *Cell* 135: 97-109
82. Hopfner KP, Karcher A, Shin DS, Craig L, Arthur LM, Carney JP, Tainer JA. 2000. Structural biology of Rad50 ATPase: ATP-driven conformational control in DNA double-strand break repair and the ABC-ATPase superfamily. *Cell* 101: 789-800
83. Hopfner KP, Craig L, Moncalian G, Zinkel RA, Usui T, Owen BA, Karcher A, Henderson B, Bodmer JL, McMurray CT, Carney JP, Petrini JH, Tainer JA. 2002. The Rad50 zinc-hook is a structure joining Mre11 complexes in DNA recombination and repair. *Nature* 418: 562-6
84. Hopfner KP, Karcher A, Shin D, Fairley C, Tainer JA, Carney JP. 2000. Mre11 and Rad50 from Pyrococcus furiosus: cloning and biochemical characterization reveal an evolutionarily conserved multiprotein machine. *J Bacteriol* 182: 6036-41
85. Hopfner KP, Tainer JA. 2003. Rad50/SMC proteins and ABC transporters: unifying concepts from high-resolution structures. *Curr Opin Struct Biol* 13: 249-55
86. Wiltzius JJ, Hohl M, Fleming JC, Petrini JH. 2005. The Rad50 hook domain is a critical determinant of Mre11 complex functions. *Nat Struct Mol Biol* 12: 403-7

87. Bhaskara V, Dupre A, Lengsfeld B, Hopkins BB, Chan A, Lee JH, Zhang X, Gautier J, Zakian V, Paull TT. 2007. Rad50 adenylate kinase activity regulates DNA tethering by Mre11/Rad50 complexes. *Mol Cell* 25: 647-61
88. Williams RS, Dodson GE, Limbo O, Yamada Y, Williams JS, Guenther G, Classen S, Glover JN, Iwasaki H, Russell P, Tainer JA. 2009. Nbs1 flexibly tethers Ctp1 and Mre11-Rad50 to coordinate DNA double-strand break processing and repair. *Cell* 139: 87-99
89. Lloyd J, Chapman JR, Clapperton JA, Haire LF, Hartsuiker E, Li J, Carr AM, Jackson SP, Smerdon SJ. 2009. A supramodular FHA/BRCT-repeat architecture mediates Nbs1 adaptor function in response to DNA damage. *Cell* 139: 100-11
90. Lee JH, Paull TT. 2004. Direct activation of the ATM protein kinase by the Mre11/Rad50/Nbs1 complex. *Science* 304: 93-6
91. Lee JH, Paull TT. 2005. ATM activation by DNA double-strand breaks through the Mre11-Rad50-Nbs1 complex. *Science* 308: 551-4
92. You Z, Chahwan C, Bailis J, Hunter T, Russell P. 2005. ATM activation and its recruitment to damaged DNA require binding to the C terminus of Nbs1. *Mol Cell Biol* 25: 5363-79
93. Durocher D, Jackson SP. 2001. DNA-PK, ATM and ATR as sensors of DNA damage: variations on a theme? *Curr Opin Cell Biol* 13: 225-31
94. Abraham RT. 2001. Cell cycle checkpoint signaling through the ATM and ATR kinases. *Genes Dev* 15: 2177-96
95. Gapud EJ, Sleckman BP. 2011. Unique and redundant functions of ATM and DNA-PKcs during V(D)J recombination. *Cell Cycle* 10: 1928-35
96. Zha S, Jiang W, Fujiwara Y, Patel H, Goff PH, Brush JW, Dubois RL, Alt FW. 2011. Ataxia telangiectasia-mutated protein and DNA-dependent protein kinase have complementary V(D)J recombination functions. *Proc Natl Acad Sci U S A* 108: 2028-33
97. Tomimatsu N, Mukherjee B, Burma S. 2009. Distinct roles of ATR and DNA-PKcs in triggering DNA damage responses in ATM-deficient cells. *EMBO Rep* 10: 629-35
98. Callen E, Jankovic M, Wong N, Zha S, Chen HT, Difilippantonio S, Di Virgilio M, Heidkamp G, Alt FW, Nussenzweig A, Nussenzweig M. 2009. Essential role for DNA-PKcs in DNA double-strand break repair and apoptosis in ATM-deficient lymphocytes. *Mol Cell* 34: 285-97
99. Pandita TK. 2003. A multifaceted role for ATM in genome maintenance. *Expert Rev Mol Med* 2003: 1-21
100. Smith GC, Cary RB, Lakin ND, Hann BC, Teo SH, Chen DJ, Jackson SP. 1999. Purification and DNA binding properties of the ataxia-telangiectasia gene product ATM. *Proc Natl Acad Sci U S A* 96: 11134-9
101. Bakkenist CJ, Kastan MB. 2003. DNA damage activates ATM through intermolecular autophosphorylation and dimer dissociation. *Nature* 421: 499-506
102. Pellegrini M, Celeste A, Difilippantonio S, Guo R, Wang W, Feigenbaum L, Nussenzweig A. 2006. Autophosphorylation at serine 1987 is dispensable for murine Atm activation in vivo. *Nature* 443: 222-5
103. Kitagawa R, Bakkenist CJ, McKinnon PJ, Kastan MB. 2004. Phosphorylation of SMC1 is a critical downstream event in the ATM-NBS1-BRCA1 pathway. *Genes Dev* 18: 1423-38
104. Nelms BE, Maser RS, MacKay JF, Lagally MG, Petrini JH. 1998. In situ visualization of DNA double-strand break repair in human fibroblasts. *Science* 280: 590-2
105. Chen HT, Bhandoola A, Difilippantonio MJ, Zhu J, Brown MJ, Tai X, Rogakou EP, Brotz TM, Bonner WM, Ried T, Nussenzweig A. 2000. Response to RAG-mediated VDJ cleavage by NBS1 and gamma-H2AX. *Science* 290: 1962-5
106. Perkins EJ, Nair A, Cowley DO, Van Dyke T, Chang Y, Ramsden DA. 2002. Sensing of intermediates in V(D)J recombination by ATM. *Genes Dev* 16: 159-64
107. Bredemeyer AL, Sharma GG, Huang CY, Helmink BA, Walker LM, Khor KC, Nuskey B, Sullivan KE, Pandita TK, Bassing CH. 2006. ATM stabilizes DNA double-strand-break complexes during V (D) J recombination. *Nature* 442: 466-70

108. Huang CY, Sharma GG, Walker LM, Bassing CH, Pandita TK, Sleckman BP. 2007. Defects in coding joint formation in vivo in developing ATM-deficient B and T lymphocytes. *J Exp Med* 204: 1371-81
109. Matei IR, Gladdy RA, Nutter LM, Canty A, Guidos CJ, Danska JS. 2006. ATM deficiency disrupts TCR{alpha} locus integrity and the maturation of CD4+CD8+ thymocytes. *Blood*
110. Vacchio MS, Olaru A, Livak F, Hodes RJ. 2007. ATM deficiency impairs thymocyte maturation because of defective resolution of T cell receptor {alpha} locus coding end breaks. *Proc Natl Acad Sci U S A* 104: 6323-8
111. Lavin MF, Shiloh Y. 1997. The genetic defect in ataxia-telangiectasia. *Annu Rev Immunol* 15: 177-202
112. Barlow C, Hirotsune S, Paylor R, Liyanage M, Eckhaus M, Collins F, Shiloh Y, Crawley JN, Ried T, Tagle D, Wynshaw-Boris A. 1996. Atm-deficient mice: a paradigm of ataxia telangiectasia. *Cell* 86: 159-71
113. Liyanage M, Weaver Z, Barlow C, Coleman A, Pankratz DG, Anderson S, Wynshaw-Boris A, Ried T. 2000. Abnormal rearrangement within the alpha/delta T-cell receptor locus in lymphomas from Atm-deficient mice. *Blood* 96: 1940-6
114. Liao MJ, Van Dyke T. 1999. Critical role for Atm in suppressing V(D)J recombination-driven thymic lymphoma. *Genes Dev* 13: 1246-50.
115. Taylor AM, Metcalfe JA, Thick J, Mak YF. 1996. Leukemia and lymphoma in ataxia telangiectasia. *Blood* 87: 423-38
116. Kobayashi Y, Tycko B, Soreng AL, Sklar J. 1991. Transrearrangements between antigen receptor genes in normal human lymphoid tissues and in ataxia telangiectasia. *J Immunol* 147: 3201-9
117. Taylor AM, Groom A, Byrd PJ. 2004. Ataxia-telangiectasia-like disorder (ATLD)-its clinical presentation and molecular basis. *DNA Repair (Amst)* 3: 1219-25
118. Stewart GS, Maser RS, Stankovic T, Bressan DA, Kaplan MI, Jaspers NG, Raams A, Byrd PJ, Petrini JH, Taylor AM. 1999. The DNA double-strand break repair gene hMRE11 is mutated in individuals with an ataxia-telangiectasia-like disorder. *Cell* 99: 577-87
119. Digweed M, Reis A, Sperling K. 1999. Nijmegen breakage syndrome: consequences of defective DNA double strand break repair. *Bioessays* 21: 649-56
120. Young BR, Painter RB. 1989. Radioresistant DNA synthesis and human genetic diseases. *Hum Genet* 82: 113-7
121. Waltes R, Kalb R, Gatei M, Kijas AW, Stumm M, Sobeck A, Wieland B, Varon R, Lerenthal Y, Lavin MF, Schindler D, Dork T. 2009. Human RAD50 deficiency in a Nijmegen breakage syndrome-like disorder. *Am J Hum Genet* 84: 605-16
122. Shiloh Y. 1997. Ataxia-telangiectasia and the Nijmegen breakage syndrome: related disorders but genes apart. *Annu Rev Genet* 31: 635-62
123. Takata M, Sasaki MS, Sonoda E, Morrison C, Hashimoto M, Utsumi H, Yamaguchi-Iwai Y, Shinohara A, Takeda S. 1998. Homologous recombination and non-homologous end-joining pathways of DNA double-strand break repair have overlapping roles in the maintenance of chromosomal integrity in vertebrate cells. *EMBO J* 17: 5497-508
124. Khanna KK, Jackson SP. 2001. DNA double-strand breaks: signaling, repair and the cancer connection. *Nat Genet* 27: 247-54
125. Symington LS. 2002. Role of RAD52 epistasis group genes in homologous recombination and double-strand break repair. *Microbiol Mol Biol Rev* 66: 630-70, table of contents
126. van Gent DC, Hoeijmakers JH, Kanaar R. 2001. Chromosomal stability and the DNA double-stranded break connection. *Nat Rev Genet* 2: 196-206
127. White CI, Haber JE. 1990. Intermediates of recombination during mating type switching in Saccharomyces cerevisiae. *EMBO J* 9: 663-73
128. Sugiyama T, Zaitseva EM, Kowalczykowski SC. 1997. A single-stranded DNA-binding protein is needed for efficient presynaptic complex formation by the Saccharomyces cerevisiae Rad51 protein. *J Biol Chem* 272: 7940-5

129. Sartori AA, Lukas C, Coates J, Mistrik M, Fu S, Bartek J, Baer R, Lukas J, Jackson SP. 2007. Human CtIP promotes DNA end resection. *Nature* 450: 509-14
130. Ira G, Pellicioli A, Balijja A, Wang X, Fiorani S, Carotenuto W, Liberi G, Bressan D, Wan L, Hollingsworth NM, Haber JE, Foiani M. 2004. DNA end resection, homologous recombination and DNA damage checkpoint activation require CDK1. *Nature* 431: 1011-7
131. Chen L, Nievera CJ, Lee AY, Wu X. 2008. Cell cycle-dependent complex formation of BRCA1.CtIP.MRN is important for DNA double-strand break repair. *J Biol Chem* 283: 7713-20
132. Huertas P, Jackson SP. 2009. Human CtIP mediates cell cycle control of DNA end resection and double strand break repair. *J Biol Chem* 284: 9558-65
133. Yu X, Chen J. 2004. DNA damage-induced cell cycle checkpoint control requires CtIP, a phosphorylation-dependent binding partner of BRCA1 C-terminal domains. *Mol Cell Biol* 24: 9478-86
134. Yuan J, Chen J. 2009. N terminus of CtIP is critical for homologous recombination-mediated double-strand break repair. *J Biol Chem* 284: 31746-52
135. You Z, Shi LZ, Zhu Q, Wu P, Zhang YW, Basilio A, Tonnu N, Verma IM, Berns MW, Hunter T. 2009. CtIP links DNA double-strand break sensing to resection. *Mol Cell* 36: 954-69
136. Yun MH, Hiom K. 2009. CtIP-BRCA1 modulates the choice of DNA double-strand-break repair pathway throughout the cell cycle. *Nature* 459: 460-3
137. Mimitou EP, Symington LS. 2008. Sae2, Exo1 and Sgs1 collaborate in DNA double-strand break processing. *Nature* 455: 770-4
138. West SC. 2003. Molecular views of recombination proteins and their control. *Nat Rev Mol Cell Biol* 4: 435-45
139. Huertas P. DNA resection in eukaryotes: deciding how to fix the break. *Nat Struct Mol Biol* 17: 11-6
140. Lieber MR. 2008. The mechanism of human nonhomologous DNA end joining. *J Biol Chem* 283: 1-5
141. Walker JR, Corpina RA, Goldberg J. 2001. Structure of the Ku heterodimer bound to DNA and its implications for double-strand break repair. *Nature* 412: 607-14
142. Featherstone C, Jackson SP. 1999. Ku, a DNA repair protein with multiple cellular functions? *Mutat Res* 434: 3-15
143. Dynan WS, Yoo S. 1998. Interaction of Ku protein and DNA-dependent protein kinase catalytic subunit with nucleic acids. *Nucleic Acids Res* 26: 1551-9
144. Weterings E, Chen DJ. 2007. DNA-dependent protein kinase in nonhomologous end joining: a lock with multiple keys? *J Cell Biol* 179: 183-6
145. Meek K, Dang V, Lees-Miller SP. 2008. DNA-PK: the means to justify the ends? *Adv Immunol* 99: 33-58
146. DeFazio LG, Stansel RM, Griffith JD, Chu G. 2002. Synapsis of DNA ends by DNA-dependent protein kinase. *EMBO J* 21: 3192-200
147. Merkle D, Douglas P, Moorhead GB, Leonenko Z, Yu Y, Cramb D, Bazett-Jones DP, Lees-Miller SP. 2002. The DNA-dependent protein kinase interacts with DNA to form a protein-DNA complex that is disrupted by phosphorylation. *Biochemistry* 41: 12706-14
148. Feldmann E, Schmiemann V, Goedecke W, Reichenberger S, Pfeiffer P. 2000. DNA double-strand break repair in cell-free extracts from Ku80-deficient cells: implications for Ku serving as an alignment factor in non-homologous DNA end joining. *Nucleic Acids Res* 28: 2585-96
149. Kabotyanski EB, Gomelsky L, Han JO, Stamato TD, Roth DB. 1998. Double-strand break repair in Ku86- and XRCC4-deficient cells. *Nucleic Acids Res* 26: 5333-42
150. Rooney S, Chaudhuri J, Alt FW. 2004. The role of the non-homologous end-joining pathway in lymphocyte development. *Immunol Rev* 200: 115-31
151. Lieber MR, Ma Y, Pannicke U, Schwarz K. 2003. Mechanism and regulation of human non-homologous DNA end-joining. *Nat Rev Mol Cell Biol* 4: 712-20

152. Ahnesorg P, Smith P, Jackson SP. 2006. XLF interacts with the XRCC4-DNA ligase IV complex to promote DNA nonhomologous end-joining. *Cell* 124: 301-13
153. Li Y, Chirgadze DY, Bolanos-Garcia VM, Sibanda BL, Davies OR, Ahnesorg P, Jackson SP, Blundell TL. 2008. Crystal structure of human XLF/Cernunnos reveals unexpected differences from XRCC4 with implications for NHEJ. *EMBO J* 27: 290-300
154. Andres SN, Modesti M, Tsai CJ, Chu G, Junop MS. 2007. Crystal structure of human XLF: a twist in nonhomologous DNA end-joining. *Mol Cell* 28: 1093-101
155. Gu J, Lu H, Tsai AG, Schwarz K, Lieber MR. 2007. Single-stranded DNA ligation and XLF-stimulated incompatible DNA end ligation by the XRCC4-DNA ligase IV complex: influence of terminal DNA sequence. *Nucleic Acids Res* 35: 5755-62
156. Gu J, Lu H, Tippin B, Shimazaki N, Goodman MF, Lieber MR. 2007. XRCC4:DNA ligase IV can ligate incompatible DNA ends and can ligate across gaps. *EMBO J* 26: 1010-23
157. Tsai CJ, Kim SA, Chu G. 2007. Cernunnos/XLF promotes the ligation of mismatched and noncohesive DNA ends. *Proc Natl Acad Sci U S A* 104: 7851-6
158. Ma Y, Pannicke U, Schwarz K, Lieber MR. 2002. Hairpin opening and overhang processing by an Artemis/DNA-dependent protein kinase complex in nonhomologous end joining and V(D)J recombination. *Cell* 108: 781-94
159. Goodarzi AA, Yu Y, Riballo E, Douglas P, Walker SA, Ye R, Harer C, Marchetti C, Morrice N, Jeggo PA, Lees-Miller SP. 2006. DNA-PK autophosphorylation facilitates Artemis endonuclease activity. *Embo J* 25: 3880-9
160. Rooney S, Alt FW, Lombard D, Whitlow S, Eckersdorff M, Fleming J, Fugmann S, Ferguson DO, Schatz DG, Sekiguchi J. 2003. Defective DNA repair and increased genomic instability in Artemis-deficient murine cells. *J Exp Med* 197: 553-65
161. Rooney S, Sekiguchi J, Zhu C, Cheng HL, Manis J, Whitlow S, DeVido J, Foy D, Chaudhuri J, Lombard D, Alt FW. 2002. Leaky Scid phenotype associated with defective V(D)J coding end processing in Artemis-deficient mice. *Mol Cell* 10: 1379-90
162. Riballo E, Kuhne M, Rief N, Doherty A, Smith GC, Recio MJ, Reis C, Dahm K, Fricke A, Krempler A, Parker AR, Jackson SP, Gennery A, Jeggo PA, Lobrich M. 2004. A pathway of double-strand break rejoining dependent upon ATM, Artemis, and proteins locating to gamma-H2AX foci. *Mol Cell* 16: 715-24
163. McVey M, Lee SE. 2008. MMEJ repair of double-strand breaks (director's cut): deleted sequences and alternative endings. *Trends Genet* 24: 529-38
164. Yan CT, Boboila C, Souza EK, Franco S, Hickernell TR, Murphy M, Gumaste S, Geyer M, Zarrin AA, Manis JP, Rajewsky K, Alt FW. 2007. IgH class switching and translocations use a robust non-classical end-joining pathway. *Nature* 449: 478-82
165. Han L, Yu K. 2008. Altered kinetics of nonhomologous end joining and class switch recombination in ligase IV-deficient B cells. *J Exp Med* 205: 2745-53
166. Weinstock DM, Brunet E, Jasin M. 2007. Formation of NHEJ-derived reciprocal chromosomal translocations does not require Ku70. *Nat Cell Biol* 9: 978-81
167. Audebert M, Salles B, Calsou P. 2004. Involvement of poly(ADP-ribose) polymerase-1 and XRCC1/DNA ligase III in an alternative route for DNA double-strand breaks rejoining. *J Biol Chem* 279: 55117-26
168. Simsek D, Brunet E, Wong SY, Katyal S, Gao Y, McKinnon PJ, Lou J, Zhang L, Li J, Rebar EJ, Gregory PD, Holmes MC, Jasin M. 2011. DNA ligase III promotes alternative nonhomologous end-joining during chromosomal translocation formation. *PLoS Genet* 7: e1002080
169. Xie A, Kwok A, Scully R. 2009. Role of mammalian Mre11 in classical and alternative nonhomologous end joining. *Nat Struct Mol Biol* 16: 814-8
170. Lee-Theilen M, Matthews AJ, Kelly D, Zheng S, Chaudhuri J. 2011. CtIP promotes microhomology-mediated alternative end joining during class-switch recombination. *Nat Struct Mol Biol* 18: 75-9
171. Zhang Y, Jasin M. 2011. An essential role for CtIP in chromosomal translocation formation through an alternative end-joining pathway. *Nat Struct Mol Biol* 18: 80-4

172. Simsek D, Jasin M. 2010. Alternative end-joining is suppressed by the canonical NHEJ component Xrcc4-ligase IV during chromosomal translocation formation. *Nat Struct Mol Biol* 17: 410-6
173. Aguilera A, Gomez-Gonzalez B. 2008. Genome instability: a mechanistic view of its causes and consequences. *Nat Rev Genet* 9: 204-17
174. Karanjawala ZE, Adachi N, Irvine RA, Oh EK, Shibata D, Schwarz K, Hsieh CL, Lieber MR. 2002. The embryonic lethality in DNA ligase IV-deficient mice is rescued by deletion of Ku: implications for unifying the heterogeneous phenotypes of NHEJ mutants. *DNA Repair (Amst)* 1: 1017-26
175. Pierce AJ, Hu P, Han M, Ellis N, Jasin M. 2001. Ku DNA end-binding protein modulates homologous repair of double-strand breaks in mammalian cells. *Genes Dev* 15: 3237-42
176. Huertas P, Cortes-Ledesma F, Sartori AA, Aguilera A, Jackson SP. 2008. CDK targets Sae2 to control DNA-end resection and homologous recombination. *Nature* 455: 689-92
177. Aylon Y, Kupiec M. 2005. Cell cycle-dependent regulation of double-strand break repair: a role for the CDK. *Cell Cycle* 4: 259-61
178. Aylon Y, Liefshitz B, Kupiec M. 2004. The CDK regulates repair of double-strand breaks by homologous recombination during the cell cycle. *EMBO J* 23: 4868-75
179. Nussenzweig A, Nussenzweig MC. 2010. Origin of chromosomal translocations in lymphoid cancer. *Cell* 141: 27-38
180. Cayuela JM, Gardie B, Sigaux F. 1997. Disruption of the multiple tumor suppressor gene MTS1/p16(INK4a)/CDKN2 by illegitimate V(D)J recombinase activity in T-cell acute lymphoblastic leukemias. *Blood* 90: 3720-6
181. Agrawal A, Schatz DG. 1997. RAG1 and RAG2 form a stable postcleavage synaptic complex with DNA containing signal ends in V(D)J recombination. *Cell* 89: 43-53.
182. Jones JM, Gellert M. 2001. Intermediates in V(D)J recombination: a stable RAG1/2 complex sequesters cleaved RSS ends. *Proc Natl Acad Sci U S A* 98: 12926-31
183. Schlissel MS. 1998. Structure of nonhairpin coding-end DNA breaks in cells undergoing V(D)J recombination. *Mol Cell Biol* 18: 2029-37
184. Besmer E, Mansilla-Soto J, Cassard S, Sawchuk DJ, Brown G, Sadofsky M, Lewis SM, Nussenzweig MC, Cortes P. 1998. Hairpin coding end opening is mediated by RAG1 and RAG2 proteins. *Mol Cell* 2: 817-28
185. Shockett PE, Schatz DG. 1999. DNA hairpin opening mediated by the RAG1 and RAG2 proteins. *Mol Cell Biol* 19: 4159-66
186. Touvrey C, Couedel C, Soulas P, Couderc R, Jasin M, de Villartay JP, Marche PN, Jouvin-Marche E, Candeias SM. 2008. Distinct effects of DNA-PKcs and Artemis inactivation on signal joint formation in vivo. *Mol Immunol* 45: 3383-91
187. Motea EA, Berdis AJ. 2010. Terminal deoxynucleotidyl transferase: the story of a misguided DNA polymerase. *Biochim Biophys Acta* 1804: 1151-66
188. Santagata S, Besmer E, Villa A, Bozzi F, Allingham JS, Sobacchi C, Haniford DB, Vezzoni P, Nussenzweig MC, Pan ZQ, Cortes P. 1999. The RAG1/RAG2 complex constitutes a 3' flap endonuclease: implications for junctional diversity in V(D)J and transpositional recombination. *Mol Cell* 4: 935-47
189. Gilfillan S, Dierich A, Lemeur M, Benoist C, Mathis D. 1993. Mice lacking TdT: mature animals with an immature lymphocyte repertoire. *Science* 261: 1175-8
190. Komori T, Pricop L, Hatakeyama A, Bona CA, Alt FW. 1996. Repertoires of antigen receptors in Tdt congenitally deficient mice. *Int Rev Immunol* 13: 317-25
191. Gellert M. 2002. V(D)J recombination: rag proteins, repair factors, and regulation. *Annu Rev Biochem* 71: 101-32
192. Yarnell Schultz H, Landree MA, Qiu JX, Kale SB, Roth DB. 2001. Joining-deficient RAG1 mutants block V(D)J recombination in vivo and hairpin opening in vitro. *Mol Cell* 7: 65-75.
193. Qiu JX, Kale SB, Yarnell Schultz H, Roth DB. 2001. Separation-of-function mutants reveal critical roles for RAG2 in both the cleavage and joining steps of V(D)J recombination. *Mol Cell* 7: 77-87

194. Tsai CL, Drejer AH, Schatz DG. 2002. Evidence of a critical architectural function for the RAG proteins in end processing, protection, and joining in V(D)J recombination. *Genes Dev* 16: 1934-49
195. Raval P, Kriatchko AN, Kumar S, Swanson PC. 2008. Evidence for Ku70/Ku80 association with full-length RAG1. *Nucleic Acids Res* 36: 2060-72
196. Corneo B, Wendland RL, Deriano L, Cui X, Klein IA, Wong SY, Arnal S, Holub AJ, Weller GR, Pancake BA, Shah S, Brandt VL, Meek K, Roth DB. 2007. Rag mutations reveal robust alternative end joining. *Nature* 449: 483-6
197. Nussenzweig A, Nussenzweig MC. 2007. A backup DNA repair pathway moves to the forefront. *Cell* 131: 223-5
198. Gostissa M, Alt FW, Chiarle R. 2011. Mechanisms that promote and suppress chromosomal translocations in lymphocytes. *Annu Rev Immunol* 29: 319-50
199. Bassing CH, Alt FW. 2004. The cellular response to general and programmed DNA double strand breaks. *DNA Repair (Amst)* 3: 781-96
200. Chen J, Trounstine M, Alt FW, Young F, Kurahara C, Loring JF, Huszar D. 1993. Immunoglobulin gene rearrangement in B cell deficient mice generated by targeted deletion of the JH locus. *Int Immunol* 5: 647-56
201. Yassai M, Hletko A, Gorski J. 1995. Forces molding circulating T-cell repertoires. Thymic events studied by recombination analysis. *Ann N Y Acad Sci* 756: 81-3
202. Callen E, Jankovic M, Difilippantonio S, Daniel JA, Chen HT, Celeste A, Pellegrini M, McBride K, Wangsa D, Bredemeyer AL, Sleckman BP, Ried T, Nussenzweig M, Nussenzweig A. 2007. ATM prevents the persistence and propagation of chromosome breaks in lymphocytes. *Cell* 130: 63-75
203. Lipkowitz S, Stern MH, Kirsch IR. 1990. Hybrid T cell receptor genes formed by interlocus recombination in normal and ataxia-telangiectasis lymphocytes. *J Exp Med* 172: 409-18
204. Matei IR, Guidos CJ, Danska JS. 2006. ATM-dependent DNA damage surveillance in T-cell development and leukemogenesis: the DSB connection. *Immunol Rev* 209: 142-58
205. Petiniot LK, Weaver Z, Barlow C, Shen R, Eckhaus M, Steinberg SM, Ried T, Wynshaw-Boris A, Hodes RJ. 2000. Recombinase-activating gene (RAG) 2-mediated V(D)J recombination is not essential for tumorigenesis in Atm-deficient mice. *Proc Natl Acad Sci U S A* 97: 6664-9
206. Rogakou EP, Pilch DR, Orr AH, Ivanova VS, Bonner WM. 1998. DNA double-stranded breaks induce histone H2AX phosphorylation on serine 139. *J Biol Chem* 273: 5858-68
207. Rogakou EP, Boon C, Redon C, Bonner WM. 1999. Megabase chromatin domains involved in DNA double-strand breaks in vivo. *J Cell Biol* 146: 905-16
208. Fernandez-Capetillo O, Lee A, Nussenzweig M, Nussenzweig A. 2004. H2AX: the histone guardian of the genome. *DNA Repair (Amst)* 3: 959-67
209. Burma S, Chen BP, Murphy M, Kurimasa A, Chen DJ. 2001. ATM phosphorylates histone H2AX in response to DNA double-strand breaks. *J Biol Chem* 276: 42462-7
210. Stiff T, O'Driscoll M, Rief N, Iwabuchi K, Lobrich M, Jeggo PA. 2004. ATM and DNA-PK function redundantly to phosphorylate H2AX after exposure to ionizing radiation. *Cancer Res* 64: 2390-6
211. Savic V, Yin B, Maas NL, Bredemeyer AL, Carpenter AC, Helmink BA, Yang-Iott KS, Sleckman BP, Bassing CH. 2009. Formation of dynamic gamma-H2AX domains along broken DNA strands is distinctly regulated by ATM and MDC1 and dependent upon H2AX densities in chromatin. *Mol Cell* 34: 298-310
212. Paull TT, Rogakou EP, Yamazaki V, Kirchgessner CU, Gellert M, Bonner WM. 2000. A critical role for histone H2AX in recruitment of repair factors to nuclear foci after DNA damage. *Curr Biol* 10: 886-95
213. Celeste A, Fernandez-Capetillo O, Kruhlak MJ, Pilch DR, Staudt DW, Lee A, Bonner RF, Bonner WM, Nussenzweig A. 2003. Histone H2AX phosphorylation is dispensable for the initial recognition of DNA breaks. *Nat Cell Biol* 5: 675-9

214. Stucki M, Clapperton JA, Mohammad D, Yaffe MB, Smerdon SJ, Jackson SP. 2005. MDC1 directly binds phosphorylated histone H2AX to regulate cellular responses to DNA double-strand breaks. *Cell* 123: 1213-26
215. Lukas C, Melander F, Stucki M, Falck J, Bekker-Jensen S, Goldberg M, Lerenthal Y, Jackson SP, Bartek J, Lukas J. 2004. Mdc1 couples DNA double-strand break recognition by Nbs1 with its H2AX-dependent chromatin retention. *EMBO J* 23: 2674-83
216. Ward IM, Minn K, Jorda KG, Chen J. 2003. Accumulation of checkpoint protein 53BP1 at DNA breaks involves its binding to phosphorylated histone H2AX. *J Biol Chem* 278: 19579-82
217. Goldberg M, Stucki M, Falck J, D'Amours D, Rahman D, Pappin D, Bartek J, Jackson SP. 2003. MDC 1 is required for the intra-S-phase DNA damage checkpoint. *Nature* 421: 952-6
218. Stewart GS, Wang B, Bignell CR, Taylor AM, Elledge SJ. 2003. MDC1 is a mediator of the mammalian DNA damage checkpoint. *Nature* 421: 961-6
219. Kolas NK, Chapman JR, Nakada S, Ylanko J, Chahwan R, Sweeney FD, Panier S, Mendez M, Wildenhain J, Thomson TM, Pelletier L, Jackson SP, Durocher D. 2007. Orchestration of the DNA-Damage Response by the RNF8 Ubiquitin Ligase. *Science*
220. Huen MS, Grant R, Manke I, Minn K, Yu X, Yaffe MB, Chen J. 2007. RNF8 Transduces the DNA-Damage Signal via Histone Ubiquitylation and Checkpoint Protein Assembly. *Cell* 131: 901-14
221. Mailand N, Bekker-Jensen S, Faustrup H, Melander F, Bartek J, Lukas C, Lukas J. 2007. RNF8 Ubiquitylates Histones at DNA Double-Strand Breaks and Promotes Assembly of Repair Proteins. *Cell* 131: 887-900
222. Stewart GS, Panier S, Townsend K, Al-Hakim AK, Kolas NK, Miller ES, Nakada S, Ylanko J, Olivarius S, Mendez M, Oldreive C, Wildenhain J, Tagliaferro A, Pelletier L, Taubenheim N, Durandy A, Byrd PJ, Stankovic T, Taylor AM, Durocher D. 2009. The RIDDLE syndrome protein mediates a ubiquitin-dependent signaling cascade at sites of DNA damage. *Cell* 136: 420-34
223. Doil C, Mailand N, Bekker-Jensen S, Menard P, Larsen DH, Pepperkok R, Ellenberg J, Panier S, Durocher D, Bartek J, Lukas J, Lukas C. 2009. RNF168 binds and amplifies ubiquitin conjugates on damaged chromosomes to allow accumulation of repair proteins. *Cell* 136: 435-46
224. Panier S, Durocher D. 2009. Regulatory ubiquitylation in response to DNA double-strand breaks. *DNA Repair (Amst)* 8: 436-43
225. Huyen Y, Zgheib O, Ditullio RA, Jr., Gorgoulis VG, Zacharatos P, Petty TJ, Sheston EA, Mellert HS, Stavridi ES, Halazonetis TD. 2004. Methylated lysine 79 of histone H3 targets 53BP1 to DNA double-strand breaks. *Nature* 432: 406-11
226. Botuyan MV, Lee J, Ward IM, Kim JE, Thompson JR, Chen J, Mer G. 2006. Structural basis for the methylation state-specific recognition of histone H4-K20 by 53BP1 and Crb2 in DNA repair. *Cell* 127: 1361-73
227. Bekker-Jensen S, Lukas C, Melander F, Bartek J, Lukas J. 2005. Dynamic assembly and sustained retention of 53BP1 at the sites of DNA damage are controlled by Mdc1/NFBD1. *J Cell Biol* 170: 201-11
228. Lou Z, Minter-Dykhouse K, Franco S, Gostissa M, Rivera MA, Celeste A, Manis JP, van Deursen J, Nussenzweig A, Paull TT, Alt FW, Chen J. 2006. MDC1 maintains genomic stability by participating in the amplification of ATM-dependent DNA damage signals. *Mol Cell* 21: 187-200
229. Melander F, Bekker-Jensen S, Falck J, Bartek J, Mailand N, Lukas J. 2008. Phosphorylation of SDT repeats in the MDC1 N terminus triggers retention of NBS1 at the DNA damage-modified chromatin. *J Cell Biol* 181: 213-26
230. Chapman JR, Jackson SP. 2008. Phospho-dependent interactions between NBS1 and MDC1 mediate chromatin retention of the MRN complex at sites of DNA damage. *EMBO Rep* 9: 795-801

231. Wu L, Luo K, Lou Z, Chen J. 2008. MDC1 regulates intra-S-phase checkpoint by targeting NBS1 to DNA double-strand breaks. *Proc Natl Acad Sci U S A* 105: 11200-5
232. Fernandez-Capetillo O, Chen HT, Celeste A, Ward I, Romanienko PJ, Morales JC, Naka K, Xia Z, Camerini-Otero RD, Motoyama N, Carpenter PB, Bonner WM, Chen J, Nussenzweig A. 2002. DNA damage-induced G2-M checkpoint activation by histone H2AX and 53BP1. *Nat Cell Biol* 4: 993-7
233. Celeste A, Petersen S, Romanienko PJ, Fernandez-Capetillo O, Chen HT, Sedelnikova OA, Reina-San-Martin B, Coppola V, Meffre E, Difilippantonio MJ, Redon C, Pilch DR, Olaru A, Eckhaus M, Camerini-Otero RD, Tessarollo L, Livak F, Manova K, Bonner WM, Nussenzweig MC, Nussenzweig A. 2002. Genomic instability in mice lacking histone H2AX. *Science* 296: 922-7
234. Bassing CH, Suh H, Ferguson DO, Chua KF, Manis J, Eckersdorff M, Gleason M, Bronson R, Lee C, Alt FW. 2003. Histone H2AX: a dosage-dependent suppressor of oncogenic translocations and tumors. *Cell* 114: 359-70
235. Bassing CH, Chua KF, Sekiguchi J, Suh H, Whitlow SR, Fleming JC, Monroe BC, Ciccone DN, Yan C, Vlasakova K, Livingston DM, Ferguson DO, Scully R, Alt FW. 2002. Increased ionizing radiation sensitivity and genomic instability in the absence of histone H2AX. *Proc Natl Acad Sci U S A* 99: 8173-8
236. Celeste A, Difilippantonio S, Difilippantonio MJ, Fernandez-Capetillo O, Pilch DR, Sedelnikova OA, Eckhaus M, Ried T, Bonner WM, Nussenzweig A. 2003. H2AX haploinsufficiency modifies genomic stability and tumor susceptibility. *Cell* 114: 371-83
237. Bassing CH, Alt FW. 2004. H2AX may function as an anchor to hold broken chromosomal DNA ends in close proximity. *Cell Cycle* 3: 149-53
238. Difilippantonio S, Gapud E, Wong N, Huang CY, Mahowald G, Chen HT, Kruhlak MJ, Callen E, Livak F, Nussenzweig MC, Sleckman BP, Nussenzweig A. 2008. 53BP1 facilitates long-range DNA end-joining during V(D)J recombination. *Nature* 456: 529-33
239. FitzGerald JE, Grenon M, Lowndes NF. 2009. 53BP1: function and mechanisms of focal recruitment. *Biochem Soc Trans* 37: 897-904
240. Jankovic M, Nussenzweig A, Nussenzweig MC. 2007. Antigen receptor diversification and chromosome translocations. *Nat Immunol* 8: 801-8
241. Ward IM, Difilippantonio S, Minn K, Mueller MD, Molina JR, Yu X, Frisk CS, Ried T, Nussenzweig A, Chen J. 2005. 53BP1 cooperates with p53 and functions as a haploinsufficient tumor suppressor in mice. *Mol Cell Biol* 25: 10079-86
242. Morales JC, Franco S, Murphy MM, Bassing CH, Mills KD, Adams MM, Walsh NC, Manis JP, Rassidakis GZ, Alt FW, Carpenter PB. 2006. 53BP1 and p53 synergize to suppress genomic instability and lymphomagenesis. *Proc Natl Acad Sci U S A* 103: 3310-5
243. Yin B, Savic V, Juntilla MM, Bredemeyer AL, Yang-Iott KS, Helmink BA, Koretzky GA, Sleckman BP, Bassing CH. 2009. Histone H2AX stabilizes broken DNA strands to suppress chromosome breaks and translocations during V(D)J recombination. *J Exp Med* 206: 2625-39
244. Meek DW. 2004. The p53 response to DNA damage. *DNA Repair (Amst)* 3: 1049-56
245. Stankovic T, Stewart GS, Fegan C, Biggs P, Last J, Byrd PJ, Keenan RD, Moss PA, Taylor AM. 2002. Ataxia telangiectasia mutated-deficient B-cell chronic lymphocytic leukemia occurs in pregerminal center cells and results in defective damage response and unrepaired chromosome damage. *Blood* 99: 300-9
246. Stankovic T, Hubank M, Cronin D, Stewart GS, Fletcher D, Bignell CR, Alvi AJ, Austen B, Weston VJ, Fegan C, Byrd PJ, Moss PA, Taylor AM. 2004. Microarray analysis reveals that TP53- and ATM-mutant B-CLLs share a defect in activating proapoptotic responses after DNA damage but are distinguished by major differences in activating prosurvival responses. *Blood* 103: 291-300
247. Rashi-Elkeles S, Elkon R, Weizman N, Linhart C, Amariglio N, Sternberg G, Rechavi G, Barzilai A, Shamir R, Shiloh Y. 2006. Parallel induction of ATM-dependent pro- and antiapoptotic signals in response to ionizing radiation in murine lymphoid tissue. *Oncogene* 25: 1584-92

248. Hirao A, Cheung A, Duncan G, Girard PM, Elia AJ, Wakeham A, Okada H, Sarkissian T, Wong JA, Sakai T, De Stanchina E, Bristow RG, Suda T, Lowe SW, Jeggo PA, Elledge SJ, Mak TW. 2002. Chk2 is a tumor suppressor that regulates apoptosis in both an ataxia telangiectasia mutated (ATM)-dependent and an ATM-independent manner. *Mol Cell Biol* 22: 6521-32
249. Hirao A, Kong YY, Matsuoka S, Wakeham A, Ruland J, Yoshida H, Liu D, Elledge SJ, Mak TW. 2000. DNA damage-induced activation of p53 by the checkpoint kinase Chk2. *Science* 287: 1824-7
250. Donehower LA, Harvey M, Slagle BL, McArthur MJ, Montgomery CA, Jr., Butel JS, Bradley A. 1992. Mice deficient for p53 are developmentally normal but susceptible to spontaneous tumours. *Nature* 356: 215-21
251. Rothe M, Sarma V, Dixit VM, Goeddel DV. 1995. TRAF2-mediated activation of NF-kappa B by TNF receptor 2 and CD40. *Science* 269: 1424-7
252. Wang CY, Mayo MW, Baldwin AS, Jr. 1996. TNF- and cancer therapy-induced apoptosis: potentiation by inhibition of NF-kappaB. *Science* 274: 784-7
253. Yamagishi N, Miyakoshi J, Takebe H. 1997. Enhanced radiosensitivity by inhibition of nuclear factor kappa B activation in human malignant glioma cells. *Int J Radiat Biol* 72: 157-62
254. Wu X, Bayle JH, Olson D, Levine AJ. 1993. The p53-mdm-2 autoregulatory feedback loop. *Genes Dev* 7: 1126-32
255. Khosravi R, Maya R, Gottlieb T, Oren M, Shiloh Y, Shkedy D. 1999. Rapid ATM-dependent phosphorylation of MDM2 precedes p53 accumulation in response to DNA damage. *Proc Natl Acad Sci U S A* 96: 14973-7
256. Dumaz N, Meek DW. 1999. Serine15 phosphorylation stimulates p53 transactivation but does not directly influence interaction with HDM2. *EMBO J* 18: 7002-10
257. Chehab NH, Malikzay A, Appel M, Halazonetis TD. 2000. Chk2/hCds1 functions as a DNA damage checkpoint in G(1) by stabilizing p53. *Genes Dev* 14: 278-88
258. Shieh SY, Ahn J, Tamai K, Taya Y, Prives C. 2000. The human homologs of checkpoint kinases Chk1 and Cds1 (Chk2) phosphorylate p53 at multiple DNA damage-inducible sites. *Genes Dev* 14: 289-300
259. Ahn JY, Schwarz JK, Piwnica-Worms H, Canman CE. 2000. Threonine 68 phosphorylation by ataxia telangiectasia mutated is required for efficient activation of Chk2 in response to ionizing radiation. *Cancer Res* 60: 5934-6
260. Melchionna R, Chen XB, Blasina A, McGowan CH. 2000. Threonine 68 is required for radiation-induced phosphorylation and activation of Cds1. *Nat Cell Biol* 2: 762-5
261. Bartek J, Falck J, Lukas J. 2001. CHK2 kinase--a busy messenger. *Nat Rev Mol Cell Biol* 2: 877-86
262. White E. 1996. Life, death, and the pursuit of apoptosis. *Genes Dev* 10: 1-15
263. Wu ZH, Shi Y, Tibbetts RS, Miyamoto S. 2006. Molecular linkage between the kinase ATM and NF-kappaB signaling in response to genotoxic stimuli. *Science* 311: 1141-6
264. Pahl HL. 1999. Activators and target genes of Rel/NF-kappaB transcription factors. *Oncogene* 18: 6853-66
265. Hayden MS, Ghosh S. 2004. Signaling to NF-kappaB. *Genes Dev* 18: 2195-224
266. Huang TT, Kudo N, Yoshida M, Miyamoto S. 2000. A nuclear export signal in the N-terminal regulatory domain of IkappaBalpha controls cytoplasmic localization of inactive NF-kappaB/IkappaBalpha complexes. *Proc Natl Acad Sci U S A* 97: 1014-9
267. Johnson C, Van Antwerp D, Hope TJ. 1999. An N-terminal nuclear export signal is required for the nucleocytoplasmic shuttling of IkappaBalpha. *EMBO J* 18: 6682-93
268. Janssens S, Tinel A, Lippens S, Tschopp J. 2005. PIDD mediates NF-kappaB activation in response to DNA damage. *Cell* 123: 1079-92
269. Huang TT, Wuerzberger-Davis SM, Wu ZH, Miyamoto S. 2003. Sequential modification of NEMO/IKKgamma by SUMO-1 and ubiquitin mediates NF-kappaB activation by genotoxic stress. *Cell* 115: 565-76

270. Bredemeyer AL, Helmink BA, Innes CL, Calderon B, McGinnis LM, Mahowald GK, Gapud EJ, Walker LM, Collins JB, Weaver BK, Mandik-Nayak L, Schreiber RD, Allen PM, May MJ, Paules RS, Bassing CH, Sleckman BP. 2008. DNA double-strand breaks activate a multi-functional genetic program in developing lymphocytes. *Nature* 456: 819-23
271. Guidos CJ, Williams CJ, Grandal I, Knowles G, Huang MT, Danska JS. 1996. V(D)J recombination activates a p53-dependent DNA damage checkpoint in scid lymphocyte precursors. *Genes Dev* 10: 2038-54
272. Callen E, Nussenzweig MC, Nussenzweig A. 2007. Breaking down cell cycle checkpoints and DNA repair during antigen receptor gene assembly. *Oncogene* 26: 7759-64
273. Hesse JE, Lieber MR, Gellert M, Mizuuchi K. 1987. Extrachromosomal DNA substrates in pre-B cells undergo inversion or deletion at immunoglobulin V-(D)-J joining signals. *Cell* 49: 775-83
274. Sadofsky MJ, Hesse JE, McBlane JF, Gellert M. 1993. Expression and V(D)J recombination activity of mutated RAG-1 proteins. *Nucleic Acids Res* 21: 5644-50
275. Hsieh CL, Arlett CF, Lieber MR. 1993. V(D)J recombination in ataxia telangiectasia, Bloom's syndrome, and a DNA ligase I-associated immunodeficiency disorder. *J Biol Chem* 268: 20105-9
276. Helmink BA, Bredemeyer AL, Lee BS, Huang CY, Sharma GG, Walker LM, Bednarski JJ, Lee WL, Pandita TK, Bassing CH, Sleckman BP. 2009. MRN complex function in the repair of chromosomal Rag-mediated DNA double-strand breaks. *J Exp Med* 206: 669-79
277. Harfst E, Cooper S, Neubauer S, Distel L, Grawunder U. 2000. Normal V(D)J recombination in cells from patients with Nijmegen breakage syndrome. *Mol Immunol* 37: 915-29
278. Li G, Alt FW, Cheng HL, Brush JW, Goff PH, Murphy MM, Franco S, Zhang Y, Zha S. 2008. Lymphocyte-specific compensation for XLF/cernunnos end-joining functions in V(D)J recombination. *Mol Cell* 31: 631-40
279. Chen YY, Wang LC, Huang MS, Rosenberg N. 1994. An active v-abl protein tyrosine kinase blocks immunoglobulin light-chain gene rearrangement. *Genes Dev* 8: 688-97
280. Muljo SA, Schlissel MS. 2003. A small molecule Abl kinase inhibitor induces differentiation of Abelson virus-transformed pre-B cell lines. *Nat Immunol* 4: 31-7
281. Strasser A, Harris AW, Cory S. 1991. bcl-2 transgene inhibits T cell death and perturbs thymic self-censorship. *Cell* 67: 889-99
282. Huang CY, Sleckman BP, Kanagawa O. 2005. Revision of T cell receptor {alpha} chain genes is required for normal T lymphocyte development. *Proc Natl Acad Sci U S A* 102: 14356-61
283. Pandita TK. 2006. Role of mammalian Rad9 in genomic stability and ionizing radiation response. *Cell Cycle* 5: 1289-91
284. Hegedus E, Kokai E, Kotlyar A, Dombradi V, Szabo G. 2009. Separation of 1-23-kb complementary DNA strands by urea-agarose gel electrophoresis. *Nucleic Acids Res* 37: e112
285. Yu X, Baer R. 2000. Nuclear localization and cell cycle-specific expression of CtIP, a protein that associates with the BRCA1 tumor suppressor. *J Biol Chem* 275: 18541-9
286. Lu L, Feng Y, Hucker WJ, Oswald SJ, Longmore GD, Yin FC. 2008. Actin stress fiber pre-extension in human aortic endothelial cells. *Cell Motil Cytoskeleton* 65: 281-94
287. Langer EM, Feng Y, Zhaoyuan H, Rauscher FJ, 3rd, Kroll KL, Longmore GD. 2008. Ajuba LIM proteins are snail/slug corepressors required for neural crest development in Xenopus. *Dev Cell* 14: 424-36
288. Brockman JA, Scherer DC, McKinsey TA, Hall SM, Qi X, Lee WY, Ballard DW. 1995. Coupling of a signal response domain in I kappa B alpha to multiple pathways for NF-kappa B activation. *Mol Cell Biol* 15: 2809-18
289. Weaver BK, Bohn E, Judd BA, Gil MP, Schreiber RD. 2007. ABIN-3: a molecular basis for species divergence in interleukin-10-induced anti-inflammatory actions. *Mol Cell Biol* 27: 4603-16

290. Weng L, Dai H, Zhan Y, He Y, Stepaniants SB, Bassett DE. 2006. Rosetta error model for gene expression analysis. *Bioinformatics* 22: 1111-21
291. Difilippantonio S, Celeste A, Fernandez-Capetillo O, Chen HT, Reina San Martin B, Van Laethem F, Yang YP, Petukhova GV, Eckhaus M, Feigenbaum L, Manova K, Kruhlak M, Camerini-Otero RD, Sharan S, Nussenzweig M, Nussenzweig A. 2005. Role of Nbs1 in the activation of the Atm kinase revealed in humanized mouse models. *Nat Cell Biol* 7: 675-85
292. Kang J, Bronson RT, Xu Y. 2002. Targeted disruption of NBS1 reveals its roles in mouse development and DNA repair. *Embo J* 21: 1447-55
293. Williams BR, Mirzoeva OK, Morgan WF, Lin J, Dunnick W, Petrini JH. 2002. A murine model of Nijmegen breakage syndrome. *Curr Biol* 12: 648-53
294. Theunissen JW, Kaplan MI, Hunt PA, Williams BR, Ferguson DO, Alt FW, Petrini JH. 2003. Checkpoint failure and chromosomal instability without lymphomagenesis in Mre11(ATLD1/ATLD1) mice. *Mol Cell* 12: 1511-23
295. Digweed M, Sperling K. 2004. Nijmegen breakage syndrome: clinical manifestation of defective response to DNA double-strand breaks. *DNA Repair (Amst)* 3: 1207-17
296. Luo G, Yao MS, Bender CF, Mills M, Bladl AR, Bradley A, Petrini JH. 1999. Disruption of mRad50 causes embryonic stem cell lethality, abnormal embryonic development, and sensitivity to ionizing radiation. *Proc Natl Acad Sci U S A* 96: 7376-81
297. Xiao Y, Weaver DT. 1997. Conditional gene targeted deletion by Cre recombinase demonstrates the requirement for the double-strand break repair Mre11 protein in murine embryonic stem cells. *Nucleic Acids Res* 25: 2985-91
298. Zhu J, Petersen S, Tessarollo L, Nussenzweig A. 2001. Targeted disruption of the Nijmegen breakage syndrome gene NBS1 leads to early embryonic lethality in mice. *Curr Biol* 11: 105-9
299. Maser RS, Monsen KJ, Nelms BE, Petrini JH. 1997. hMre11 and hRad50 nuclear foci are induced during the normal cellular response to DNA double-strand breaks. *Mol Cell Biol* 17: 6087-96
300. Gatei M, Young D, Cerosaletti KM, Desai-Mehta A, Spring K, Kozlov S, Lavin MF, Gatti RA, Concannon P, Khanna K. 2000. ATM-dependent phosphorylation of nibrin in response to radiation exposure. *Nat Genet* 25: 115-9
301. Wu X, Ranganathan V, Weisman DS, Heine WF, Ciccone DN, O'Neill TB, Crick KE, Pierce KA, Lane WS, Rathbun G, Livingston DM, Weaver DT. 2000. ATM phosphorylation of Nijmegen breakage syndrome protein is required in a DNA damage response. *Nature* 405: 477-82
302. Lim DS, Kim ST, Xu B, Maser RS, Lin J, Petrini JH, Kastan MB. 2000. ATM phosphorylates p95/nbs1 in an S-phase checkpoint pathway. *Nature* 404: 613-7
303. Buis J, Wu Y, Deng Y, Leddon J, Westfield G, Eckersdorff M, Sekiguchi JM, Chang S, Ferguson DO. 2008. Mre11 nuclease activity has essential roles in DNA repair and genomic stability distinct from ATM activation. *Cell* 135: 85-96
304. Yeo TC, Xia D, Hassouneh S, Yang XO, Sabath DE, Sperling K, Gatti RA, Concannon P, Willerford DM. 2000. V(D)J rearrangement in Nijmegen breakage syndrome. *Mol Immunol* 37: 1131-9
305. Ziv Y, Bielopolski D, Galanty Y, Lukas C, Taya Y, Schultz DC, Lukas J, Bekker-Jensen S, Bartek J, Shiloh Y. 2006. Chromatin relaxation in response to DNA double-strand breaks is modulated by a novel ATM- and KAP-1 dependent pathway. *Nat Cell Biol* 8: 870-6
306. White DE, Negorev D, Peng H, Ivanov AV, Maul GG, Rauscher FJ, 3rd. 2006. KAP1, a novel substrate for PIKK family members, colocalizes with numerous damage response factors at DNA lesions. *Cancer Res* 66: 11594-9
307. Scherer DC, Brockman JA, Chen Z, Maniatis T, Ballard DW. 1995. Signal-induced degradation of I kappa B alpha requires site-specific ubiquitination. *Proc Natl Acad Sci U S A* 92: 11259-63

308. May MJ, D'Acquisto F, Madge LA, Glockner J, Pober JS, Ghosh S. 2000. Selective inhibition of NF-kappaB activation by a peptide that blocks the interaction of NEMO with the IkappaB kinase complex. *Science* 289: 1550-4
309. Pearce G, Angeli V, Randolph GJ, Junt T, von Andrian U, Schnittler HJ, Jessberger R. 2006. Signaling protein SWAP-70 is required for efficient B cell homing to lymphoid organs. *Nat Immunol* 7: 827-34
310. Feng C, Woodside KJ, Vance BA, El-Khoury D, Canelles M, Lee J, Gress R, Fowlkes BJ, Shores EW, Love PE. 2002. A potential role for CD69 in thymocyte emigration. *Int Immunol* 14: 535-44
311. Matloubian M, Lo CG, Cinamon G, Lesneski MJ, Xu Y, Brinkmann V, Allende ML, Proia RL, Cyster JG. 2004. Lymphocyte egress from thymus and peripheral lymphoid organs is dependent on S1P receptor 1. *Nature* 427: 355-60
312. Rosen SD. 2004. Ligands for L-selectin: homing, inflammation, and beyond. *Annu Rev Immunol* 22: 129-56
313. Johnson K, Hashimshony T, Sawai CM, Pongubala JM, Skok JA, Aifantis I, Singh H. 2008. Regulation of Immunoglobulin Light-Chain Recombination by the Transcription Factor IRF-4 and the Attenuation of Interleukin-7 Signaling. *Immunity* 28: 335-45
314. Richardson C, Jasin M. 2000. Frequent chromosomal translocations induced by DNA double-strand breaks. *Nature* 405: 697-700
315. Spycher C, Miller ES, Townsend K, Pavic L, Morrice NA, Janscak P, Stewart GS, Stucki M. 2008. Constitutive phosphorylation of MDC1 physically links the MRE11-RAD50-NBS1 complex to damaged chromatin. *J Cell Biol* 181: 227-40
316. Stucki M, Jackson SP. 2004. MDC1/NFBD1: a key regulator of the DNA damage response in higher eukaryotes. *DNA Repair (Amst)* 3: 953-7
317. Li S, Ting NS, Zheng L, Chen PL, Ziv Y, Shiloh Y, Lee EY, Lee WH. 2000. Functional link of BRCA1 and ataxia telangiectasia gene product in DNA damage response. *Nature* 406: 210-5
318. Lengsfeld BM, Rattray AJ, Bhaskara V, Ghirlando R, Paull TT. 2007. Sae2 is an endonuclease that processes hairpin DNA cooperatively with the Mre11/Rad50/Xrs2 complex. *Mol Cell* 28: 638-51
319. Buck D, Malivert L, de Chasseval R, Barraud A, Fondaneche MC, Sanal O, Plebani A, Stephan JL, Hufnagel M, le Deist F, Fischer A, Durandy A, de Villartay JP, Revy P. 2006. Cernunnos, a novel nonhomologous end-joining factor, is mutated in human immunodeficiency with microcephaly. *Cell* 124: 287-99
320. Dai Y, Kysela B, Hanakahi LA, Manolis K, Riballo E, Stumm M, Harville TO, West SC, Oettinger MA, Jeggo PA. 2003. Nonhomologous end joining and V(D)J recombination require an additional factor. *Proc Natl Acad Sci U S A* 100: 2462-7
321. Zha S, Alt FW, Cheng HL, Brush JW, Li G. 2007. Defective DNA repair and increased genomic instability in Cernunnos-XLF-deficient murine ES cells. *Proc Natl Acad Sci U S A* 104: 4518-23
322. Ward JF. 1988. DNA damage produced by ionizing radiation in mammalian cells: identities, mechanisms of formation, and reparability. *Prog Nucleic Acid Res Mol Biol* 35: 95-125
323. Petrij-Bosch A, Peelen T, van Vliet M, van Eijk R, Olmer R, Drusedau M, Hogervorst FB, Hageman S, Arts PJ, Ligtenberg MJ, Meijers-Heijboer H, Klijn JG, Vasen HF, Cornelisse CJ, van 't Veer LJ, Bakker E, van Ommen GJ, Devilee P. 1997. BRCA1 genomic deletions are major founder mutations in Dutch breast cancer patients. *Nat Genet* 17: 341-5
324. Menon AG, Anderson KM, Riccardi VM, Chung RY, Whaley JM, Yandell DW, Farmer GE, Freiman RN, Lee JK, Li FP, et al. 1990. Chromosome 17p deletions and p53 gene mutations associated with the formation of malignant neurofibrosarcomas in von Recklinghausen neurofibromatosis. *Proc Natl Acad Sci U S A* 87: 5435-9

325. Runnebaum IB, Tong XW, Moebus V, Heilmann V, Kieback DG, Kreienberg R. 1994. Multiplex PCR screening detects small p53 deletions and insertions in human ovarian cancer cell lines. *Hum Genet* 93: 620-4
326. Bassing CH, Ranganath S, Murphy M, Savic V, Gleason M, Alt FW. 2008. Aberrant V(D)J recombination is not required for rapid development of H2ax/p53-deficient thymic lymphomas with clonal translocations. *Blood* 111: 2163-9